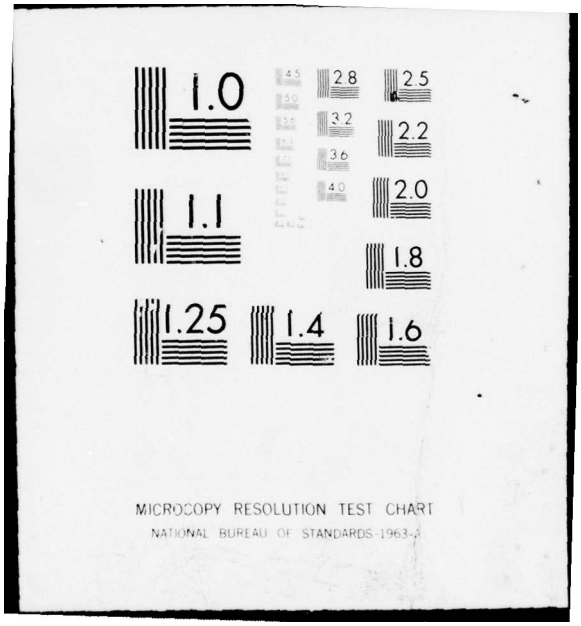
AD-A064 759 AIR FORCE INST OF TECH WRIGHT-PATTERSON AFB OHIO SCH--ETC F/G 15/3.1
A PRACTICAL THREE DIMENSIONAL , 11 STATE EXTENDED KALMAN FILTER--ETC(U)
DEC 78 C W HLAVATY

UNCLASSIFIED AFIT/GGC/EE/78-7-VOL-1 NL

1 OF 2
AD
AD 64759




1.0
1.1
1.25
1.4
1.6
1.8
2.0
2.2
2.5
2.8
3.2
3.6
4.0
4.5
5.0
5.6
MICROCOPY RESOLUTION TEST CHART
NATIONAL BUREAU OF STANDARDS-1963-A

AD A064759

DDC FILE COPY

LEVEL II

AIR FORCE INSTITUTE OF TECHNOLOGY



AIR UNIVERSITY
UNITED STATES AIR FORCE



SCHOOL OF ENGINEERING

DDC
RECEIVED
FEB 22 1979
A

WRIGHT-PATTERSON AIR FORCE BASE, OHIO

DISTRIBUTION STATEMENT A
Approved for public release;
Distribution Unlimited

79 01 30 168

AFIT/GGC/EE/78-7

(1) LEVEL II

DDC FILE COPY AD A064759

(6)

A PRACTICAL THREE DIMENSIONAL, 11 STATE EXTENDED KALMAN FILTER FOR USE IN A FIRE CONTROL SYSTEM AGAINST NON-THRUSTING MISSILES

(9) Master's THESIS VOLUME I

AFIT/GGC/EE/78-7

(10) Charles W. Hlavaty
Capt USAF

(11) Dec 78

(12) 144 p.

DDC
RECEIVED
FEB 22 1979
A

Approved for public release; distribution unlimited

012 225

AFIT/GGC/EE/78-7

A PRACTICAL THREE DIMENSIONAL, 11 STATE EXTENDED KALMAN FILTER FOR USE IN A FIRE CONTROL SYSTEM AGAINST NON-THRUSTING MISSILES

THESIS VOLUME I

Presented to the Faculty of the School of Engineering

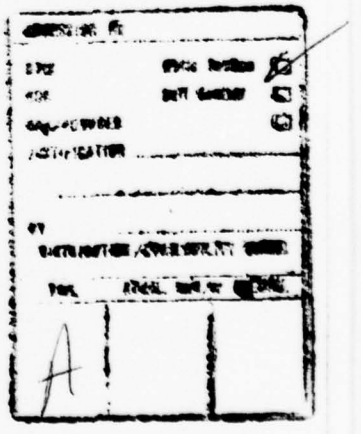
of the Air Force Institute of Technology

Air Training Command

in Partial Fulfillment of the

Requirements for the Degree of

Master of Science



by

Charles W. Hlavaty, B.S.E.E., M.S.

Capt USAF

Graduate Electrical Engineering

December 1978

Approved for public release; distribution unlimited.

Acknowledgements

"See to it that no one takes you captive through philosophy and empty deception, according to the tradition of men, according to the elementary principles of the world, rather than according to Christ.[1] In the beginning, God created the heavens and the earth. And the earth was formless and void, and darkness was over the surface of the deep; and the Spirit of God was moving over the surface of the waters.[2] Then the Lord God formed man of dust from the ground, and breathed into his nostrils the breath of life; and man became a living being.[3] But the Helper, the Holy Spirit, whom the Father will send in My name, He will teach you all things, and bring to your remembrance all that I said to you.[4] But the wisdom from above is first pure, then peaceable, gentle, reasonable, full of mercy and good fruits, unwavering, without hypocrisy.[5]"

I wish to thank Professor Peter S. Maybeck and Professor George Orr, whose help and guidance mapped new footpaths around the obstacles I created. Their service was always enthusiastically given. In addition, I wish to thank the Holy Spirit, whose teaching not only provided me with insights to the system I designed, but whose workings taught me much about myself, about God, and about this world; and gave me peace and comfort through two trying periods of my life.

---

[1]Colossians 2:8 NASB
[2]Genesis 1:1-2 NASB
[3]Genesis 1:7 NASB
[4]John 14:26 NASB
[5]James 3:17 NASB

Volume I

Contents

		Page
Acknowledgements		ii
Volume II Contents		v
List of Figures		vi
List of Tables		ix
Abstract		x
I.	Purpose of Thesis	1
	Introduction	1
	Statement of the Problem	3
	Monte Carlo Analysis	5
II.	System Truth Models	8
	Introduction	8
	Missile Model	8
	Seeker Block	11
	Guidance Block	24
	Autopilot/Dynamics Block	27
	Target Model	34
III.	Extension of Two Dimensional Filter	46
	Introduction	46
	First Proposal	47
	Second Proposal	49
	Third Proposal	77
IV.	11 State Three Dimensional Filter	86
	Introduction	86
	Filter State Space	87
	Filter Tests	94
V.	Results and Recommendations	97
	Results	97
	Recommendations	99

Page

Bibliography 101

Appendix A Rotation of a Vector 103

Appendix B Derivation of 11 State Filter 106

Vita 129

Volume II

Contents

	Page
Appendix C	1
Appendix D	75
Appendix E	113

List of Figures

Figure		Page
1	Variance Convergence	7
2	Inertial Frame at T=0	10
3	Missile Body Frame	12
4	Seeker Frame	13
5	Seeker Field of View	15
6	The Vector $\underline{\theta}$	16
7	Three Dimensional Seeker Mechanization	19
8	Definition of $\underline{W}_{s1}$	20
9	Symmetrical Cruciform Missile	28
10-A	K Set One Trajectory	39
10-B	K Set Two Trajectory	40
10-C	K Set Three Trajectory	41
10-D	K Set Three Trajectory	42
11	A Missile's Turn	43
12	B Frame Components of Turn for an Arbitrary Time Constant	44
13	Two Dimensional Pictorial Depiction of the First Five States of the 2D Filter	48
14	2D Filter's XY Plane Orientation at Two Time Instants for Three Dimensional Application	50
15	Double Filter	51
16	Difference Between Filter States and Measurement for Double Filter	53

17	Angle Measurement Double Filter	55
18	Range Double Filter	56
19	Range Rate Double Filter	57
20	Angle Measurement Sigmas Double Filter	59
21	Range Sigmas Double Filter	60
22	Range Rate Sigmas Double Filter	61
23	Angle Measurement Double Filter	62
24	Range Double Filter	63
25	Range Rate Double Filter	64
26	Angle Measurement Sigmas Double Filter	65
27	Range Sigmas Double Filter	66
28	Range Rate Sigmas Double Filter	67
29	Angle Measurement Double Filter	69
30	Range Double Filter	70
31	Range Rate Double Filter	71
32	Angle Measurement Sigmas Double Filter	72
33	Range Sigmas Double Filter	73
34	Range Rate Sigmas Double Filter	74
35	Vector Rotation Effects on Its Planar Projection	75
36	Summarized Filter Plane Results of Figure 35	76
37	Relationship Between Computed Line of Sight Acceleration and Filter Modeled Acceleration	78
38	Angle Measurement Double Filter	80
39	Range Double Filter	81
40	Range Rate Double Filter	82
41	Angle Measurement Sigmas Double Filter	83
42	Range Sigmas Double Filter	84

43	Range Rate Sigmas Double Filter	85
44	The Three Filter Frames	89
45	Angular Orientation Between i and l Frames	90
46	Angular Orientation Between v and l Frames	91
47	Missile Model Roll	93
A-1	Rotation of a Unit Vector	104
B-1	Points m, t, and j in the Line of Sight Frame	108
B-2	Angular Orientation Between v and l Frames	111
B-3	11 State Filter Model's $\underline{v}$ Relationship for Time t_1 .	116
B-4	11 State Filter Model's $\underline{v}$ Relationship for Time t_2 .	118
B-5	Angular Orientation Between i and l frames	120
B-6	Mathematical Constraint on ω_3	123

List of Tables

Table		Page
I	Sigmas and Time Constants for Line of Sight Noise	24
II	Sigmas and Time Constants for Measurements Noise	36
III	K Set Parameters	38
IV	Missile Response Comparisons of Trajectories	46

Abstract

A previously designed extended Kalman filter, based upon the proportional guidance law, aerodynamic drag equation, and a first order lag model of the missile time response; is modified for three dimensional use. Its purpose is to estimate various states of an offensive missile by processing the line of sight measurements made by the target aircraft. A six-degree-of-freedom, stochastic missile model is developed and presented in Fortran code. Monte Carlo analyses of the filter's performance are generated for four different trajectories. These trajectories test for different orientations of the line of sight, different acceleration profiles of the missile, and different amounts of roll induced upon the missile by a three dimensional, conic turn.

The extended Kalman filter is designed in the line of sight frame and is composed of eleven states. They are: two line of sight orientation angles, two inertial angular velocities of the line of sight, range, closing velocity, two lateral accelerations of the missile, and three constant parameters. The constant parameters are the proportional navigation constant (which exploits an assumed missile guidance scheme), a time constant (for the first order lag model of missile time response), and the missile's mass over surface ratio (for computing aerodynamic drag of the missile). The filter assumes that the missile is non-rolling with respect to the line of sight frame, and that the line of sight frame is non-rolling with respect to the inertial frame. It also assumes that the missile is non-thrusting.

Preliminary results are promising. The filter is only tuned for one trajectory due to time limitations, yet its estimation of the pointing-tracking states provide good aiding for all trajectories. Parameter estimates and missile acceleration estimates for the other trajectories are degraded due to improper tuning of the two parameters. However, it is felt that additional tuning of those parameters will increase the filter's accuracy for the other trajectories. Plots of the Monte Carlo results are provided, as well as the Fortran computer program used in the simulation.

A PRACTICAL THREE DIMENSIONAL, 11 STATE EXTENDED KALMAN FILTER FOR USE IN A FIRE CONTROL SYSTEM AGAINST NON-THRUSTING MISSILES

I. Purpose of Thesis

Introduction

In tomorrow's wartime environment, offensive missiles will play a leading role. Future aircraft must either neutralize the missile threat or avoid it altogether. Current research is focused primarily on neutralization methods involving, among other things, laser weapons. However, certain information must be available before a laser can be used to neutralize a missile.

The most obvious requirement is information about the missile's velocity and position. Accuracies required by a laser weapon are generally beyond the reach of most pointing-tracking systems. Aided pointing and tracking systems - those systems which use a stochastic kinematics model of the object being tracked to predict future position and velocity - have met with varying degrees of success (Refs 1,4,5,9). Generally, research has shown that the more accurate the stochastic model, the more accurate the pointing and tracking. Yet, the model must be simple enough to be practical. By limiting the variety of tracked objects to an attacking missile - particularly a non-thrusting missile guided by proportional navigation - Cusumano and DePonte

demonstrated the feasibility of a planar (two dimensional) eight state extended Kalman filter based upon a first order lag model of the missile's lateral acceleration response. This filter model, when compared to filters incorporating less structural acceleration models (such as first order Gauss-Markov models), increases the accuracy of two dimensional pointing and tracking against a wide variety of proportional navigation missiles. But other requirements must be fulfilled as well.

A not-so-obvious requirement is threat evaluation. Obviously, if a missile is not, or will not, be a threat, no action against it is required. In a multiple missile environment, knowledge of each missile's threat may mean the difference between life and death. Not only is it necessary to neutralize the most threatening missile; it is also necessary to quit neutralizing as soon as the missile loses track and to move on to the next threat. In this way, the aircraft's defensive capability is greatly increased.

It appears, however, that laser weapons will require a rather large airframe. Therefore, fighter aircraft will still need to practice avoidance techniques. Current avoidance techniques rely on intelligence reports to help plan a low threat route. When something goes awry and the aircraft is attacked, it attempts to "lose" the missile through the use of special maneuvers. In fact, "wild weasels" purposely engaged surface-to-air missiles during the Vietnam war to discover launch sites. These special mission aircraft successfully outmaneuvered the missile and destroyed the launch site.

However, these techniques rely on humans to maneuver the aircraft. Studies show humans are limited in the number of tasks that can be

handled at one time as well as the speed of accomplishment (Ref 15:17-39). In future wars, low threat routes may not be available. In addition, a multiple missile threat will probably be too fast-paced and complex for humans to handle. Therefore, some machine must be used to extend the human capabilities.

One such machine could be a computerized autopilot that employs a stochastic missile model. This type of autopilot could obtain estimates of missile lateral accelerations and dynamic response characteristics. With this knowledge, special algorithms would choose the best maneuver that would cause the missile to attempt to exceed its performance limitations. Thus, the missile is avoided. Missile threats could be handled one at a time or, ultimately, all at once. But this method is definitely beyond the scope of this thesis. Rather, the objective of this thesis is to take one more step towards a stochastic model capable of being used in a system for threat neutralization and threat avoidance.

Statement of the Problem

The research of Cusumano and DePonte demonstrates that a reduced order model for the missile's lateral acceleration response (specifically, a first order lag), can be used in an extended Kalman filter as an effective aid to pointing and tracking (Ref 1). However, the extended Kalman filter, and the model upon which it is based, is planar (two dimensional)*. In addition, the filter's performance is proven for only two, missile-target trajectories. Therefore, this

Note: Throughout this thesis, the term "dimensional" will refer to the physical system, i.e. two dimensional is planar, three dimensional is the physical world. The size of a filter will be referred to as "states", such as "eight states" and "11 states".

thesis will build two extended Kalman filters appropriate to a realistic three dimensional environment and test them under a variety of trajectories.

Two ways to build a filter are proposed. The first way projects three dimensional line of sight (the vector that points from the missile to the target) motion into two, orthogonal, vertical planes. A two dimensional, eight state extended Kalman filter is used in each plane to obtain state estimates of the two projections. These two sets of state estimates are then used to obtain three dimensional estimates of the line of sight motion, thus aiding the three dimensional pointing and tracking problem. But this filter is limited to the performance demonstrated by Cusumano and DePonte. Approximations necessary for three dimensional application will most probably reduce the filter's accuracy unacceptably. The second way builds an extended Kalman filter based upon a three dimensional missile model and is potentially more accurate.

The three dimensional missile model will "split" the missile into two orthogonal planes. A first order lag model of missile response will be used for each missile plane. The two missile response models will be coupled to the three dimensional measurements available from a pointing-tracking system. It is conceivable that a different choice of state space and/or the processing of additional information available from sensors within the target aircraft could improve filter performance beyond the capability demonstrated by Cusumano and DePonte. Therefore, these factors will be investigated.

Since the second approach shows greater promise than the first, the following objectives are established:

1. The three dimensional application of 2, eight-state filters will be investigated, primarily as a learning tool for gaining the physical insights into a missile-target encounter which are required to accomplish the second objective. No attempt will be made to produce a proven, workable filter since this approach is not fruitful in generating a filter with acceptable performance.
2. A three dimensional missile model will be designed and incorporated into an extended Kalman filter. This model will be an extension of the work accomplished by Cusumano and DePonte. The filter will be tested against a representative variety of trajectories. Recommendations will be made to direct future research.

In both the above objectives, the results obtained by Cusumano and DePonte (Ref 1,2) will be used as a baseline for comparison. Time constraints imposed upon this thesis will have a major impact upon the accomplishment of these objectives.

Monte Carlo Analysis

Both objectives require tests to be performed on extended Kalman filters. The evaluation of an extended Kalman filter requires the use of a Monte Carlo analysis. A complete description of a Monte Carlo analysis is contained in Reference 7.

In a Monte Carlo analysis, the filter's estimates of the states are compared to the true values of those states (which are computed by a "truth model") during one missile-target engagement. To produce one test, the engagement is repeated several times with different

samples of simulated noises. The comparisons from each engagement are statistically averaged to demonstrate the filter's performance. The more engagements that are averaged, the closer the test results demonstrate the true statistical performance of the filter. However, each engagement, or run, adds to the cost of a Monte Carlo analysis. Therefore, an appropriate number of runs, p, must be chosen.

To demonstrate the validity of the choice for p, a variance conversion chart is constructed (see Figure 1). The variance observed for one particular data point as the number of runs, p, is increased is plotted. As p increases, the computed sample variance converges to the true variance value. However, not all data points converge at the same rate. Since it is possible that this data point will converge quickly, thus falsely indicating convergence for all data points after only a few runs, four data points are analyzed. The variance of the slowest converging data point is used to determine an appropriate p. The tests performed in this thesis show excellent variance conversion for p equal to twenty. The Monte Carlo results, which are contained in the appendices, have variance conversion charts for each test.

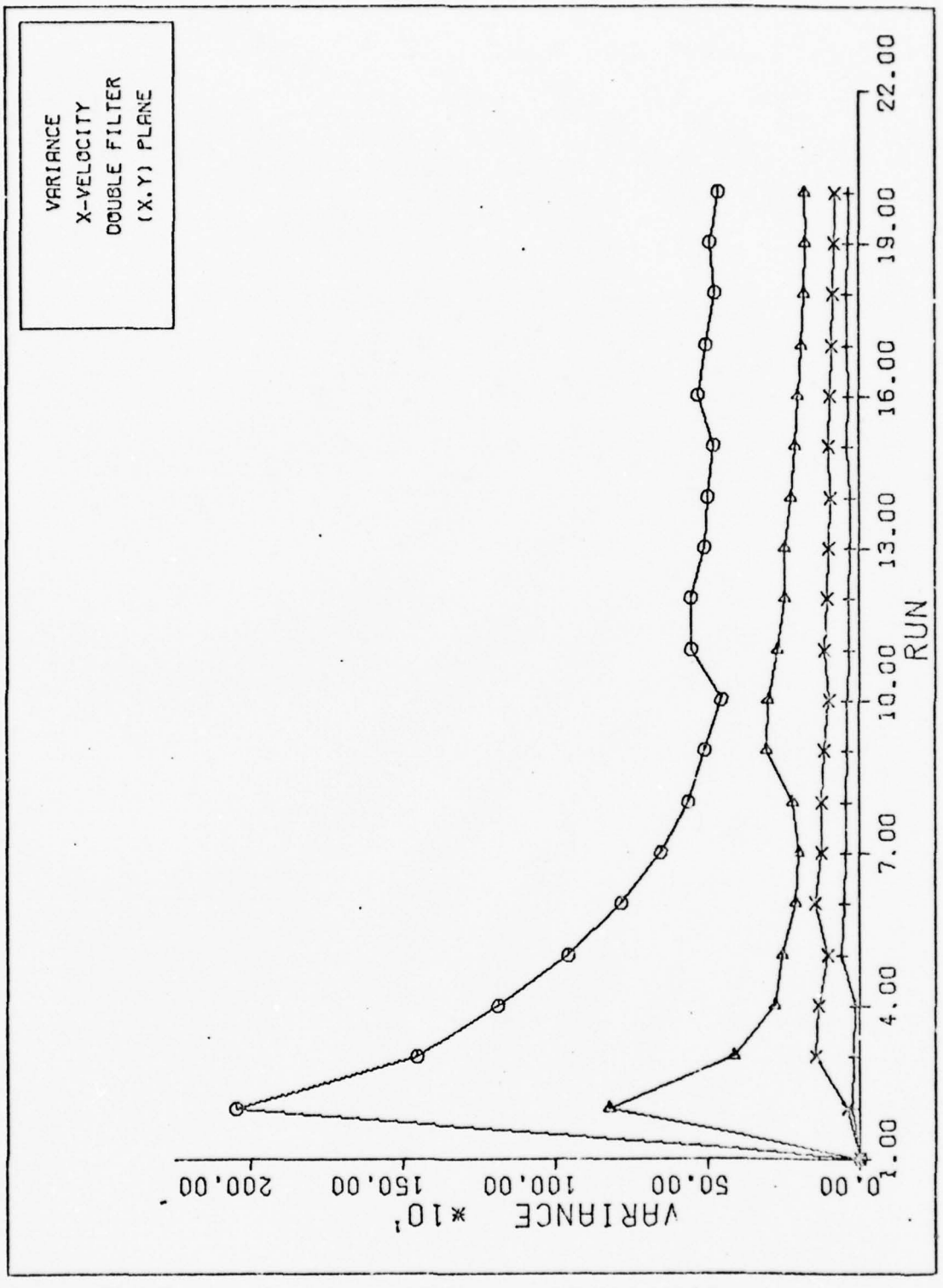


Fig. 1. VARIANCE CONVERGENCE

II. System Truth Models

Introduction

The truth model which is required in a Monte Carlo analysis is an accurate mathematical representation of the real world. It is used to test and fine tune the performance of the extended Kalman filter by providing true values of the states which the filter is estimating. Thus, errors in the filter's state estimates can be evaluated statistically. Any errors or invalid assumptions in the truth model will corrupt the "true values" and degrade the effectiveness of filter verification. Therefore, it is essential for the truth model to portray the real world phenomena as accurately as possible.

The truth model used in this Monte Carlo analysis is composed of two component system models - one for the missile and one for the target. Previous theses are used extensively for the numerical details of each system model (Ref 1,5). However, the modeling approach for the missile is significantly altered to insure an accurate, three-dimensional representation. The target truth model requires only minor modification.

Missile Model

Models for guided missiles can be partitioned into three blocks: the seeker block, the guidance block, and the autopilot/dynamics block. The seeker block measures the target's relative position and/or dynamics. The guidance block uses these measurements to determine

missile acceleration commands (or actuator commands) that will cause target intercept. The autopilot/dynamics block transforms the acceleration commands into lifting forces, which produce lateral accelerations. Time lags, errors in design assumptions, and environmental disturbances can cause errors in target intercept.

This missile truth model uses a vector approach, representing necessary information as inertially coordinatized vectors, uncoordinatized vectors, and scalars. An inertially coordinatized vector, which is a set of three component values, is represented as a capital letter with an underline ($\underline{R}$). Underlined small letters ($\underline{r}$) represent coordinatized unit vectors. The uncoordinatized vector, which is a single value, is represented as a capital letter without underline (R). An uncoordinatized vector is simply a magnitude (length) of a vector with sign (direction) information. Thus, R=5 points in the opposite direction of R=-5. However, R is not defined in relation to inertial space. A scalar is represented as a small letter without an underline (k).

Three reference frames are used in the missile model: the inertial frame (i), the missile body frame (b), and the missile seeker frame (s). The origin of the inertial frame is located at the target's position at the start of the engagement and remains inertially fixed (see Figure 2). The missile's initial position is in the ($\underline{i}_1$, $\underline{i}_2$) plane (the plane formed by the two axes $\underline{i}_1$ and $\underline{i}_2$). The axes $\underline{i}_1$ and $\underline{i}_3$ are horizontal, and $\underline{i}_2$ is vertical (up). The axis $\underline{i}_1$ points away from the missile, as in the figure. The inertial angular velocity of the earth is assumed to be negligible during the short period of engagement.

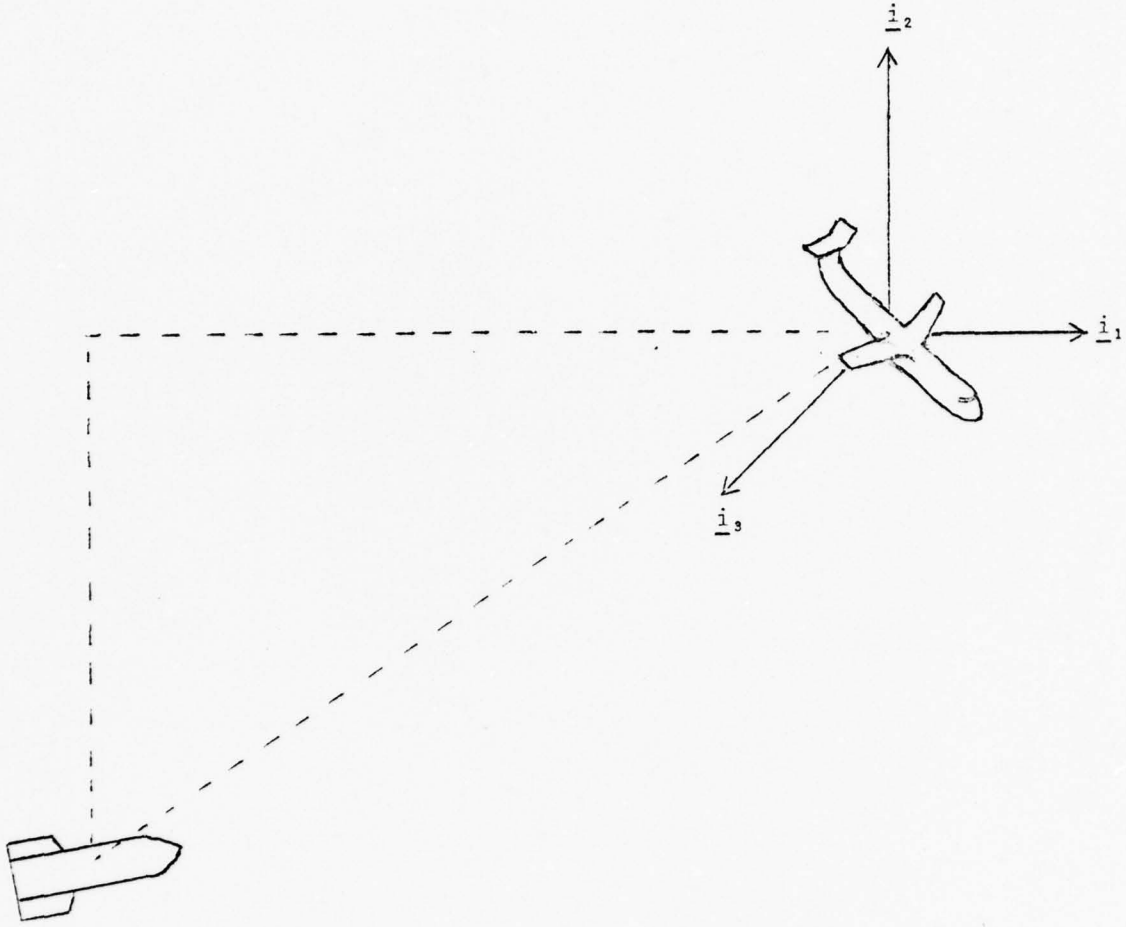


Fig. 2. Inertial Frame at T=0

Therefore, the ($\underline{i}_1$, $\underline{i}_3$) plane is always horizontal. Gravity is assumed to be in the $-\underline{i}_2$ direction with constant magnitude.

The origin of the missile body (b) frame is the missile's center of mass (see Figure 3). The missile centerline is the $\underline{b}_1$ axis. However, unlike conventional body frames, the $\underline{b}_2$ axis points out of the top of the missile (negative conventional yaw axis) and the $\underline{b}_3$ axis points out of the missile's right side (positive conventional pitch axis). This unconventional body frame allows easier modification of previously developed computer software (Ref 1).

To simplify the missile model, the seeker's inertial angular velocity is assumed to be independent of the missile's inertial angular velocity (inertially stablized seeker). Moreover, the distance between the missile's center of mass and the seeker is assumed to be negligible relative to other distances in the problem, such as range. Therefore, the origin of the seeker (s) frame is assumed to be the missile's center of mass. Located at this origin is the seeker pivot point (see Figure 4). The seeker's centerline is the $\underline{s}_1$ axis. The $\underline{s}_3$ axis is constrained to the ($\underline{b}_1$,$\underline{b}_3$) plane. The $\underline{s}_2$ axis finishes the right-hand orthogonal s frame. Thus, the three coordinate frames are defined.

Seeker Block

The missile seeker contains a sensor (much like the human eye looking through a rifle scope) that develops an output if the target is not centered in its field of view. This output is fed back into a driving mechanism or driver (the arms holding the rifle), which moves the sensor to center the target. When the target is centered, the sensor output is zero.

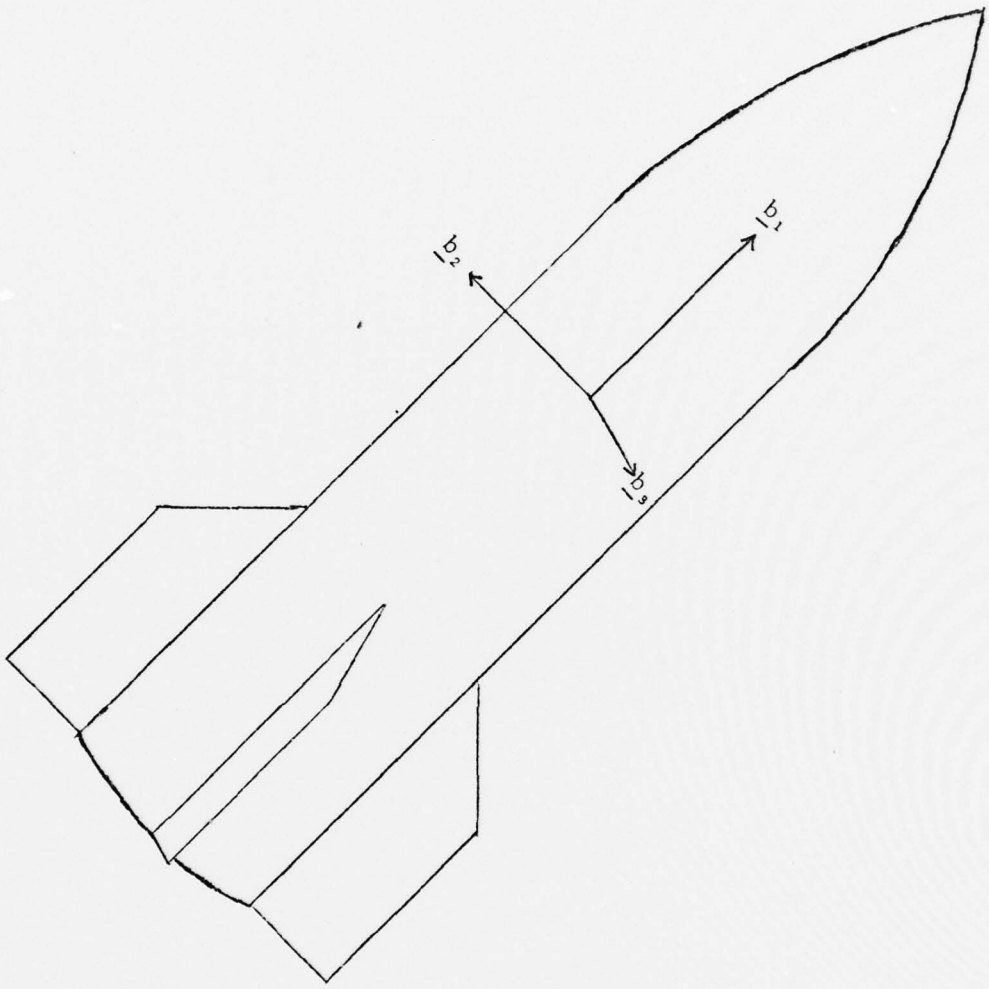


Fig. 3. Missile Body Frame

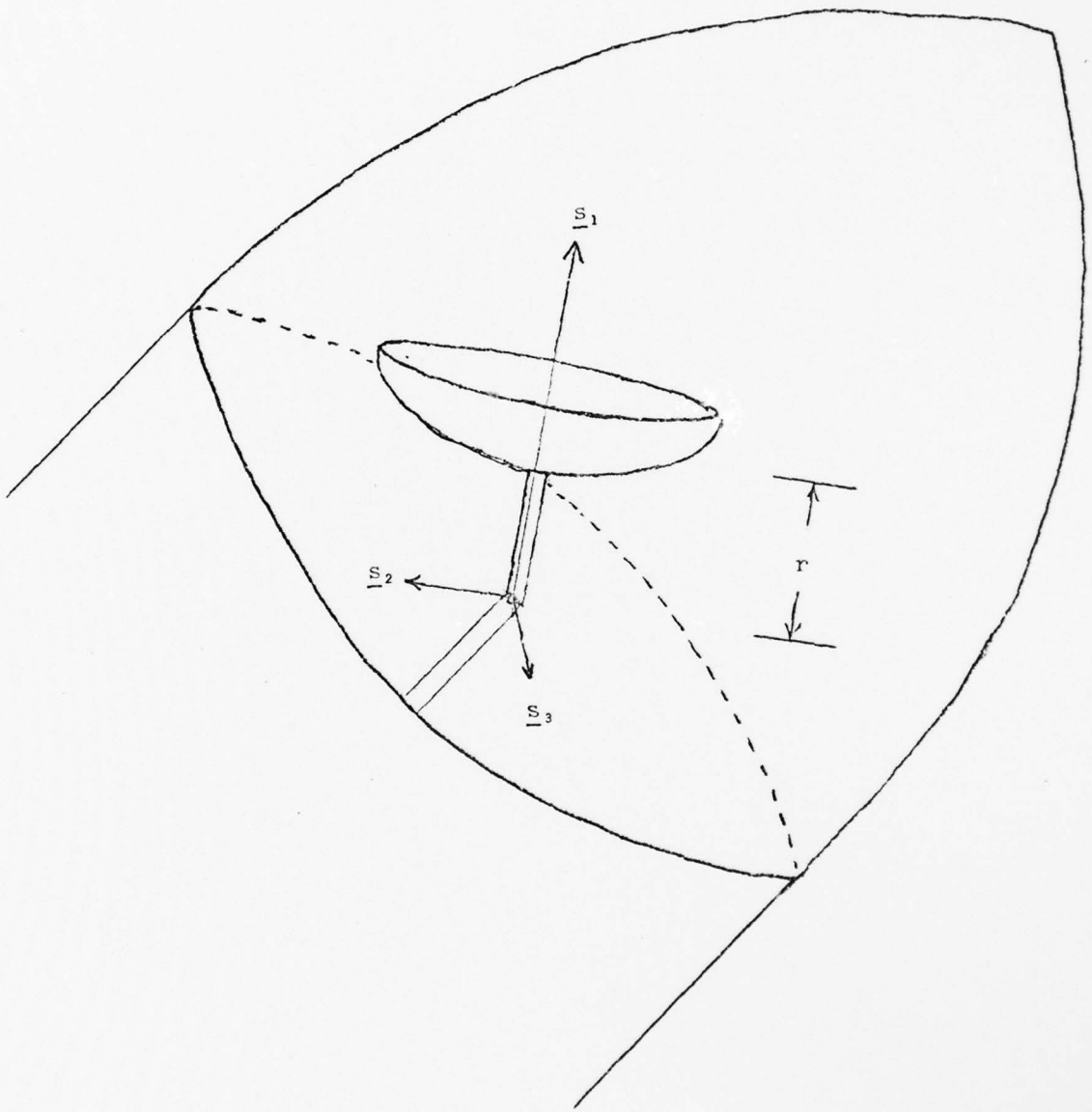


Fig. 4. Seeker Frame

The sensor's field of view can be represented as a circular disc parallel to the ($\underline{s}_2$, $\underline{s}_3$) plane. Its center is located an arbitrary distance from the seeker pivot point (see Figure 5). The crosshairs of the sensor are in the $\underline{s}_2$ and $\underline{s}_3$ directions, respectively. The drivers are located at the seeker pivot point and produce inertial angular motion of the seeker. One driver produces inertial rotation in the $\underline{s}_2$ direction only; the other driver produces inertial rotation only in the $\underline{s}_3$ direction. The pivot point is physically constructed such that $\underline{s}_3$ remains in the ($\underline{b}_1$, $\underline{b}_3$) plane. In this way, the pitch and yaw axes of the seeker remain properly oriented to the pitch and yaw axes of the missile, allowing seeker outputs to be directly coupled to the guidance block.

Most two dimensional seekers can be modeled as two independent first order lag networks - one for each direction (Ref 11:32). The inertial angular rate of the sensed line of sight vector is the network's input; the angle θ, between the sensed line of sight vector, $\underline{r}_{SLOS}$, and the seeker centerline, $\underline{s}_1$, is the network's output. Seeker block outputs, however, are often the inertial angular rates of the seeker - the feedback portion of the first order lags. (The sensed line of sight vector points from the missile to the apparent position of the target.) Since θ must be small for most sensors to lock on to the target, it can be treated as a vector and broken into components corresponding to each lag circuit (see Figure 6). (If large angles are admissable, order of rotation becomes important, making this type of sensor nonlinear.) A linear sensor will produce two voltage outputs, each proportional to the respective error angle component. These voltages are amplified into currents and fed into the drivers.

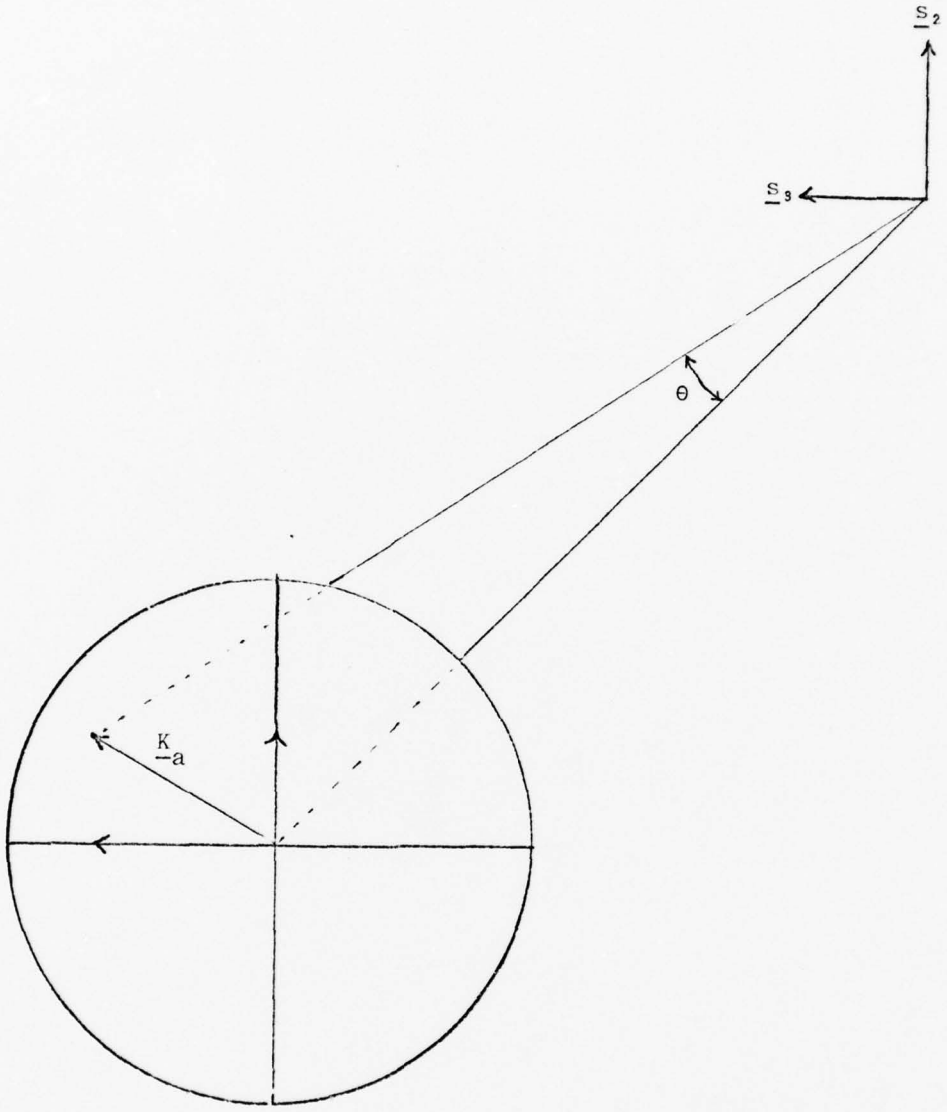


Fig. 5. Seeker Field of View

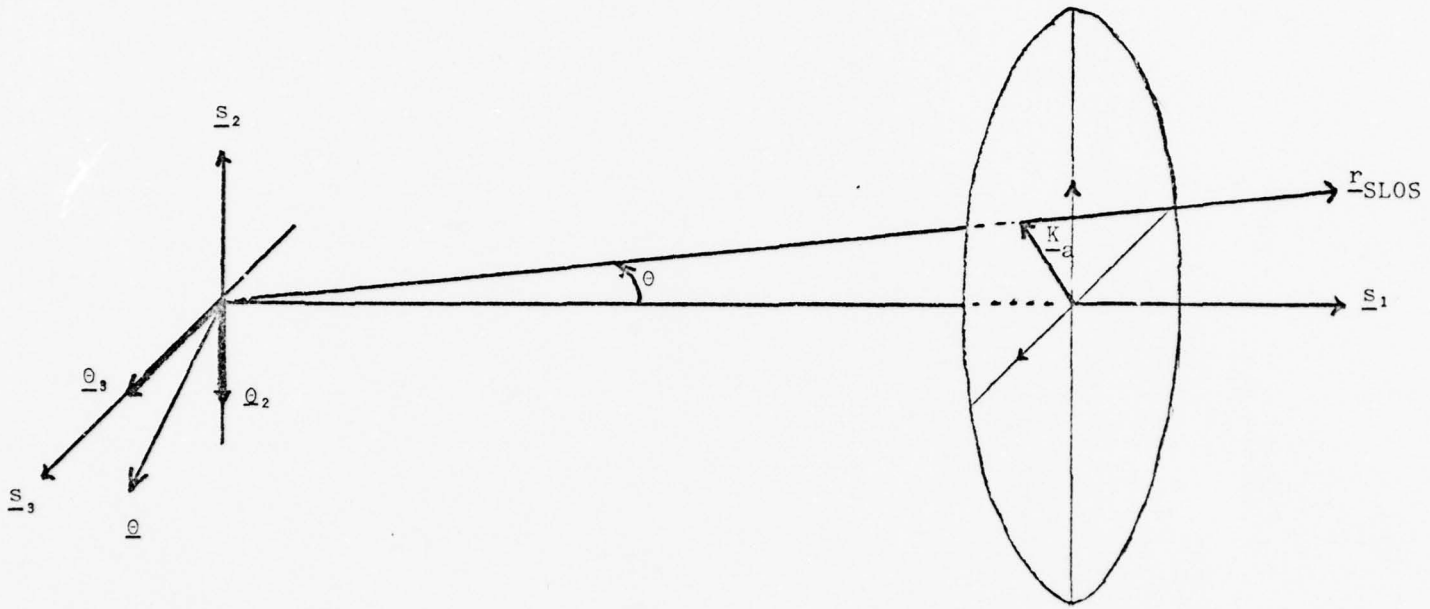


Fig. 6. The Vector $\underline{\theta}$

A constant current coupled to a linear driver on a frictionless pivot produces a constant angular rate of the seeker (Ref 3). It is assumed that this ideal seeker model adequately represents seeker performance.

To mechanize the seeker models, the error angle component vectors, $\underline{\theta}_2$ and $\underline{\theta}_3$ (which are the component vectors of $\underline{\theta}$) must be modeled. These angular components can be defined in terms of θ; and the unit vector that points from the intersection of the seeker centerline and the sensor field of view, to the intersection of the sensed line of sight $\underline{r}_{SLOS}$ and the sensor field of view (see Figures 5 and 6). The equations that describe this relationship are:

$$\theta_2 = \theta(\underline{s}_3 \cdot \underline{k}_a) \tag{1}$$

$$\theta_3 = \theta(\underline{s}_2 \cdot \underline{k}_a) \tag{2}$$

where $\underline{k}_a$ = the unit vector that points in the direction of the sensor error. The unit vector $\underline{k}_a$ can be approximated as:

$$\underline{k}_a \approx \frac{\underline{r}_{SLOS} - \underline{s}_1}{|\underline{r}_{SLOS} - \underline{s}_1|} \tag{3}$$

Note: Equations (1), (2), and (3) require θ to be small enough to be treated as a vector.

The error angle, θ, is defined through the dot product formula to be:

$$\theta = \cos^{-1} (\underline{s}_1 \cdot \underline{r}_{SLOS}) \tag{4}$$

where the valid region of θ is $0 \leq \theta \leq \pi$

Note that the definitions of θ and $\underline{k}_a$ determine the directions of $\underline{\theta}_2$

and $\underline{\theta}_3$ in equations (1) and (2). Positive $\underline{\theta}_2$ is a rotation about the $-\underline{s}_2$ axis, and positive $\underline{\theta}_3$ is a rotation about the $\underline{s}_3$ axis. This convention allows equations from both missile planes (equations (1) and (2)) to be identical - a practice that will also be used in the dynamics block. When these components are used in the first order lag seeker model, the set of equations becomes:

$$\frac{\theta_2}{W_2} = \frac{-1}{s + \frac{1}{\tau_1}} \tag{5}$$

$$\frac{\theta_3}{W_3} = \frac{1}{s + \frac{1}{\tau_1}} \tag{6}$$

where W_2, W_3 = $\underline{s}_2$, $\underline{s}_3$ components of the inertial angular velocity of $\underline{r}_{SLOS}$ (rad/sec)

θ_2, θ_3 = $-\underline{s}_2$, $\underline{s}_3$ components of the error angle, $\underline{\theta}$ (rad)

s = Laplace transform s

τ_1 = seeker time constant (sec)

Different seeker time constants could be specified to model a seeker with different dynamic characteristics about its two pivot axes.

The outputs of the seeker block, $\underline{W}_{s2}$ and $\underline{W}_{s3}$, are the feedback portions of the two first order lag models (see Figure 7). They are also two of the three seeker frame components of the seeker frame inertial angular velocity. The third seeker frame component, $\underline{W}_{s1}$, is in the $\underline{s}_1$ direction. The vector addition of $\underline{W}_{s1}$ and $\underline{W}_{s2}$ must be in the $\underline{b}_2$ direction to maintain the constraints imposed by the seeker frame's definition, i.e. the constraint on $\underline{s}_3$ to lie in the ($\underline{b}_1$, $\underline{b}_3$) plane. From geometry (see Figure 8)

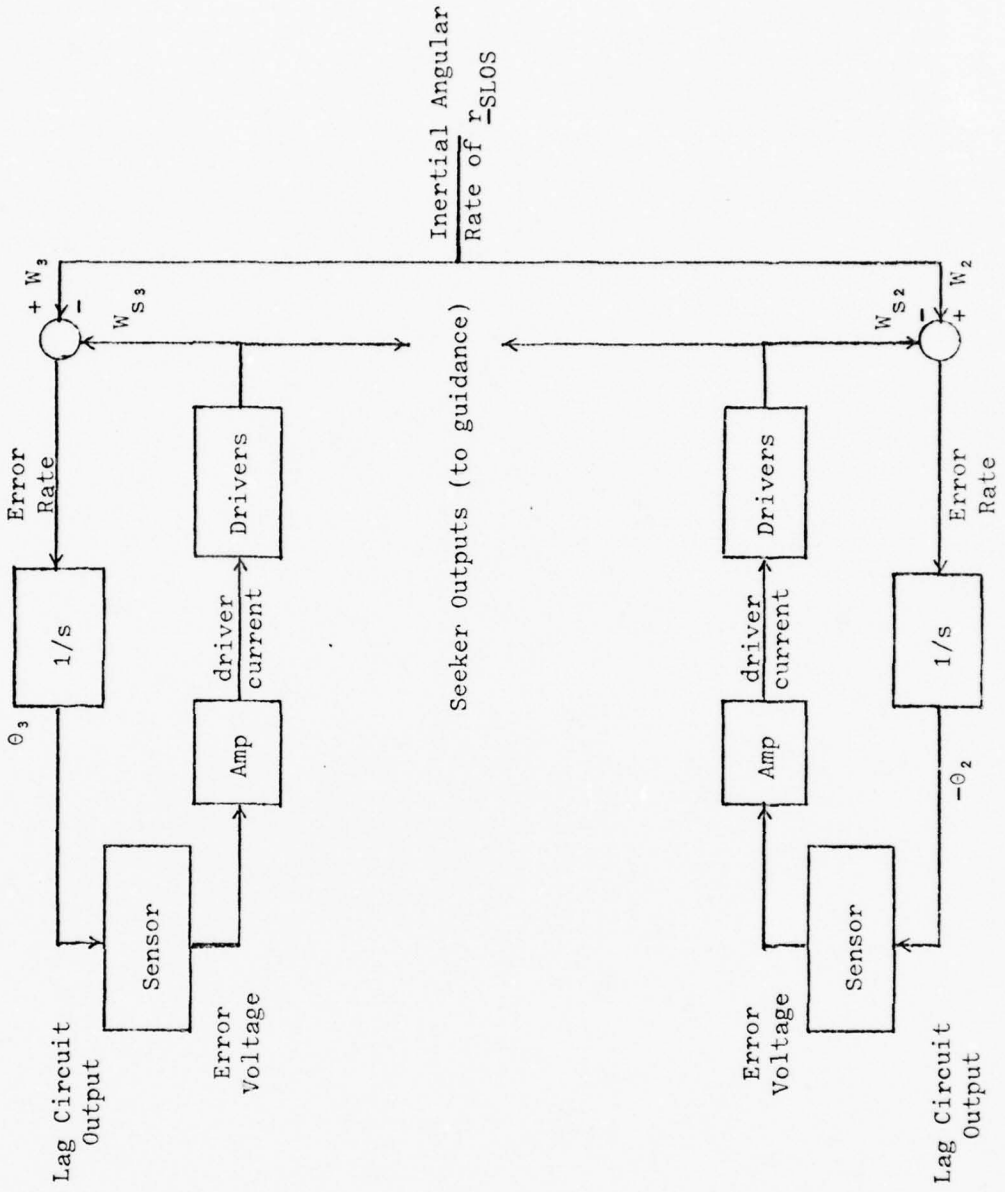


Fig. 7. Three Dimensional Seeker Mechanization

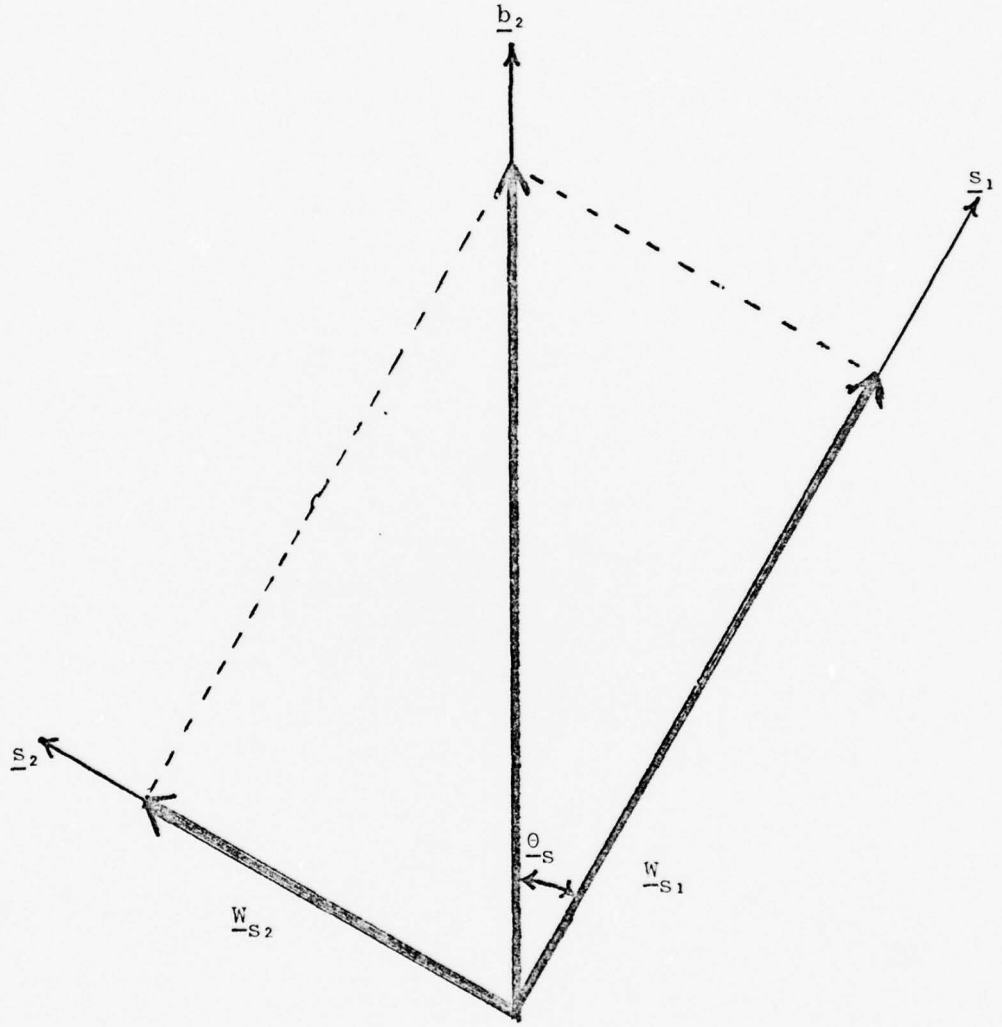


Fig. 8. Definition of $\underline{W}_{s1}$

$$W_{s_1} = W_{s_2} \cos\theta_s \tag{7}$$

where θ_s = the angle between $\underline{s}_1$ and $\underline{b}_2$ (rad)

W_{s1} = inertial angular velocity of seeker along $\underline{s}_1$ axis (rad/sec)

W_{s2} = inertial angular velocity of seeker along $\underline{s}_2$ axis (rad/sec)

The seeker frame inertial angular velocity (in inertial coordinates) is

$$\underline{W}_s = \underline{W}_{s1} + \underline{W}_{s2} + \underline{W}_{s3} \tag{8}$$

and

$$\underline{W}_s = \begin{bmatrix} \omega_{sx} \\ \omega_{sy} \\ \omega_{sz} \end{bmatrix} \tag{9}$$

where ω_{sx} = seeker frame inertial angular velocity in $\underline{i}_1$ direction (rad/sec)

ω_{sy} = seeker frame inertial angular velocity in $\underline{i}_2$ direction (rad/sec)

ω_{sz} = seeker frame inertial angular velocity in $\underline{i}_3$ direction (rad/sec)

$\underline{W}_s$ will be used to determine the orientation of the seeker frame.

The orientation of the seeker frame in terms of the inertial frame is defined to be:

$$s_1 = C_i^s [1\ 0\ 0]^T \tag{10}$$

$$s_2 = C_i^s [0\ 1\ 0]^T \tag{11}$$

$$s_3 = C_i^s [0\ 0\ 1]^T \tag{12}$$

where C_i^s = direction cosine matrix from i to s frame.

The dynamics of the direction cosine matrix are specified by (Ref 16:23)

$$pC_i^s = C_i^s \, W_{is}^{ik} \tag{13}$$

where p = first derivative with respect to time

$$W_{is}^{ik} = \begin{bmatrix} 0 & -\omega_{sz} & \omega_{sy} \\ \omega_{sz} & 0 & -\omega_{sx} \\ -\omega_{sy} & \omega_{sx} & 0 \end{bmatrix}$$

By integrating equation (13), the orientation of the seeker frame is specified. Thus, the dynamics of the seeker block, from the sensed line of sight to the seeker block outputs, $\underline{W}_{s_2}$ and $\underline{W}_{s_3}$, are specified. To complete the description of the seeker block, the sensed line of sight, $\underline{r}_{SLOS}$, must be specified.

The sensed line of sight, $\underline{r}_{SLOS}$, is derived in the simulation from the true line of sight, $\underline{r}_{LOS}$, which is the unit vector that points from the missile position to the true target position. The true line of sight is bent and distorted, much like the image of a fish in water is displaced and distorted by water ripples and angle of sight. The missile's nose cone produces aberration error, similar to errors caused by the refraction of light. Glint, thermal, and scintillation noises (Ref 5:27-30) further corrupt the image position, like ripples in the water. To account for these effects, the true line of sight, $\underline{r}_{LOS}$, is rotated by an aberration error angle and two noise angles.

One simple model for the aberration error angle (which assumes a symmetrical nose cone) is (Ref 5:11-13)

$$\underline{\Phi}_A = k_r \underline{\Phi} \tag{14}$$

where k_r = proportionality constant

$\underline{\Phi}$ = the angle from missile centerline to the true line of sight.

The angle Φ is found from the dot product formula to be:

$$\Phi = \cos^{-1}(\underline{b}_1 \cdot \underline{r}_{LOS}) \tag{15}$$

The direction of rotation of Φ is the direction of $\underline{b}_1 \times \underline{r}_{LOS}$. Thus, the coordinatized vector, $\underline{\Phi}$ is defined. The true line of sight, $\underline{r}_{LOS}$, is rotated through the angle $\underline{\Phi}_A$ to produce the intermediate line of sight vector, $\underline{r}_{ILOS}$, which must be further rotated by two noise angles to produce $\underline{r}_{SLOS}$. (See Appendix A for planar rotations of vectors.)

Lutter found that noise which corrupts the line of sight's direction can be modeled as a combination of exponentially correlated Gaussian noise added to a Gaussian white noise (Ref 5:30). From the assumption of symmetry, two orthogonal noise angles with identical statistics can be used to account for three dimensional line of sight noises. The statistics used for the two noise angles, $\underline{\Phi}_{n1}$ and $\underline{\Phi}_{n2}$, are obtained from previous research and are presented in Table I (Ref 5:30-31). Although noise angles are small, the computer software developed in Appendix A is easier to apply if order of rotation is modeled. Therefore, the directions of $\underline{\Phi}_{n1}$ and $\underline{\Phi}_{n2}$ are modeled orthogonal to the vector each corrupts and to each other. The direction of $\underline{\Phi}_{n1}$ is chosen to be the direction of $\underline{b}_1 \times \underline{r}_{ILOS}$. The intermediate line of sight, $\underline{r}_{ILOS}$, is rotated through the angle $\underline{\Phi}_{n1}$. This new

TABLE I

Sigmas and Time Constants
for Line of Sight Noise

NOISE ANGLE	SIGMA	TIME CONTROL
Φ_{n_1}	.003 rad .000894 rad	--- 0.1 sec
Φ_{n_2}	.003 rad .000894 rad	--- 0.1 sec

direction of $\underline{r}_{ILOS}$, ($\underline{r}'_{ILOS}$), is crossed into $\underline{\Phi}_{n_1}$ to define the direction of $\underline{\Phi}_{n_2}$. The vector $\underline{r}'_{ILOS}$ is rotated through the angle $\underline{\Phi}_{n_2}$ to produce the sensed line of sight, $\underline{r}_{SLOS}$.

The seeker block of the missile has been fully modeled, from the corruption of the true line of sight to the seeker outputs, $\underline{W}_{S_2}$ and $\underline{W}_{S_3}$. The orientation of the seeker frame is specified for all time. The seeker outputs are passed directly to the guidance block, which produces commanded accelerations.

Guidance Block

Ideally, if the seeker has no inertial angular velocity ($\underline{W}_{S_2} = \underline{W}_{S_3} = 0$) for all time, the missile will hit the target. Another way of stating this is that the inertial angular orientation of the true line of sight, $\underline{r}_{LOS}$, remains unchanged. If, however, $\underline{r}_{LOS}$ has an inertial angular velocity, the missile is not on a collision course with the target. The guidance block's purpose is to generate a set of control commands that will drive the missile to the target.

Various complexities of guidance laws exist, but the most common and easiest to use is proportional navigation. Although this guidance

law is not optimal for most engagements, other developed guidance schemes are too complex for on-line implementation, or approximate proportional navigation in some form (Ref 11,12). In an ideal model, the proportional navigation rule commands a missile acceleration* proportional to the closing velocity times the inertial angular velocity of the true line of sight. The three dimensional scalar equations expressed in vector notation are: (Ref 11:13)

$$\underline{A}_c = n(\underline{W}_L \times \underline{V}_C) \tag{16}$$

where $\underline{W}_L$ = inertial angular velocity of $\underline{r}_{LOS}$ (rad/sec)

$\underline{V}_C$ = closing velocity of the missile (ft/sec)

n = proportional navigation constant

$\underline{A}_c$ = missile acceleration required to null angular motion of the line of sight vector (ft/sec^2)

The proportionality constant, n, is chosen by the missile designer and typically ranges between three and five (Ref 11:18). The closing velocity, V_C, is the line of sight velocity of the missile relative to the target. In practice, the closing velocity is either derived from the seeker or its magnitude is estimated before launch and set as a constant. The missile in this study uses a noise corrupted measurement of the closing velocity.

The guidance block does not have the angular velocity of the true line of sight at its disposal. Instead, a noise corrupted measurement of $\underline{W}_L$ is available. Therefore, a first order lag

* Lateral acceleration is equal to the lift generated by the missile flight control surfaces divided by the missile mass.

pre-filter is used to smooth out the measurements. In addition, the acceleration required by this rule must be perpendicular to the line of sight. Yet the missile produces accelerations through lifting forces perpendicular to the missile centerline. Since the missile centerline does not usually coincide with the line of sight, the missile produced acceleration is not colinear with the required acceleration. A correction factor must be used to modify the produced acceleration. In this way, the component of missile lateral acceleration that is perpendicular to the line of sight will equal the acceleration required by the proportional navigation law. (Ref 11:13-14). The correction factor, although different for different trajectories, is relatively constant throughout one trajectory. Therefore, many missile designs incorporate the correction into n by increasing its value. Proportional navigation laws using this type of correction have n ranging from 3 to 10 (Ref 13:7). If a larger range for n is used as compensation, then the two guidance equations that describe the guidance block outputs (which assume a symmetrical guidance block) are:

$$A_{C_2} = \frac{nW_{S_3}V_C}{s\tau_2 + 1} \tag{17}$$

$$A_{C_3} = \frac{-nW_{S_2}V_C}{s\tau_2 + 1} \tag{18}$$

where A_{C_2} = commanded acceleration along $\underline{b}_2$ axis (ft/sec^2)

A_{C_3} = commanded acceleration along $\underline{b}_3$ axis (ft/sec^2)

n = proportional navigation constant

s = laplace transform "s"

τ_2 = prefilter time constant (sec)

Equations (17) and (18) are used in the missile truth model to describe the missile guidance block.

Autopilot/Dynamics Block

Commanded accelerations, $\underline{A}_{C_2}$ and $\underline{A}_{C_3}$, are processed by the autopilot and airframe dynamics to develop corresponding actual lateral accelerations $\underline{A}_{L2}$ and $\underline{A}_{L3}$. In actual missiles, these produced accelerations are not equal to the commanded accelerations due to time lags, design errors, and environmental disturbances. The autopilot's purpose is to manipulate the missile's flight control surfaces such that the produced accelerations equal the commanded accelerations as quickly and as accurately as possible. The missile in this study uses an adaptive autopilot (one that produces uniform response over varying flight conditions) to accomplish this goal.

To develop the equations of motion for a missile, certain assumptions must be made about the missile's airframe. First of all, the missile is assumed to have no inertial angular velocity along its roll axis. This assumption simplifies the set of dynamics equations for missile motion. Second, the airframe is assumed to be shaped like a cruciform (see Figure 9), which decouples airframe dynamics into two identical sets of equations - one set for the missile's pitch axis and one set for the missile's yaw axis. Since most missile boosters have a powerful, but short, burn time, a constant mass, non-thrusting missile is the third assumption. Finally, small angle approximations are assumed to be valid for angle of attack.

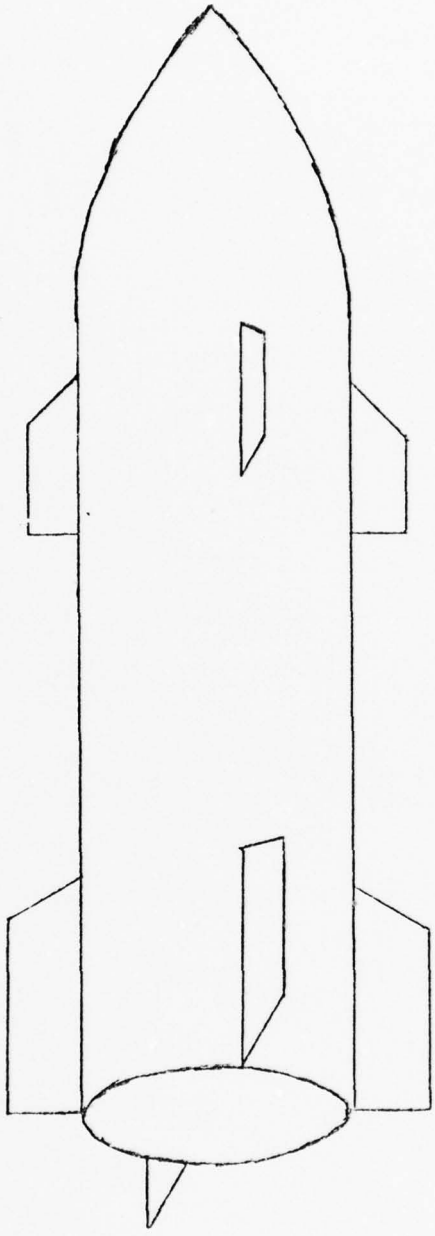


Fig. 9. Symmetrical Cruciform Missile

Under these assumptions, the four equations which describe the dynamics of the missile pitch plane are (Ref 1:35; 6:14; 5:20-21; 10: Chap. 8, p.3):

$$A_{L2}(t) = -V_m\{A_3(t) - Q_3(t)\} \tag{19}$$

$$\dot{Q}_3(t) = m_q Q_3(t) + m_\alpha A_3(t) + m_\delta \Delta_3(t) \tag{20}$$

$$\dot{A}_3(t) = Q_3(t) - l_\alpha A_3(t) - l_\delta \Delta_3(t) \tag{21}$$

$$\dot{\Delta}_3(t) = -\lambda \Delta_3(t) + \lambda U_3(t) \tag{22}$$

where A_{L2} = missile produced acceleration in the $\underline{b}_2$ direction (ft/sec^2)

V_m = missile velocity assumed to be in the $\underline{b}_1$ direction (ft/sec)

$A_3(t)$ = missile angle of attack, rotation in the $\underline{b}_3$ direction, (rad)

$Q_3(t)$ = missile pitch rate in the $\underline{b}_3$ direction (rad/sec)

$\Delta_3(t)$ = control surface deflection, rotation in the $\underline{b}_3$ direction (rad)

$U_3(t)$ = control command, rotation in the $\underline{b}_3$ direction (rad)

$-\lambda$ = actuator response pole (sec^{-1})

$m_q, m_\alpha, m_\delta,$

l_α, l_δ = missile stability derivatives (sec^{-1})

If $Q_2(t)$, $A_2(t)$, $\Delta_2(t)$, and $U_2(t)$ are defined along the $-\underline{b}_2$ axis, vector relationships for the yaw plane are identical to the pitch plane. The four equations for the missile yaw plane are

$$A_{L3} = -V_m\{A_2(t) - Q_2(t)\} \tag{23}$$

$$\dot{Q}_2(t) = m_q\, Q_2(t) + m_\alpha\, A_2(t) + m_\delta\, \Delta_2(t) \tag{24}$$

$$\dot{A}_2(t) = Q_2(t) - l_\alpha\, A_2(t) - l_\delta\, \Delta_2(t) \tag{25}$$

$$\dot{\Delta}_2(t) = -\lambda\, \Delta_2(t) + \lambda\, U_2(t) \tag{26}$$

where A_{L3} = missile produced acceleration in the $\underline{b}_3$ direction (ft/sec)

$Q_2(t)$ = missile yaw rate in the $-\underline{b}_2$ direction (rad/sec)

$A_2(t)$ = missile angle of attack, rotation in the $-\underline{b}_2$ direction (rad)

$\Delta_2(t)$ = control surface deflection, rotation in the $-b_2$ direction (rad)

$U_2(t)$ = control surface command, rotation in the $-b_2$ direction (rad)

The control commands, $U_2(t)$ and $U_3(t)$, are modeled as a function of commanded accelerations, pitch rate, and produced accelerations:

$$U_3(t) = K_\delta\, A_{c2}(t) - H_2\, A_{L2}(t) - h_1\, Q_3(t) \tag{27}$$

$$U_2(t) = K_\delta\, A_{c3}(t) - H_2\, A_{L3}(t) - h_1\, Q_2(t) \tag{28}$$

where K_δ = autopilot gain in $\underline{b}_1$ direction, yet to be defined (sec^2/ft)

H_2 = autopilot gain in $\underline{b}_1$ direction, yet to be defined (sec^2/ft)

h_1 = scalar adaptive autopilot gain, yet to be defined (sec)

By taking the derivative of equation (23), substituting in equations (24) and (25), and performing some algebraic manipulation, equations (19), (20), (21), (22), and (27) can be formed into:

$$\begin{bmatrix} \dot{A}_{L2}(t) \\ \dot{Q}_3(t) \\ \dot{\Delta}_3(t) \end{bmatrix} = \begin{bmatrix} -(l_\alpha + H_2 \lambda V_m l_\delta) & (V_m l_\alpha - h_1 \lambda V_m l_\delta) & -(\lambda V_m l_\delta) \\ (m_\alpha / V_m l_\alpha) & m_q & (m_q - (m_\alpha l_\delta / l_\alpha)) \\ -H_2 \lambda & -h_1 \lambda & -\lambda \end{bmatrix} \begin{bmatrix} A_{L2}(t) \\ Q_3(t) \\ \Delta_3(t) \end{bmatrix} + \begin{bmatrix} K_\delta \lambda V_m l_\delta \\ 0 \\ \lambda K_\delta \end{bmatrix} A_{c2} \tag{29}$$

Similarly, equations (23), (24), (25), (26), and (28) can be formed into:

$$\begin{bmatrix} \dot{A}_{L3}(t) \\ \dot{Q}_2(t) \\ \dot{\Delta}_2(t) \end{bmatrix} = \begin{bmatrix} -(l_\alpha + H_2 \lambda V_m l_\delta) & (V_m l_\alpha - h_1 \lambda V_m l_\delta) & -(\lambda V_m l_\delta) \\ (m_\alpha / V_m l_\alpha) & m_q & (m_q - (m_\alpha l_\delta / l_\alpha)) \\ -H_2 \lambda & -h_1 \lambda & -\lambda \end{bmatrix} \begin{bmatrix} A_{L3}(t) \\ Q_2(t) \\ \Delta_2(t) \end{bmatrix} + \begin{bmatrix} K_\delta \lambda V_m l_\delta \\ 0 \\ \lambda K_\delta \end{bmatrix} A_{c3} \tag{30}$$

In an adaptive autopilot, the autopilot gains are varied to maintain a specific missile response. If actuator dynamics are much quicker than airframe dynamics, actuator dynamics can be neglected. The adaptive controller is designed so that the missile response is essentially second order of the form:

$$\frac{A_{L2}}{A_{c2}} = \frac{A_{L3}}{A_{c3}} = \frac{\omega_n^2}{s^2 + 2\zeta \omega_n s + \omega_n^2} \tag{31}$$

where ω_n = natural frequency (rad/sec)

ζ = damping ratio

To obtain the second order response, h_1, H_2, and K_δ must equal (Ref 5:26-27)

$$h_1 = \frac{-l_\alpha m_\alpha - \frac{m_\delta}{l_\delta} l_\alpha + \omega_n^2 + (2\zeta\omega_n + m_q)\left(\frac{m_q}{l_\delta} + m_q\right)}{m_\delta m_\alpha - \frac{m_\delta}{l_\delta} l_\alpha + \omega_n^2 + (m_q + 2\zeta\omega_n)(l_\delta m_\alpha - m_\delta l_\alpha)} \tag{32}$$

$$H_2 = \frac{l_\delta m_\alpha (l_\alpha - 2\zeta\omega_n - m_q) + m_\delta l_\alpha (2\zeta\omega_n - l_\alpha) - \omega_n^2 - m_\alpha}{V_m l_\delta m_\delta \left(m_\alpha - \frac{m_\delta}{l_\delta} l_\alpha + \omega_n^2\right) + (m_q + 2\zeta\omega_n)(l_\delta m_\alpha - m_\delta l_\alpha)} \tag{33}$$

$$K_\delta = \frac{1}{V_m}\left(h_1 - \frac{m_\alpha + l_\alpha m_\delta}{l_\alpha m_\delta - m_\alpha l_\delta}\right) + H_2 \tag{34}$$

The stability derivatives are determined by a cubic fit to actual missile data provided by the Air Force Avionics Laboratory. A specific second order response is obtained when ω_n and ζ are specified. For this study, ω_n = 7.07 radians per second, and ζ = .707: realistic values that result in minimum settling time (Ref 10:3).

The inertial angular velocity of the missile, $\underline{W}_b$ is equal to the sum of the pitch and yaw inertial angular velocities, since roll is assumed to be zero:

$$\underline{W}_b = \underline{Q}_2 + \underline{Q}_3 \tag{35}$$

$$\underline{W}_b = \begin{bmatrix} \omega_{bx} \\ \omega_{by} \\ \omega_{bz} \end{bmatrix} \tag{36}$$

where ω_{bx} = missile inertial angular velocity in the $\underline{i}_1$ direction

ω_{by} = missile inertial angular velocity in the $\underline{i}_2$ direction

ω_{bz} = missile inertial angular velocity in the $\underline{i}_3$ direction

The orientation of the missile body frame in terms of the inertial frame is defined to be:

$$\underline{b}_1 = C_i^b [1\ 0\ 0]^T \tag{37}$$

$$\underline{b}_2 = C_i^b [0\ 1\ 0]^T \tag{38}$$

$$\underline{b}_3 = C_i^b [0\ 0\ 1]^T \tag{39}$$

where C_i^b is the direction cosine matrix from i to b frame.

Similar to equation (13), the dynamics of the direction cosine matrix are:

$$pC_i^b = -C_i^b W_{ib}^{ik} \tag{40}$$

where p = first derivative with respect to time

$$W_{ib}^{ik} = \begin{bmatrix} 0 & -\omega_{bz} & \omega_{by} \\ \omega_{bz} & 0 & -\omega_{bx} \\ -\omega_{by} & \omega_{bx} & 0 \end{bmatrix}$$

Integration of equation (40) specifies the orientation of the b frame. The linear acceleration of the missile is made up of three components:

1. $\underline{A}_{L2}$ - the produced acceleration in the $\underline{b}_2$ direction (ft/sec²)
2. $\underline{A}_{L3}$ - the produced acceleration in the $\underline{b}_3$ direction (ft/sec²)
3. $\underline{A}_D$ - the acceleration due to drag opposite the velocity's direction (ft/sec²)

The first two accelerations have been specified. The third must still be defined.

The acceleration due to drag is dependent upon the magnitude of missile velocity as well as the magnitude of produced lateral accelerations (Ref 1:38-39)

$$A_D = \tfrac{1}{2} \frac{1}{\left(\frac{m}{s}\right)} \rho \; c_D \; V_m^2 \tag{41}$$

where ρ = air density (slug/ft^3)

(m/s) = missile mass to reference area ratio (slug/ft^2)

c_D = coefficient of drag.

The coefficient of drag is approximated by

$$c_D = 2\left(\frac{MACH}{V_m}\right)^{\frac{1}{2}} + \frac{2A_L}{c_{n\alpha} \; \rho \; V_m^2} \; (m/s) \tag{42}$$

where MACH = speed of sound (ft/sec)

$c_{n\alpha}$ = stability derivative

A_L = total produced acceleration (ft/sec^2)

This totally specifies the linear acceleration of the missile.

The linear acceleration of the missile is integrated to provide linear velocity and position information. Along with the orientation of the missile's body frame and seeker frame, the missile is totally modelled.

Target Model

The target model is composed of two parts - the tracker and the target's kinematics. The tracker provides line of sight measurements every 0.02 seconds, as required by each extended Kalman filter. The

target's kinematics produces various maneuvers which in turn evoke a range of missile responses, which tests the filter's ability to provide accurate state estimates under different scenarios.

The tracker part of the target model resembles a typical radar used by fighter aircraft. It has the capability of measuring line of sight orientation as a function of two angles. The four other available measurements are: line of sight inertial angular velocity in two components, missile range, and range rate. Each measurement is simulated by corrupting the truth model's true value of these quantities with an appropriate strength random noise. It is assumed that measurement noises can be adequately modeled by a first order Gauss-Markov process combined with a constant strength white Gaussian noise (Ref 5:27-31). It is also assumed that the tracker part is symmetrical, resulting in identical noise statistics for both angle measurements, and identical noise statistics for both angular velocity measurements. The noise statistics are obtained from Lutter, the Air Force Avionics Laboratory, and Northrop; and are presented in Table II (Ref 5:3).

The target's kinematics part of the target model is a simple set of equations for linear acceleration. Since each extended Kalman filter will consider only the inertial motion of the missile, realistic modeling of target kinematics is not crucial. What is necessary is a set of realistic missile responses that will test each extended Kalman filter over a wide range of scenarios.

The linear acceleration equations are:

$$\underline{A}_{T1} = -\underline{K}_2 \, \omega_T^2 \cos \omega_T t_i \tag{43}$$

$$\underline{A}_{T2} = -\underline{K}_4 \, \omega_T^2 \sin \omega_T t_i \tag{44}$$

TABLE II

Sigmas and Time Constants for Measurement Noise

Measure	Sigma	Time Constant
RANGE		
Uncorrelated	11.7 ft	- - -
Correlated	10.0 ft	0.5 sec
RANGE RATE		
Uncorrelated	7.0 ft/sec	- - -
Correlated	4.242 ft/sec	1.0 sec
LINE OF SIGHT Angular Velocity (Both components)		
Uncorrelated	0.001745 rad/sec	- - -
Correlated	0.0008726 rad/sec	10.0 sec
LINE OF SIGHT Angular Orientation (Both angles)		
Uncorrelated	0.00126 rad	- - -
Correlated	0.00168 rad	0.5 sec

$$\underline{A}_{T3} = -\underline{K}_6 \ \omega_T^2 \ \sin(\omega_T t_i - .76) \tag{45}$$

where $\underline{K}_2$, $\underline{K}_4$, $\underline{K}_6$ = linear constants in the $\underline{i}_1$, $\underline{i}_2$, and $\underline{i}_3$ directions respectively (ft)

ω_T = scalar constant for angular rate (rad/sec)

$\underline{A}_{T1}$, $\underline{A}_{T2}$, $\underline{A}_{T3}$ = target linear accelerations in the $\underline{i}_1$, $\underline{i}_2$, and $\underline{i}_3$ directions respectively (ft/sec^2)

t_i = time (sec)

The phase term, (.76), of equation (45) insures that the target's motion is not planar. Appropriate integration of equations (43) through (45) produces target velocity and position. Initial velocity conditions are:

$$\underline{V}_{T1} = \underline{K}_1 \tag{46}$$

$$\underline{V}_{T2} = \underline{K}_3 + \underline{K}_4 \, \omega_T \tag{47}$$

$$\underline{V}_{T3} = \underline{K}_5 + \underline{K}_6 \, \omega_T \sin (.76) \tag{48}$$

where $\underline{K}_1$, $\underline{K}_3$, $\underline{K}_5$ = linear velocity constants along the $\underline{i}_1$, $\underline{i}_2$, and $\underline{i}_3$ directions respectively (ft/sec)

V_{T1}, V_{T2}, V_{T3} = target linear velocities along the $\underline{i}_1$, $\underline{i}_2$, and $\underline{i}_3$ directions respectively (ft/sec)

The initial target position is the origin of the i frame. A set of constants, K_1 through K_6, as well as an ω_T, determine a specific target trajectory and are referred to as a K set. Four trajectories are available to test each extended Kalman filter. The K set parameters are listed in Table III. Trajectories are shown in two dimensions in Figures 10-A through 10-D.

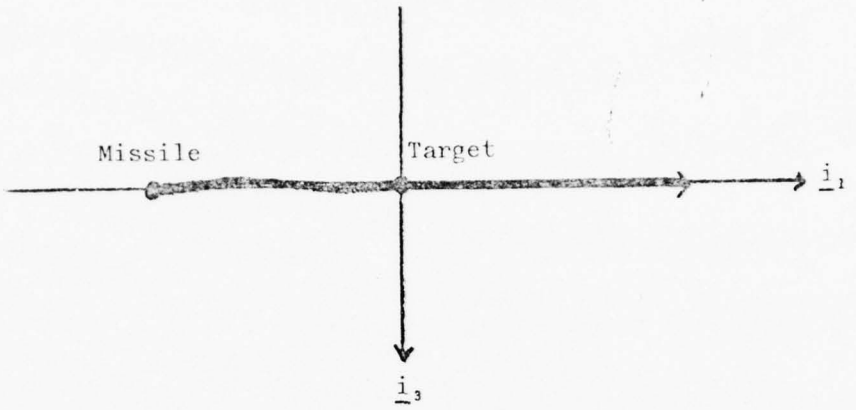
Before the trajectories are numerically compared a key concept must be presented. The missile model developed in this chapter is a full six degree of freedom model. It accurately portrays the roll that is induced by conservation of momentum when a missile performs a turn. To demonstrate this effect, suppose that a missile turns with respect to the inertial frame as shown in Figure 11. Since the missile is flying in free space, the b frame (missile) is not constrained to any orientation with respect to the i frame, i.e., the vertical tail fin is not constrained to remain vertical as the missile turns. If the

TABLE III

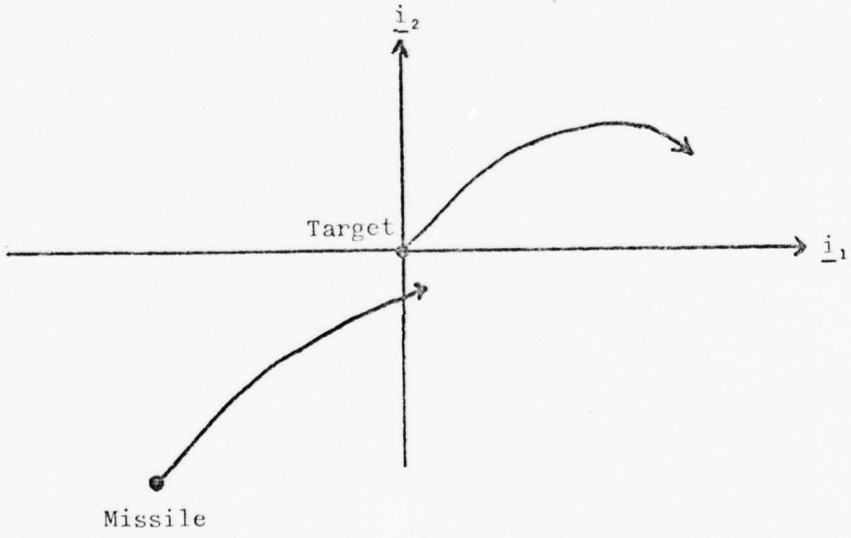
K Set Parameters

	K Set 1	K Set 2	K Set 3	K Set 4
K_1	100	0	850	500
K_2	-2000	0	200	2864.51
K_3	200	700	100	800
K_4	1000	500	200	0
K_5	0	750	250	0
K_6	0	-900	-590	0
ω	0.4	0.4	0.6	0.4

angular velocity vector of the turn, $\underline{T}$, is broken into its b frame components, $\underline{T}_1$ and $\underline{T}_5$, then $\underline{T}_1$ is along the $\underline{b}_1$ axis, and $\underline{T}_5$ is in the ($\underline{b}_1$, $\underline{i}_2$) plane (see Figure 12). $\underline{T}_1$ causes the b frame to rotate with respect to inertial space, i.e. the missile rolls. Thus, $\underline{T}_5$ appears to rotate around the missile to an observer on the missile (theorem of Coriolis), yet always lies in the ($\underline{b}_1$, $\underline{i}_2$) plane. This vector, $\underline{T}_5$, is generated by the missile when the pitch and yaw inertial angular velocities of the missile are appropriately periodic and out of phase. Thus, what dynamically appears to be a rotating angular velocity vector to the missile is an inertial turn as depicted in Figure 11. Because of the conservation of momentum, the missile rolls as it turns (Ref 14:113-118). These effects are modelled in the truth model to insure that this roll, which is not modeled by the filters, does not produce adverse state estimation errors.

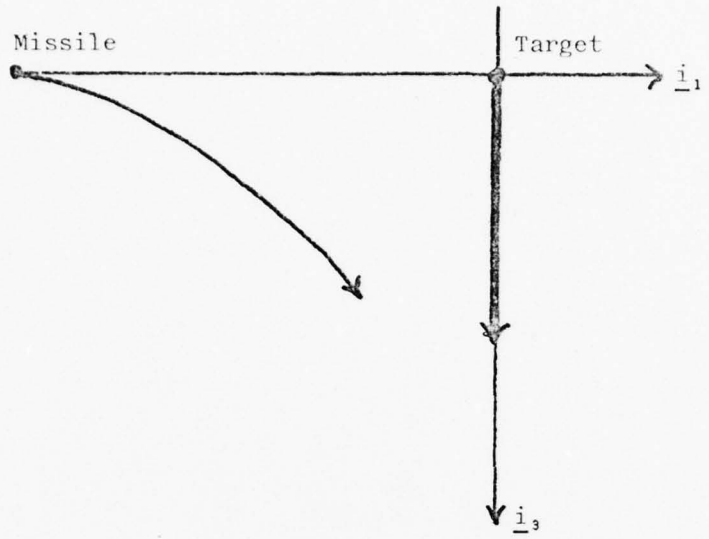


Top View

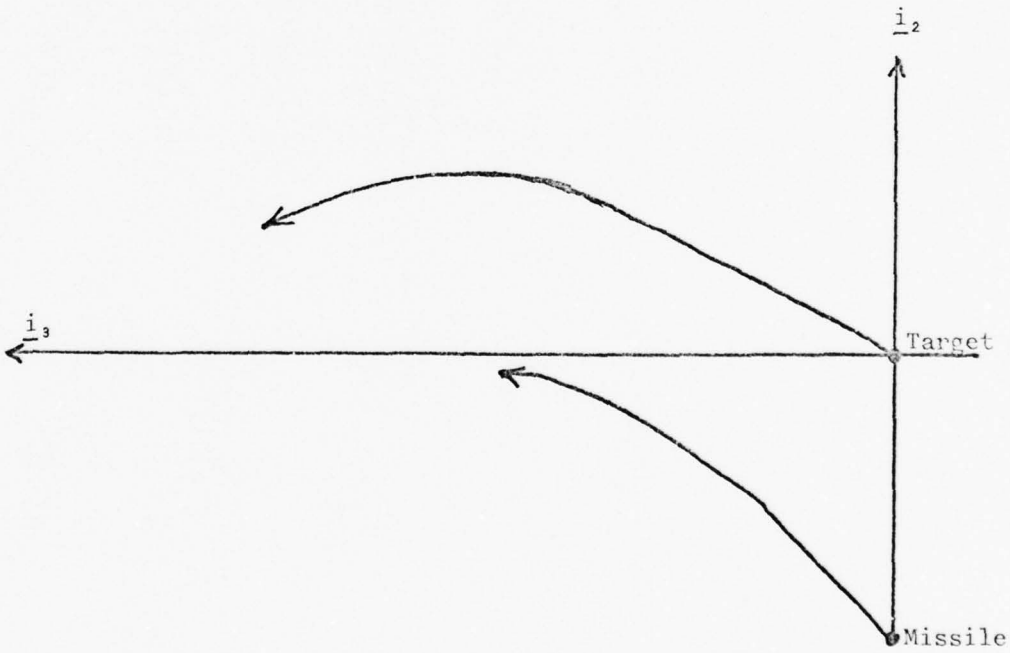


Side View

Fig. 10-A. K Set One Trajectory

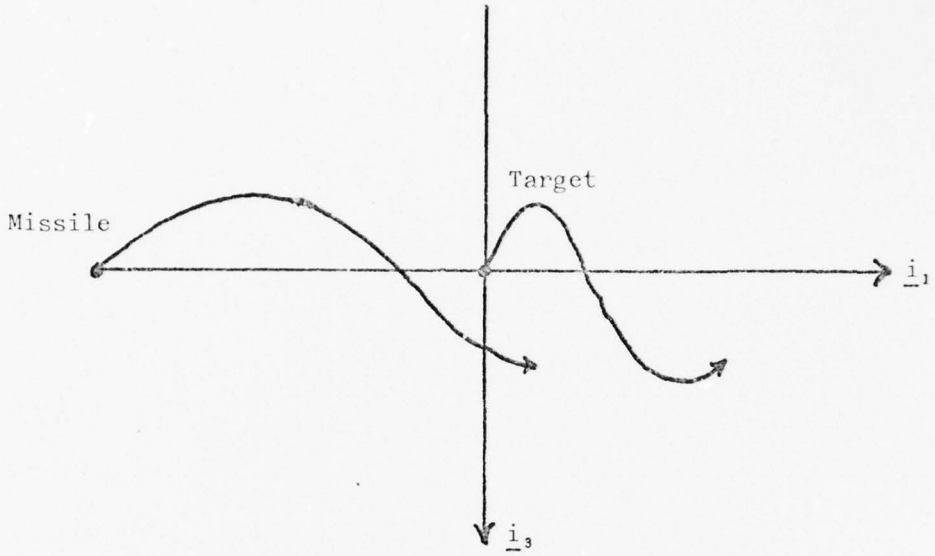


Top View

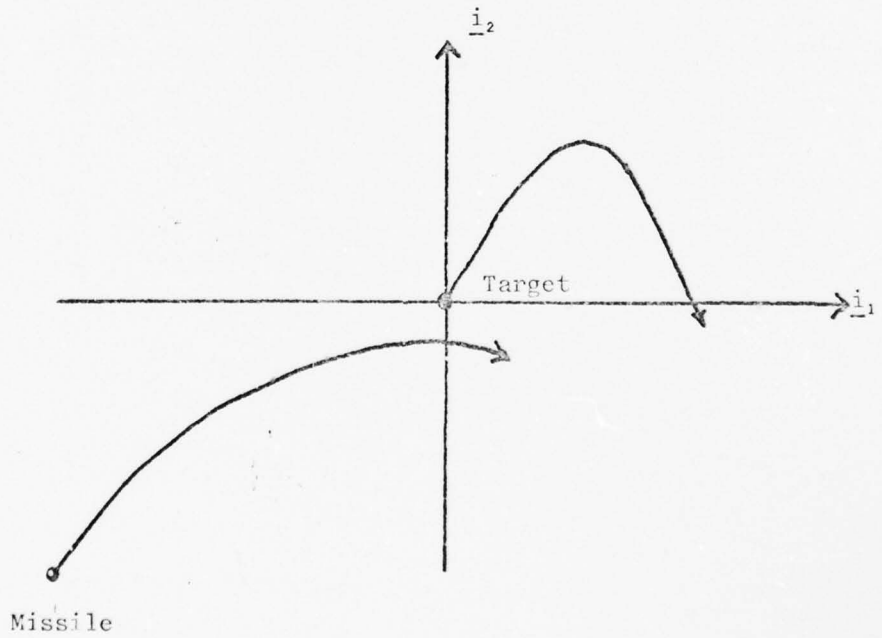


Front View

Fig. 10-B. K Set Two Trajectory

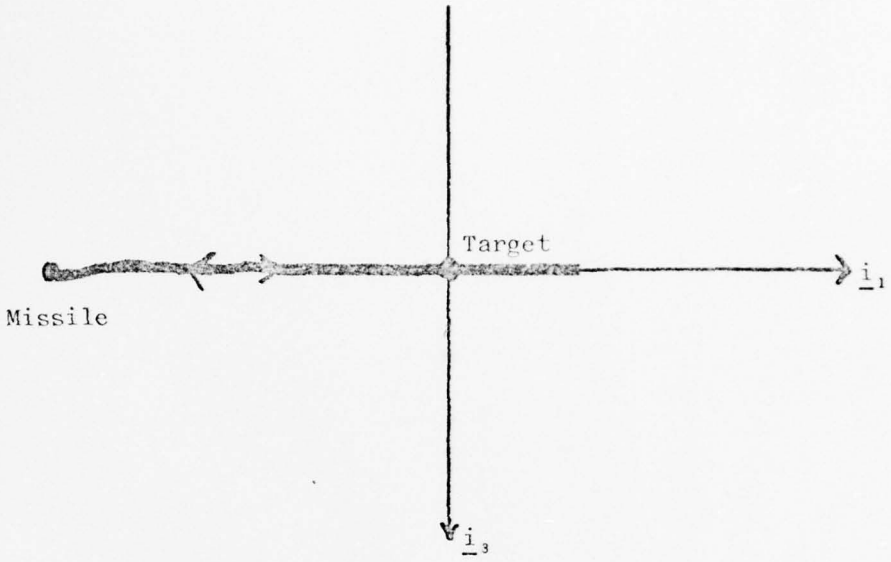


Top View

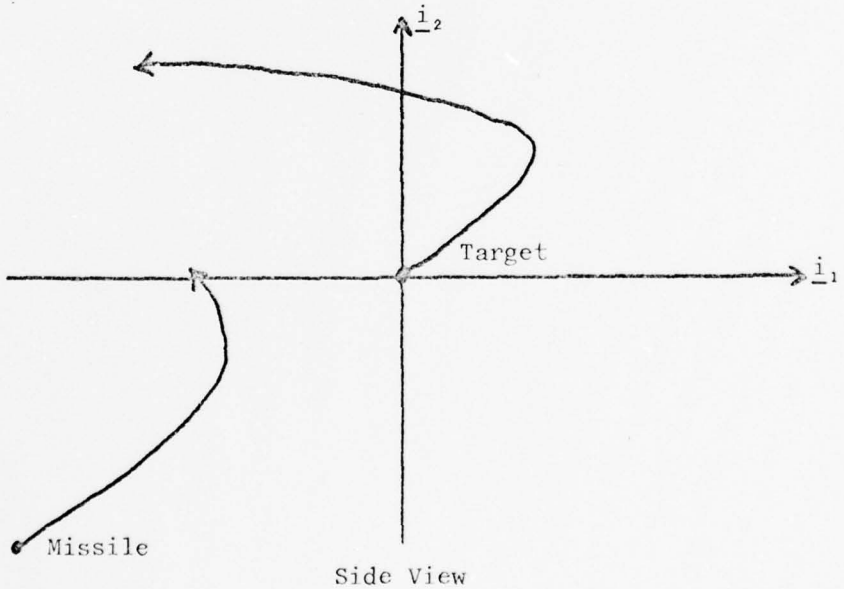


Side View

Fig. 10-C. K Set Three Trajectory



Top View



Side View

Fig. 10-D. K Set Four Trajectory

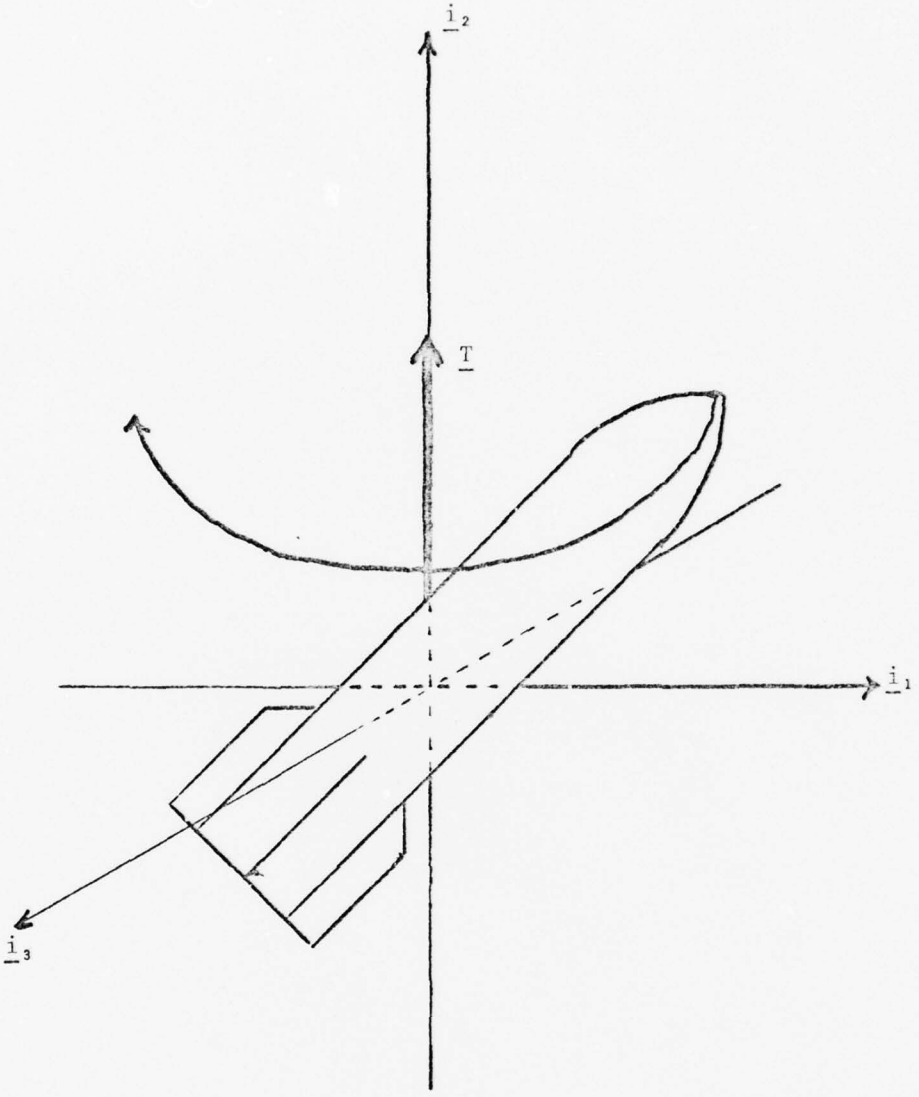


Fig. 11. A Missile's Turn

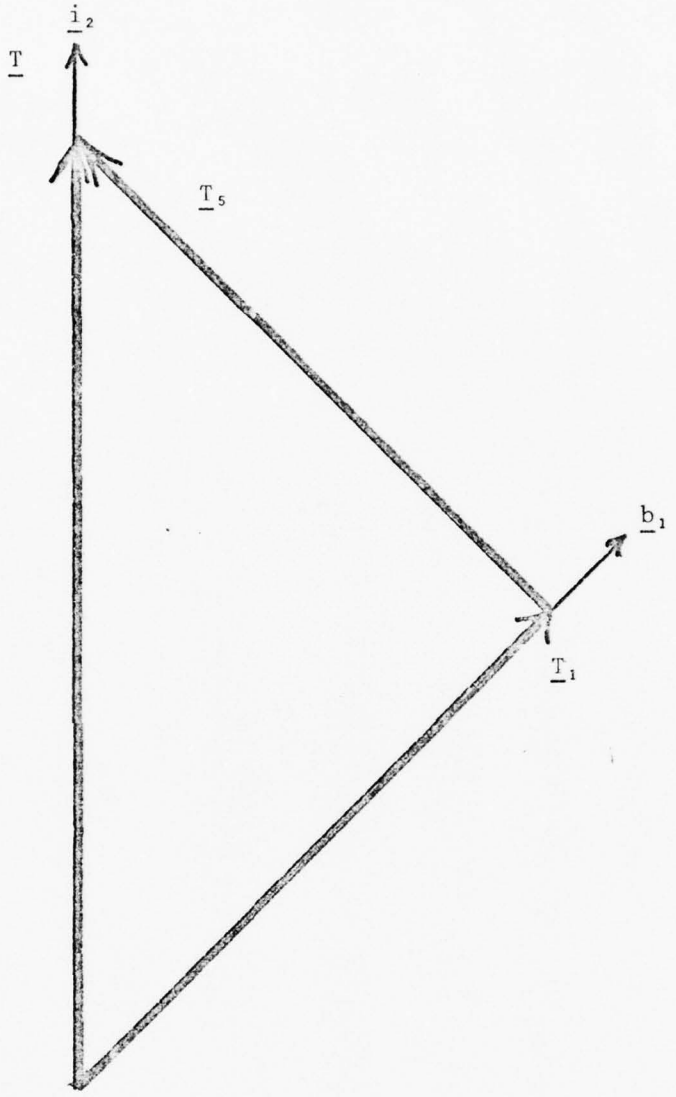


Fig. 12. B Frame Components of Turn
For an Arbitrary Time Instant

The amount of induced missile roll is one of several factors that distinguish each K set. Other factors include missile lateral acceleration, missile lateral acceleration rate, and line of sight movement. The line of sight movement is defined to be that angle which the line of sight vector, $\underline{r}_{LOS}$, makes with the ($\underline{i}_1$, $\underline{i}_2$) plane. (This definition is chosen since the line of sight is contained by the ($\underline{i}_1$, $\underline{i}_2$) plane at the start of each trajectory.) This angle, along with the missile roll, gives some measure as to how close the scenario resembles a scenario confined to a single plane. The four trajectories are compared in Table IV.

No other trajectories are used for testing. It is understood that these four trajectories do not test for all possible factors that may affect the extended Kalman filters, such as a vertical line of sight. K set four approaches a vertical line of sight to within .04 radians. In Cusumano and DePonte's filter (Chapter III), a vertical line of sight produces an undefined equation if a change of states (V_{mx} to V_{my}) and state equations is not accomplished. The filter accomplishes this change automatically. In the 11 state filter (Chapter IV), the restriction placed on the $\underline{l}_2$ axis ($\underline{l}_2$ must lie in the ($\underline{i}_1$, $\underline{i}_3$) plane) does not uniquely define the l frame when the line of sight is vertical. However, it is felt that they cover enough factors to provide insights to filter performance. The computer program that implements both truth models is Subroutine Traj in Appendix D.

TABLE IV

Missile Response Comparisons of Trajectories

	K Set 1	K Set 2	K Set 3	K Set 4
Maximum Magnitude Pitch Acceleration (ft/sec^2)	610	270	720	770
Maximum Magnitude Yaw Acceleration (ft/sec^2)	110	384	420	100
Maximum Pitch Acceleration Rate ($ft/sec^2/sec$)	450	310	840	580
Maximum Yaw Acceleration Rate ($ft/sec^2/sec$)	40	180	420	110
Maximum Missile Roll (degrees)	0.8	30	27	1.5
Maximum Line of Sight Movement (degrees)	1.0	13	21	0.9
Dominant Quality	Approximates Two Dimensional	Low Acceleration	High Acceleration Rate	Cusumano & DePonte Trajectory

III. Extension of Two Dimensional Filter

Introduction

The research performed by Cusumano and DePonte shows that an extended Kalman filter, based upon a refined missile acceleration model, is an effective aid to a fire control system under two dimensional conditions (Ref 1). Their two dimensional filter uses eight states to provide real time estimates of range, range rate, azimuth angle, and missile acceleration. From these estimates, two dimensional pointing and tracking become more precise. However, the question remains as to the validity of the two dimensional, i.e. planar case, filter in a three dimensional world.

At first glance, it can be argued that a two dimensional filter should be valid under three dimensional conditions. The proportional navigation law employed by the missile attempts to null any inertial angular motion of the line of sight vector. Thus, the scenario should reduce to perturbations about a nominal plane, perhaps allowing the nominal plane to rotate appropriately. To test this hypothesis, three three-dimensional applications of the Cusumano and DePonte eight state, two dimensional, extended Kalman filter (hereafter, the 2D filter) are proposed. These three proposals are: a moving reference plane 2D filter; two fixed, 2D filters with four measurements; and two fixed, 2D filters with two measurements. It is recognized that other, perhaps better, proposals exist that are not considered.

Before the three proposals are presented, the assumptions and limitations of the 2D filter must be understood. The eight states of the 2D filter, using the notation developed by Cusumano and DePonte, are (Ref 1:43-72)

θ_T - line of sight angle, as seen by the target, in the XY plane

R - line of sight range in the XY plane

$\dot{R}$ - line of sight range rate in the XY plane

V^I_{mx} - X velocity of the missile

A_L - lateral acceleration of the missile in the XY plane

(These first five states are depicted for an arbitrary time instant in Figure 13.)

n - missile's proportional navigation constant

τ - time lag of filter's first order lag missile model

(m/s) - ratio of missile mass to effective surface area (for drag computations)

(These three parameters are hereafter referred to as states.)

The 2D filter uses measurements of θ_T, R, and $\dot{R}$. In the development of these eight states, Cusumano and DePonte assume that the filter's XY plane is inertially fixed and horizontal. All proposed three dimensional applications of the 2D filter violate this assumption to some degree, making them inherently less accurate than the two dimensional application.

First Proposal

In the first proposal, the 2D filter's XY plane is defined by the gravity vector and the line of sight vector. This relates θ_T to the elevation angle. However, the XY plane is no longer an inertial plane,

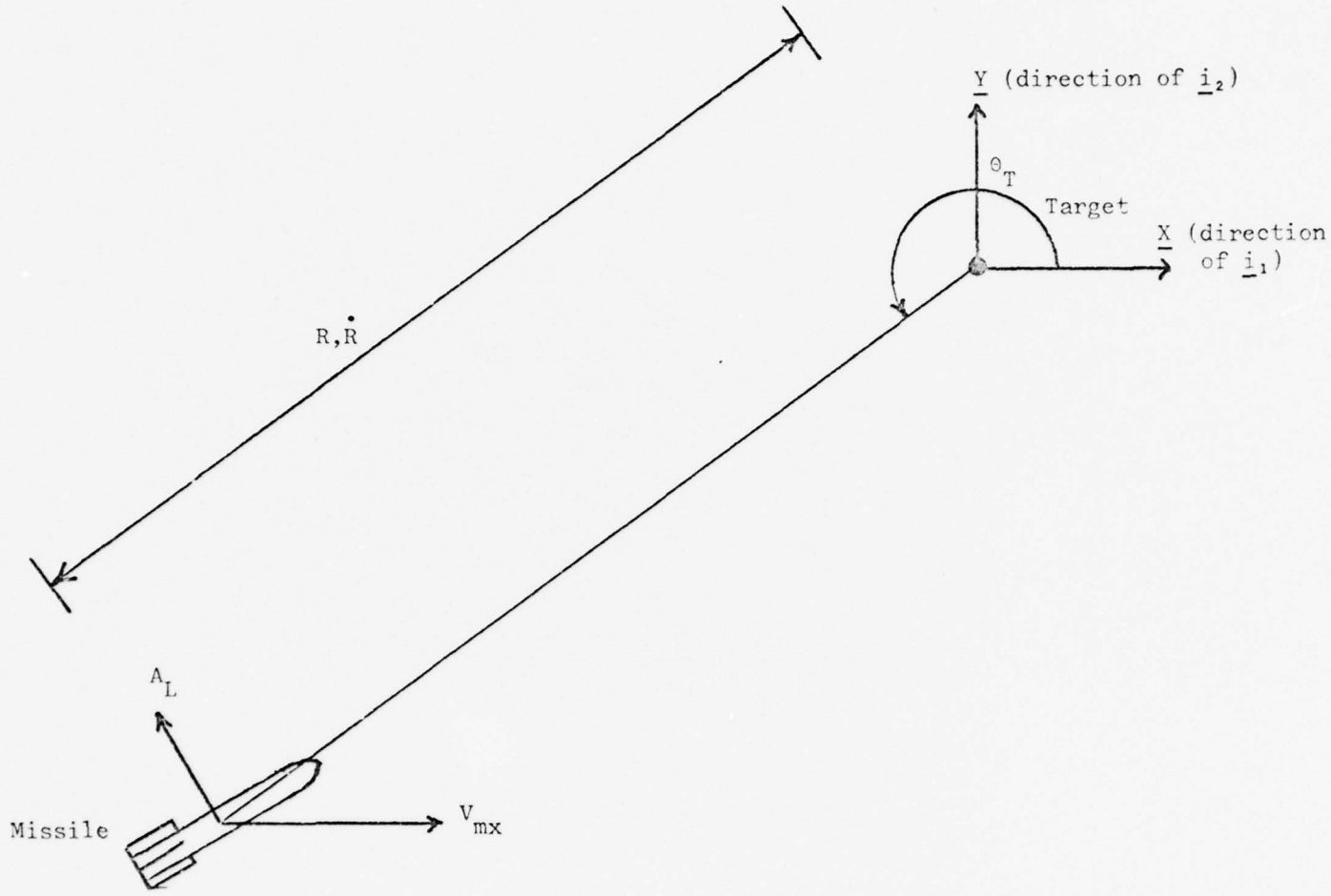


Fig. 13. Two Dimensional Pictorial Depiction of the First Five States of the 2D Filter

since the line of sight vector changes inertial orientation throughout the encounter (see Figure 14). In addition, the filter equations should be modified to account for gravity, since gravity effects may be significant. Unfortunately, no estimate of azimuth angle is available, so this application is not investigated.

Second Proposal

The second three dimensional application, which is similar to the third, is called the double filter. Two 2D filters are used - one whose XY plane is the inertial ($\underline{i}_1$, $\underline{i}_2$) plane (X 2D filter); the other whose XY plane is the inertial ($\underline{i}_2$, $\underline{i}_3$) plane (Z 2D filter) (see Figure 15). Each filter performs estimates on the planar projections of the 3-D scenario. Thus, the inertial orientation of the double filter's states remains fixed throughout the scenario. To avoid modification of established computer software, gravity effects are ignored. Since most K set trajectories induce missile accelerations greater than 10 g's, it is assumed that gravity errors will be small enough such that other error sources can be discerned. Had this method seemed more fruitful, a more proper accounting for gravity effects would have been made in the filter. The inertial orientation of the line of sight vector can be expressed as a function of the angle state from each 2D filter, Θ_{TX} and Θ_{TZ}. Therefore, the double filter is capable of providing estimates of the line of sight azimuth and elevation angles.

There is one drawback, however. The target radar's measurements of range and range rate are not direct measurements of either 2D filter's R and $\dot{R}$ states, since the line of sight is generally not

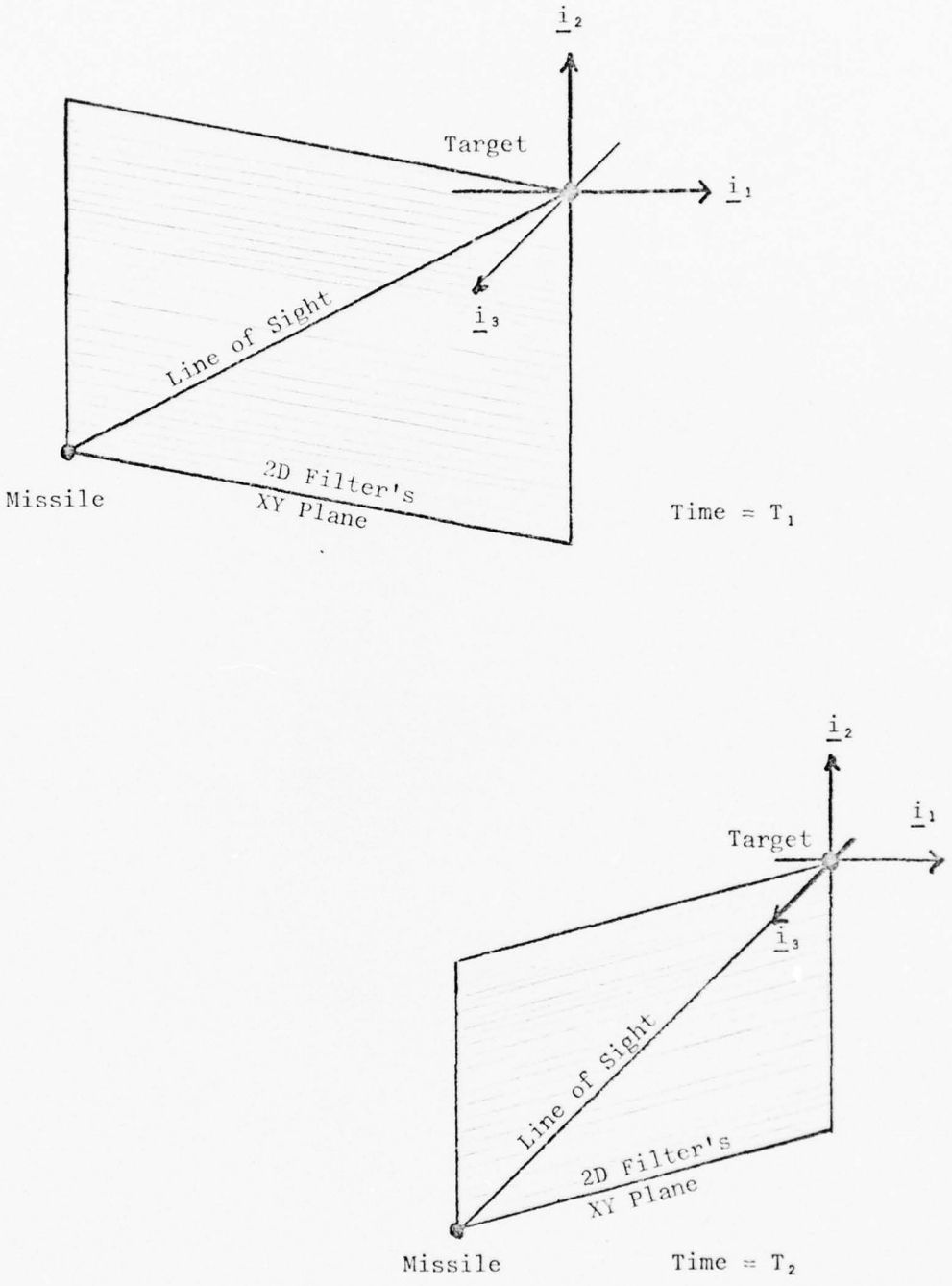


Fig. 14. 2D Filter's XY Plane Orientation at Two Time Instants for First Three Dimensional Application

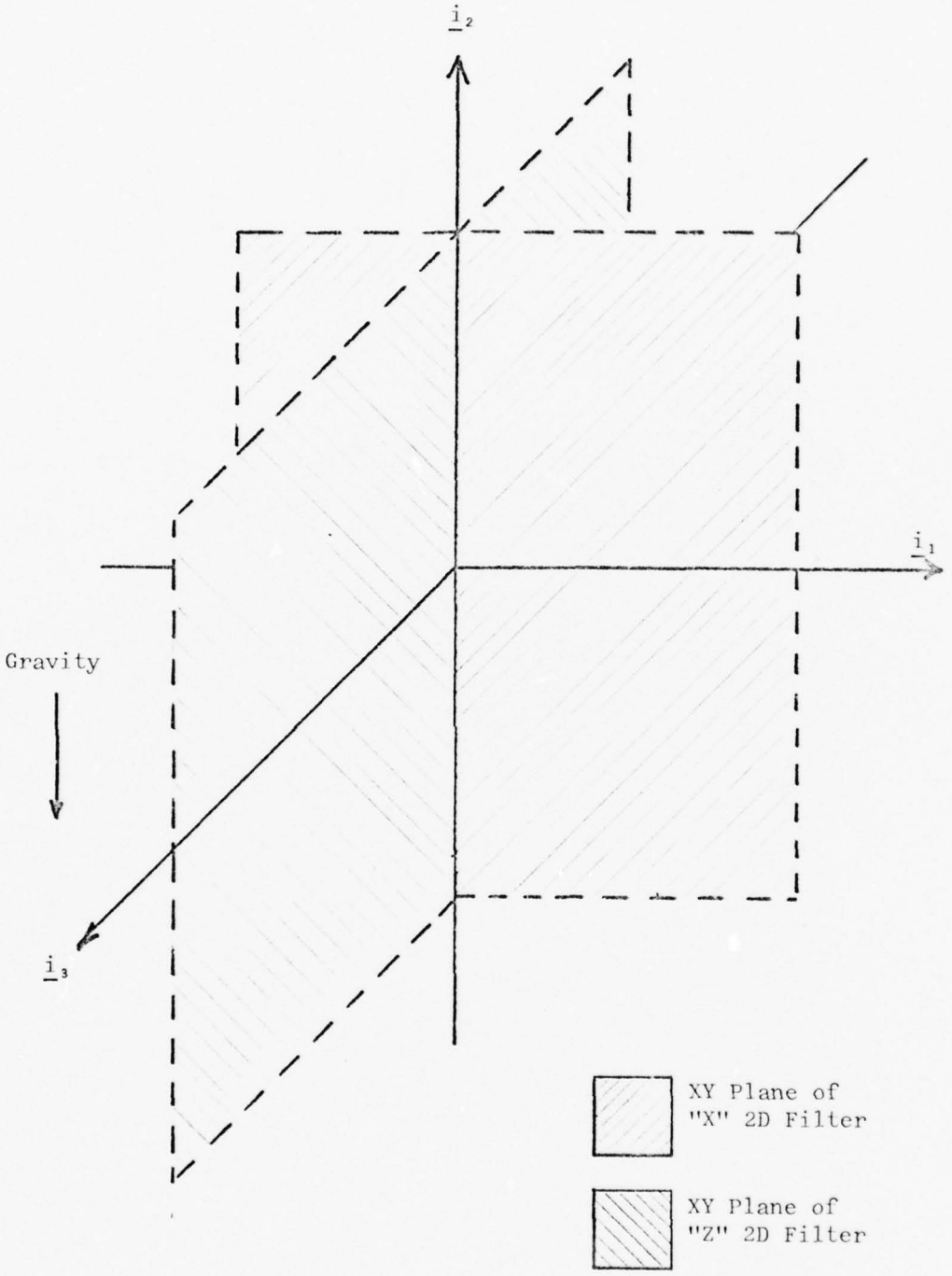


Fig. 15. Double Filter

coplanar to the 2D filter planes (see Figure 16). (The two angle states can be uniquely defined from radar azimuth and elevation angles, or the radar can be so constructed such that the radar angle measurements correspond directly to the filter's angle states.) Therefore, these measurements must be projected into the filter planes by an appropriate transformation. One transformation must be used to find the range and range rate projection into the X 2D filter plane; another transformation must be used to find the range and range rate projection into the Z 2D filter plane.

These transformations require knowledge of the inertial orientation of the line of sight vector, which requires the angle state from both 2D filters. This requirement couples the X and Z 2D filters. This weakly coupled system may yield adequate results, but observability problems and/or cross coupling of errors through the angle states are a concern. To avoid these potential problems, transformation are not based on the double filter's estimate of line of sight orientation. Instead, transformations are initially defined from measurements and held constant (or can be periodically redefined). Another alternative, which is the third application, is to avoid R and $\dot{R}$ measurements entirely.

In the simulation, the true values of θ_{TX} and θ_{TZ} are used to determine the three dimensional orientation of the line of sight vector, $\underline{r}_{LOS}$. (In practice, several measurements of these states can be averaged to determine the orientation of $\underline{r}_{LOS}$.) Next, $\underline{r}_{LOS}$ is projected into each 2D filter plane to determine the proper transformation constant for each 2D filter. The range and range rate measurements, multiplied by the transformation constant, yield the R and $\dot{R}$ states. The double filter is then initialized with the transformation constants and allowed to estimate the states.

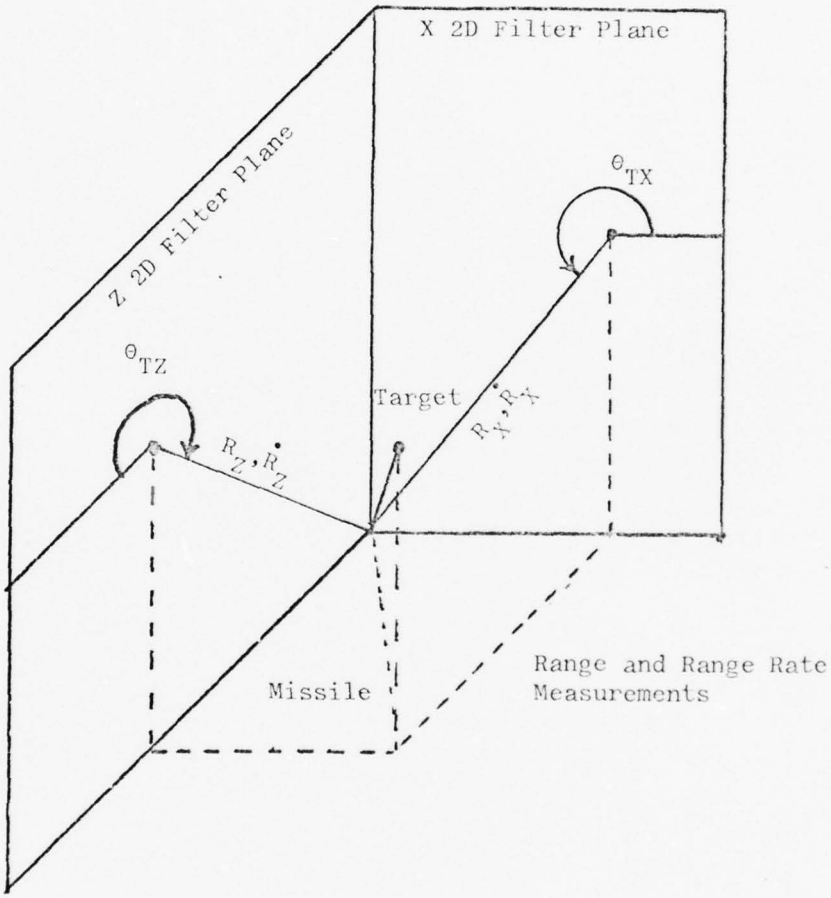


Fig. 16. Difference Between Filter States and Measurements for Double Filter

The double filter with four measurements is first tested with trajectory K set one, which is the closest trajectory to two dimensional motion. Filter states are initialized with zero error, and tuning parameters specified by Cusumano and DePonte for a two dimensional K set four trajectory are used (Ref 2:328-329). These tuning parameters are chosen as the best available. Extensive 2D filter testing is not accomplished to determine the best tuning parameters for each trajectory due to time limitations.

The line of sight vector is initially contained in the X 2D filter plane. This simplifies analysis to one 2D filter, since the transformation constant for the X 2D filter is one; the transformation constant for the Z 2D filter is zero; and the transformations are held constant throughout the test. (Normal implementation would initially orient the inertial coordinate frame such that both double filters would use identical transformation constants.) In addition, the X 2D filter's transformation constant is at its smallest sensitivity to transverse line of sight movement. Therefore, if the X 2D filter cannot perform adequately under these initial conditions, then the double filter is not feasible. The converse is not true, since the double filter is being tested under ideal conditions.

The results of this test (which are contained with all other results of this chapter in Appendix C) are compared to the results obtained by Cusumano and DePonte and show unacceptable filter performance (Ref 2:308-347). Half of the states, including two of the four states used for pointing and tracking (R and V_{mx}), have severe biases (see Figures 17, 18, and 19). Yet, the standard deviations of the filter state estimates are generally less than the filter's estimate

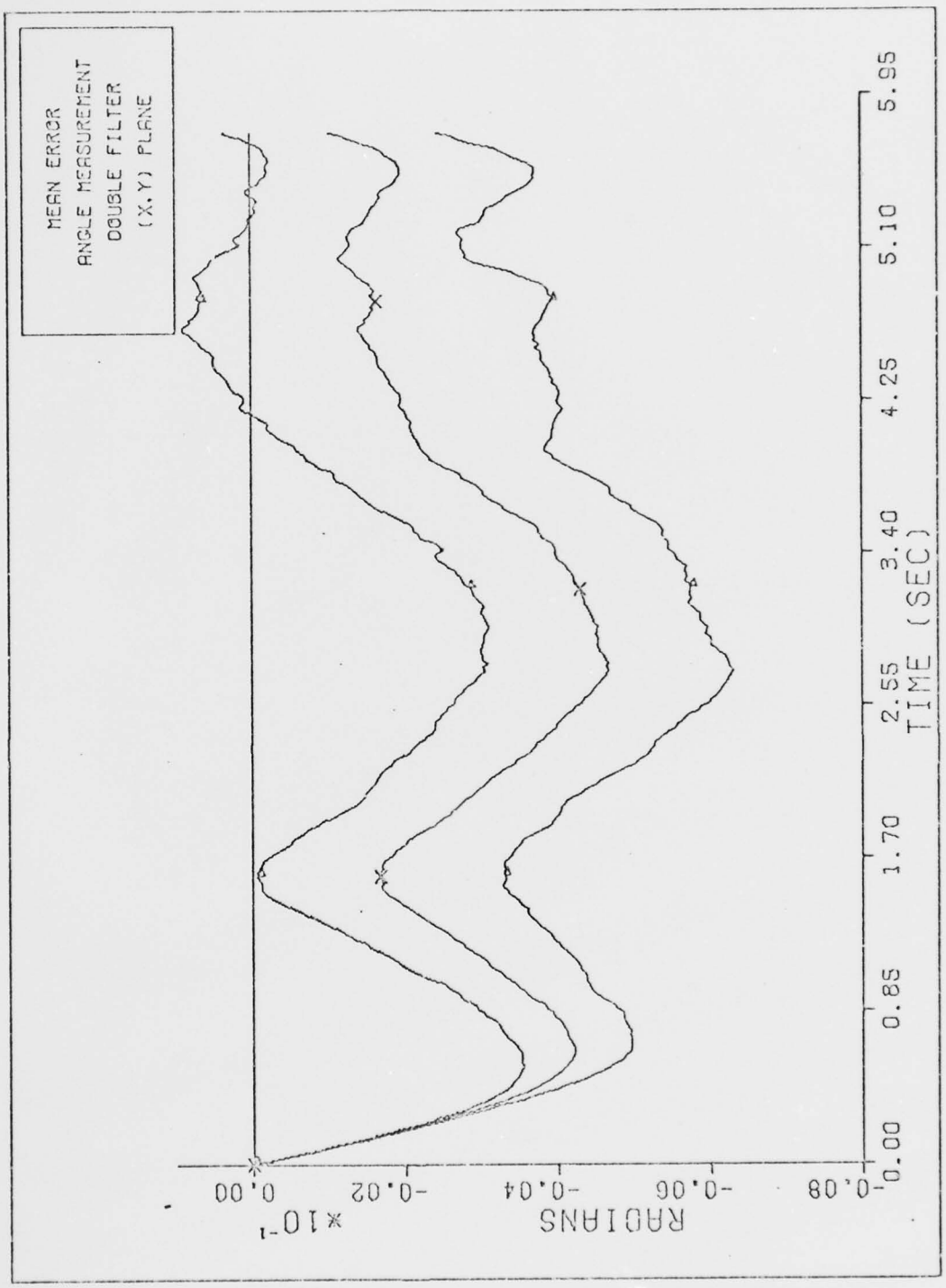


Fig. 17. ANGLE MEASUREMENT DOUBLE FILTER

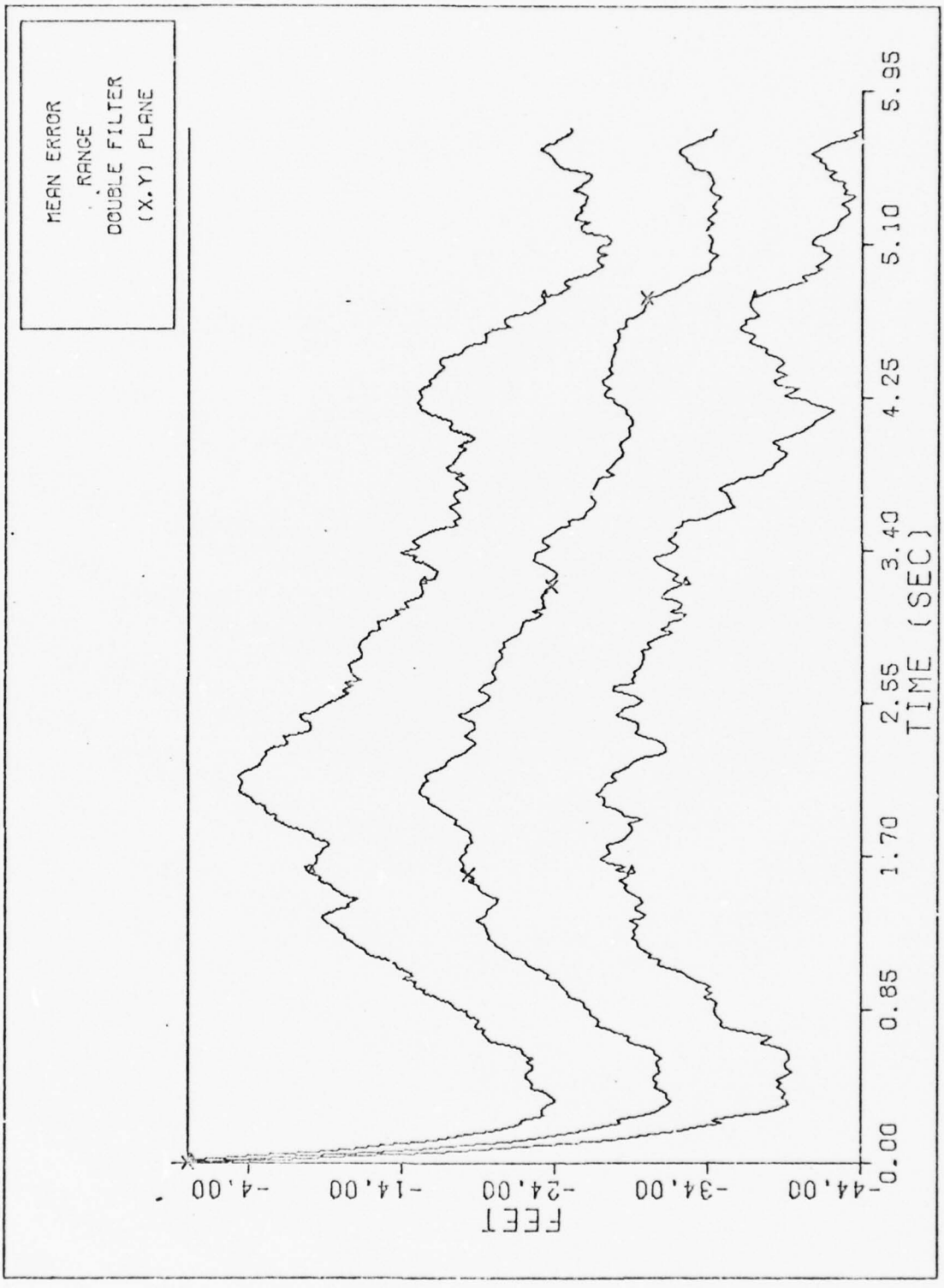


Fig. 18. RANGE DOUBLE FILTER

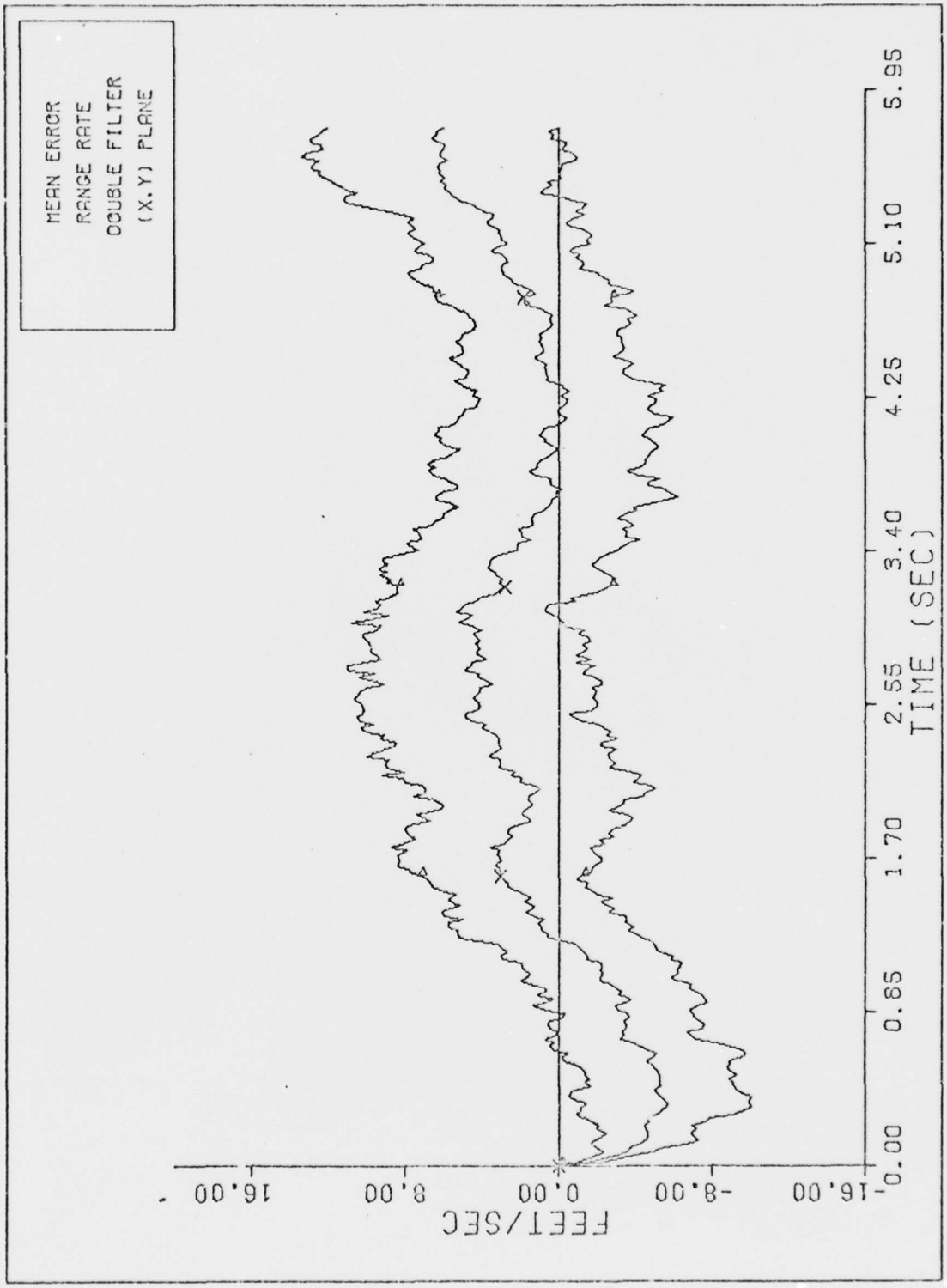


Fig. 19. RANGE RATE DOUBLE FILTER

of the standard deviations and compare favorably with Cusumano and DePonte's results (Ref 2:308-347) (see Figures 20, 21, and 22). This indicates that gravity effects (which can be easily modeled) and/or measurement transformation errors are significant. However, it is conceivable that under the K set one target trajectory, errors are caused by improper filter tuning. Cusumano and DePonte note that because the 2D filter is "optimally tuned for a given trajectory, the robustness observed over that one trajectory may not be observed for other scenarios without retuning the filter" (Ref 1:118-119). Therefore, to insure that the biases are not caused by the differences in trajectories, the double filter is tested against the target trajectory used by Cusumano and DePonte - K set four.

When the double filter performs state estimates on a three dimensional missile attacking the K set four target trajectory, good state estimates occur after an initial transient (see Figures 23, 24, and 25). The comparison of filter state standard deviations to the filter's estimate of those standard deviations shows good filter tuning (see Figures 26, 27, and 28). Therefore, this test indicates that the double filter is capable of aiding a three dimensional tracking and pointing system, but its tuning is sensitive to the trajectory. Adaptive tuning may overcome this problem.

To eliminate the effects of errors in the transformation constant, the line of sight vector is restricted to the ($\underline{i}_1$, $\underline{i}_2$) plane when the target flies trajectory K set four. This is accomplished by restricting missile motion to the ($\underline{i}_1$, $\underline{i}_2$) plane. Thus, the line of sight is always in the 2D filter plane. The results from this test are almost identical to the previous test, indicating that errors in the

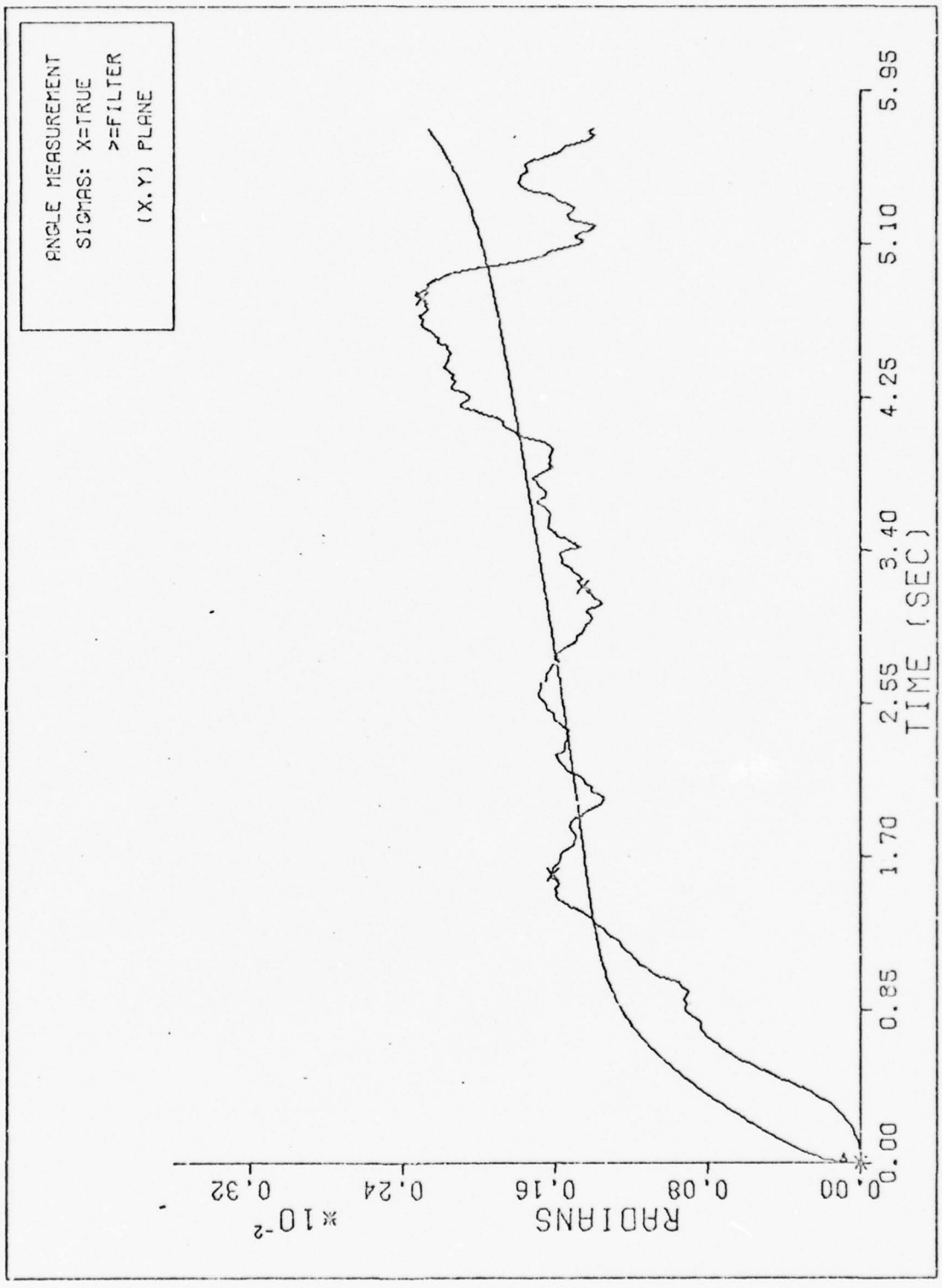


Fig. 20. ANGLE MEASUREMENT SIGMAS DOUBLE FILTER

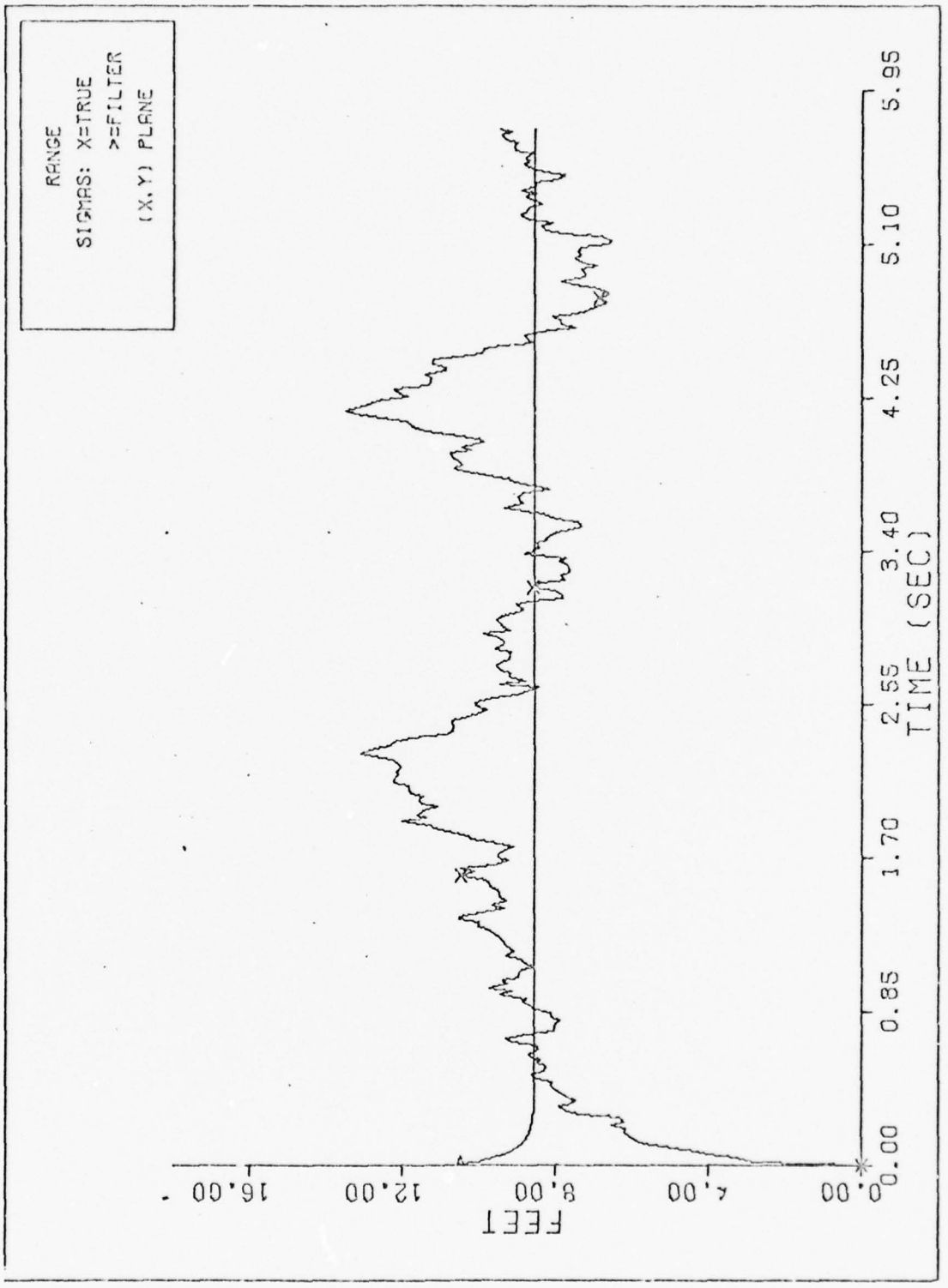


Fig. 21. RANGE SIGMAS DOUBLE FILTER

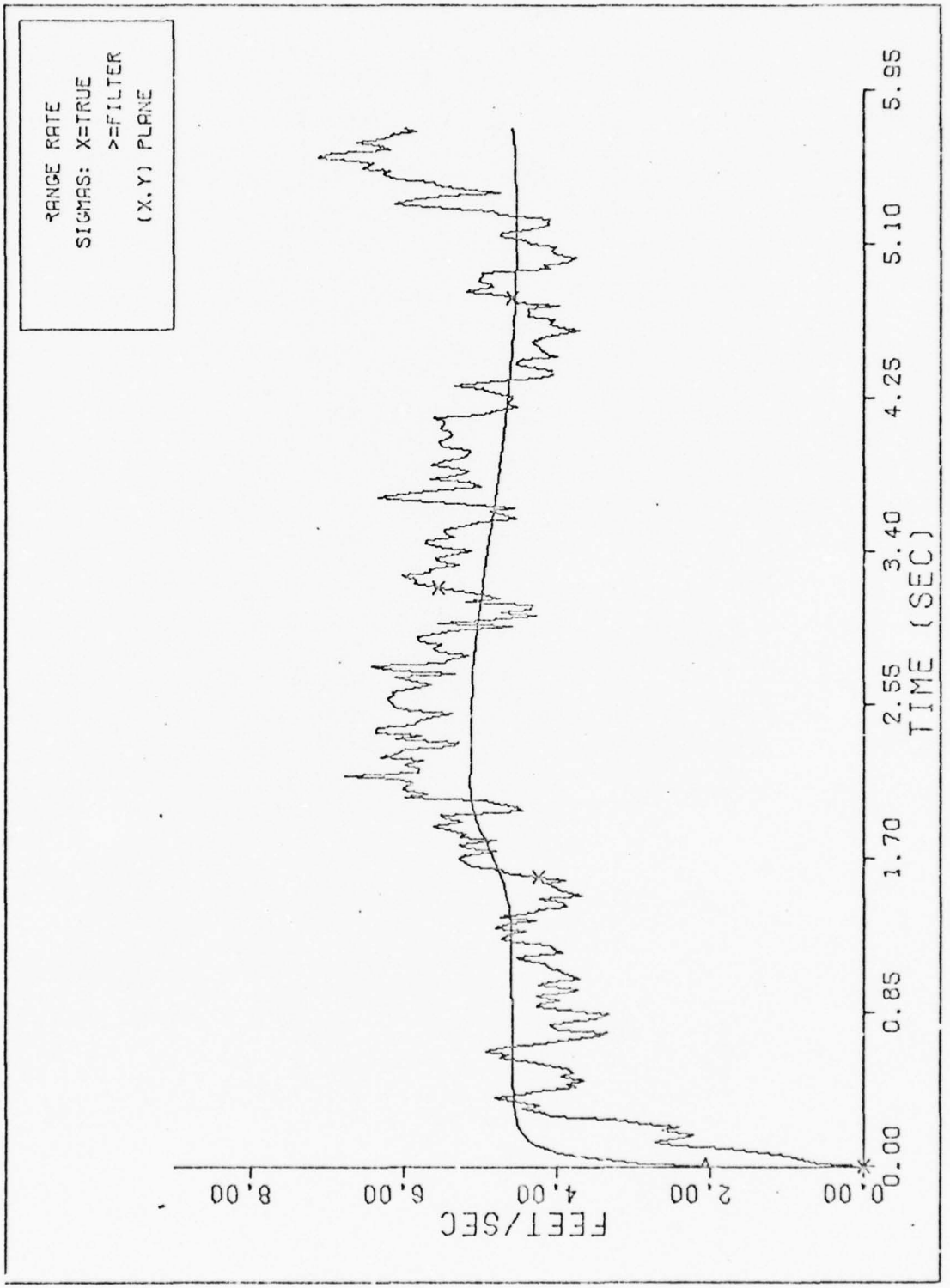


Fig. 22. RANGE RATE SIGMAS DOUBLE FILTER

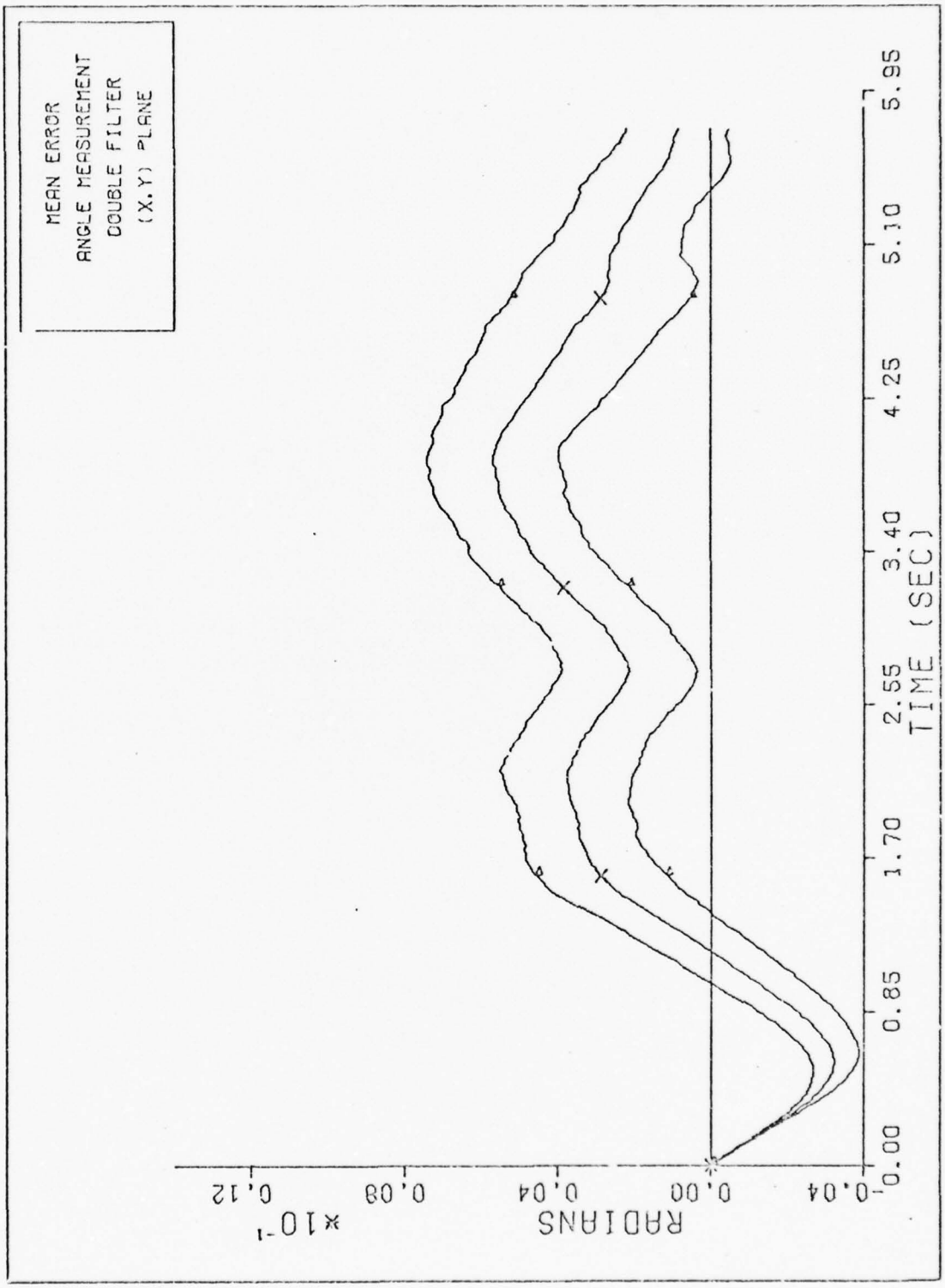


Fig. 23. ANGLE MEASUREMENT DOUBLE FILTER

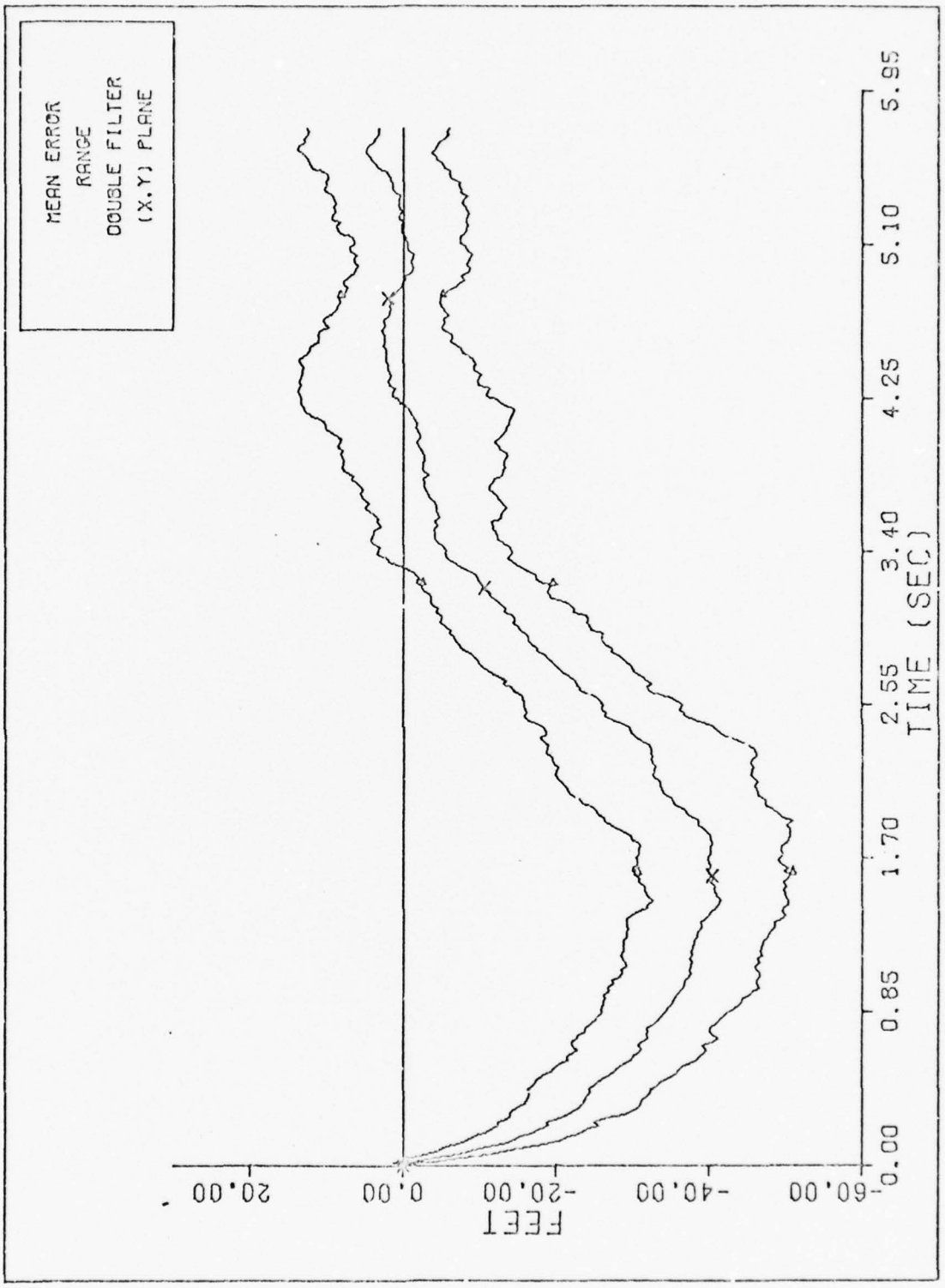


Fig. 24. RANGE DOUBLE FILTER

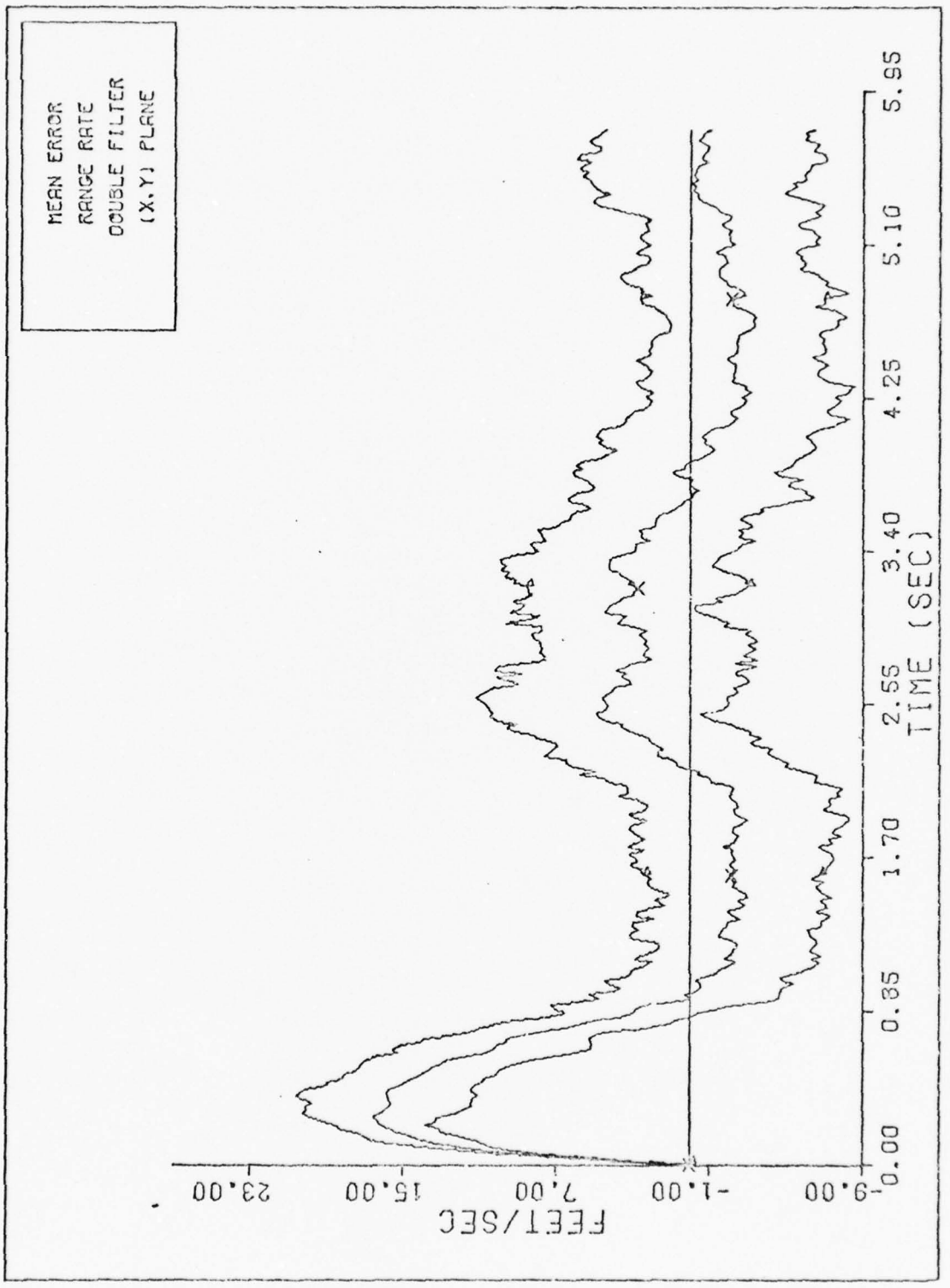


Fig. 25. RANGE RATE DOUBLE FILTER

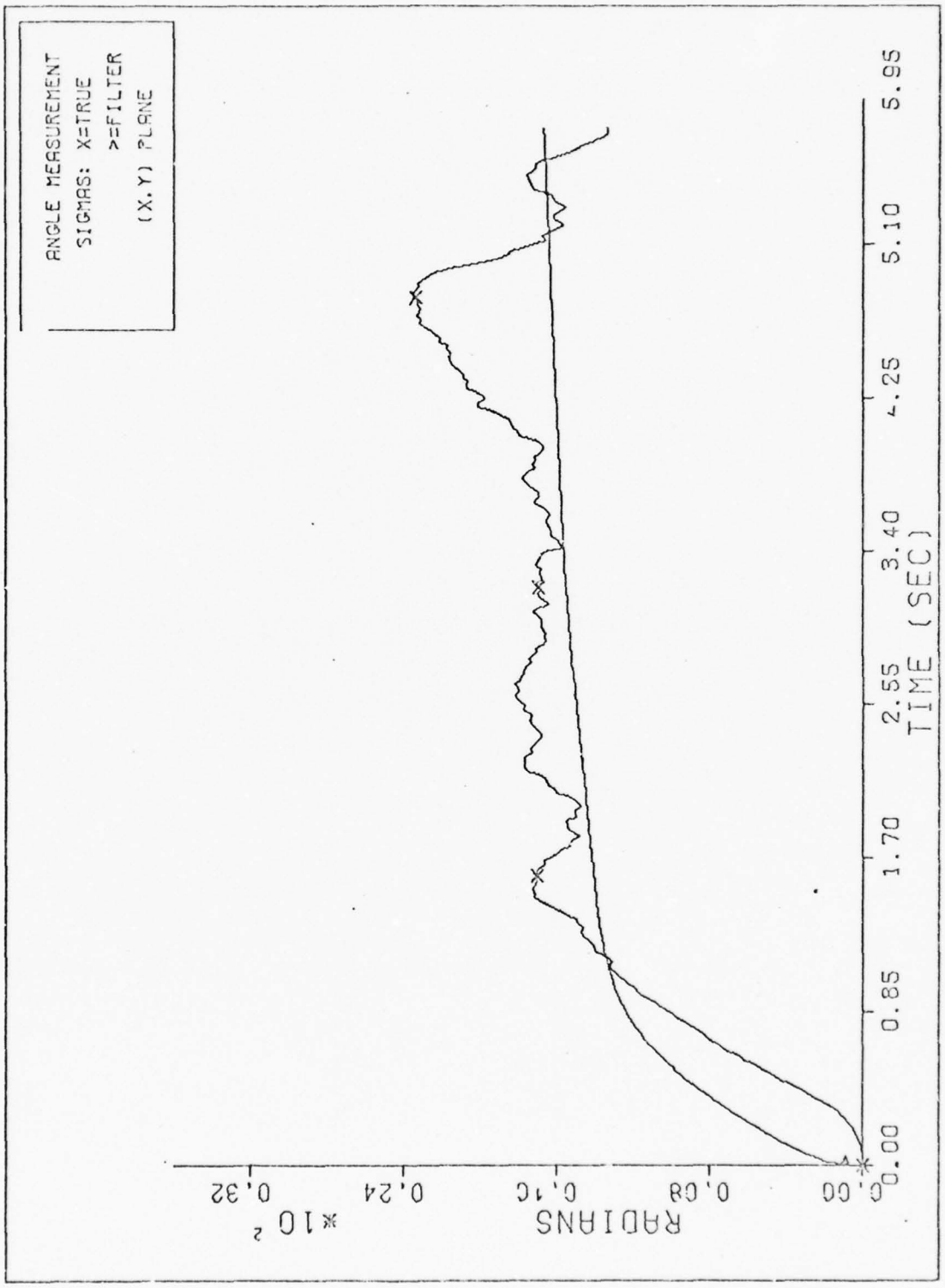


Fig. 26. ANGLE MEASUREMENT SIGMAS DOUBLE FILTER

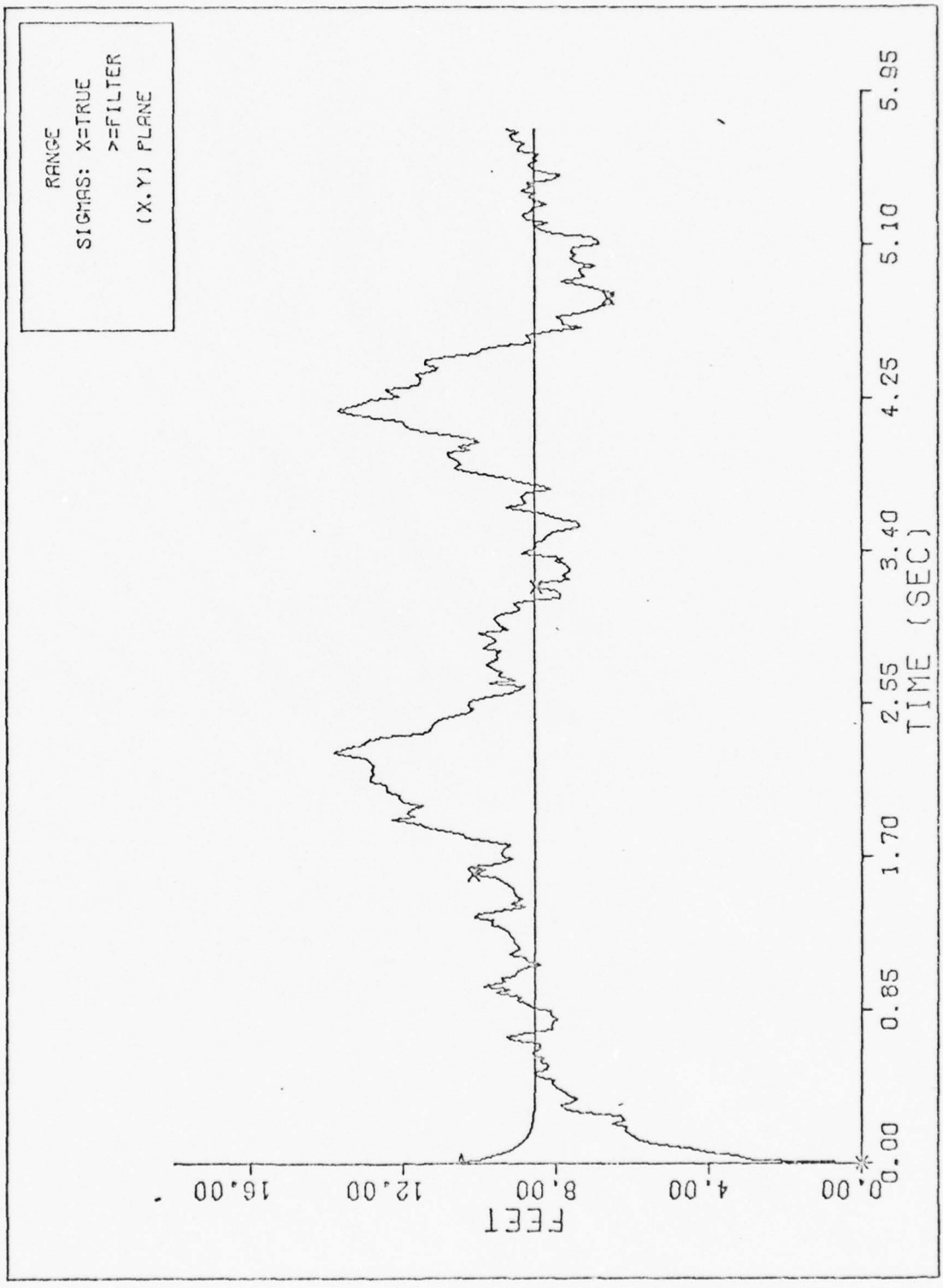


Fig. 27. RANGE SIGMAS DOUBLE FILTER

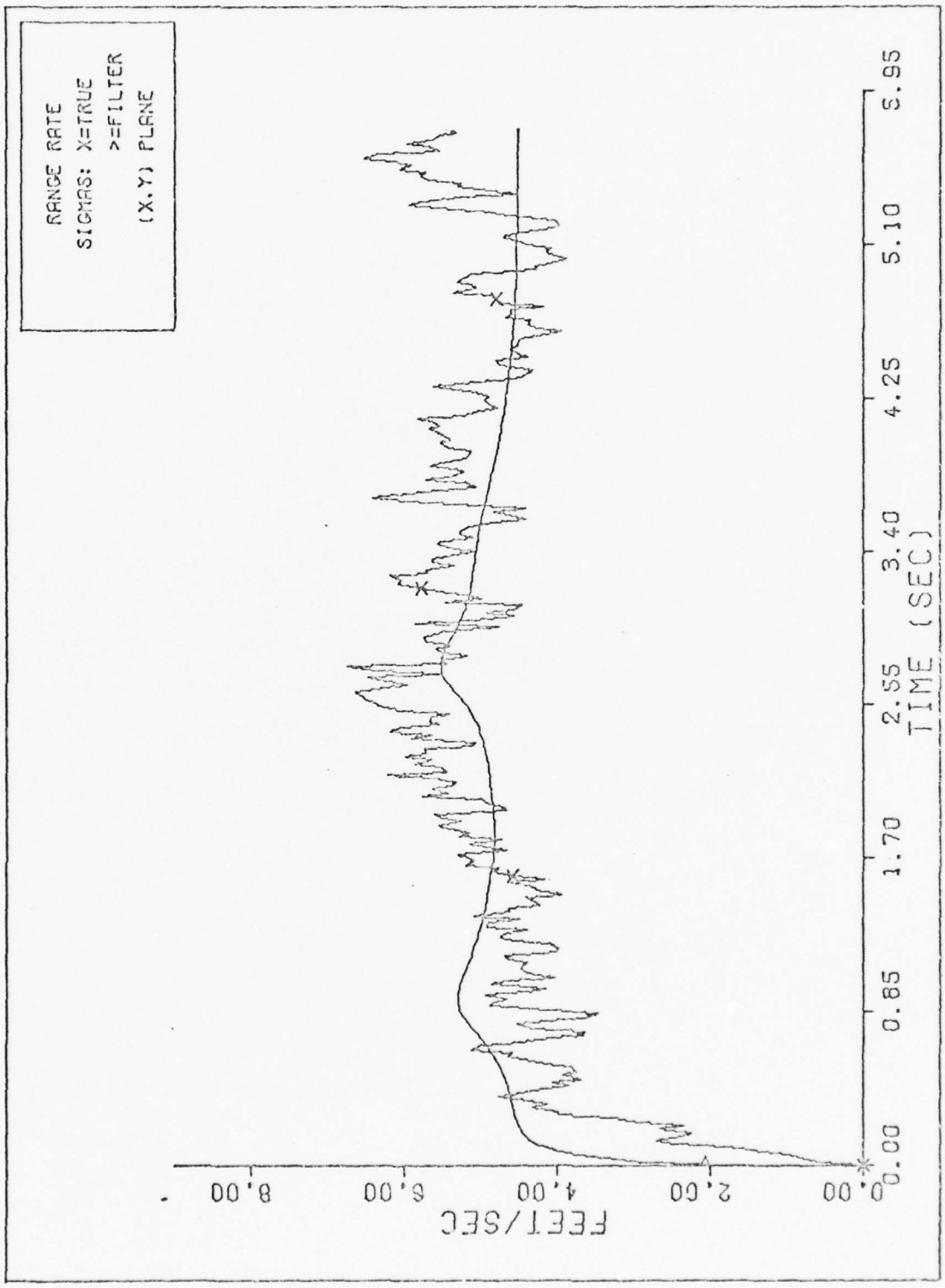


Fig. 28. RANGE RATE SIGMAS DOUBLE FILTER

transformation constant (when the line of sight is within one degree of the filter plane) have little effect on filter performance. The initial transients are apparently due to gravity (see Figures 29-34). However, these tests are inherently two dimensional, with transverse line of sight motion less than a degree. The double filter must still be tested when the line of sight vector exhibits greater changes in orientation, such as with the K set three trajectory.

The K set three trajectory produces larger, quicker changes to the line of sight orientation than do the other K sets. This tests the validity of the transformation constants. Under this test, the double filter encounters computer caused numerical difficulties with the (m/s) variance computations. The specific values of the filter states, up to the time of numerical failure, are analyzed. These values show that when the line of sight vector rotates transverse to the 2D filter plane, an error in the R and $\dot{R}$ states is induced. This effect is similar to the changes that occur to a planar projection of a rotating unit vector (see Figure 35). Note that when the unit vector rotates, derivative information of its projection, i.e. velocity and acceleration, is also affected. To understand why numerical difficulties are encountered, the 2D filter is analyzed.

In a two dimensional environment, measurement errors in θ_T, R, and $\dot{R}$ (states of the 2D filter) are appropriately modeled. In a three dimensional environment, transverse line of sight movement causes measurement errors that are not modeled by the filter (see Figure 36).

The measurements are used by the 2D filter to compute the linear and angular accelerations of the line of sight vector. Unmodeled measurement errors are treated as a part of the filter's computed line

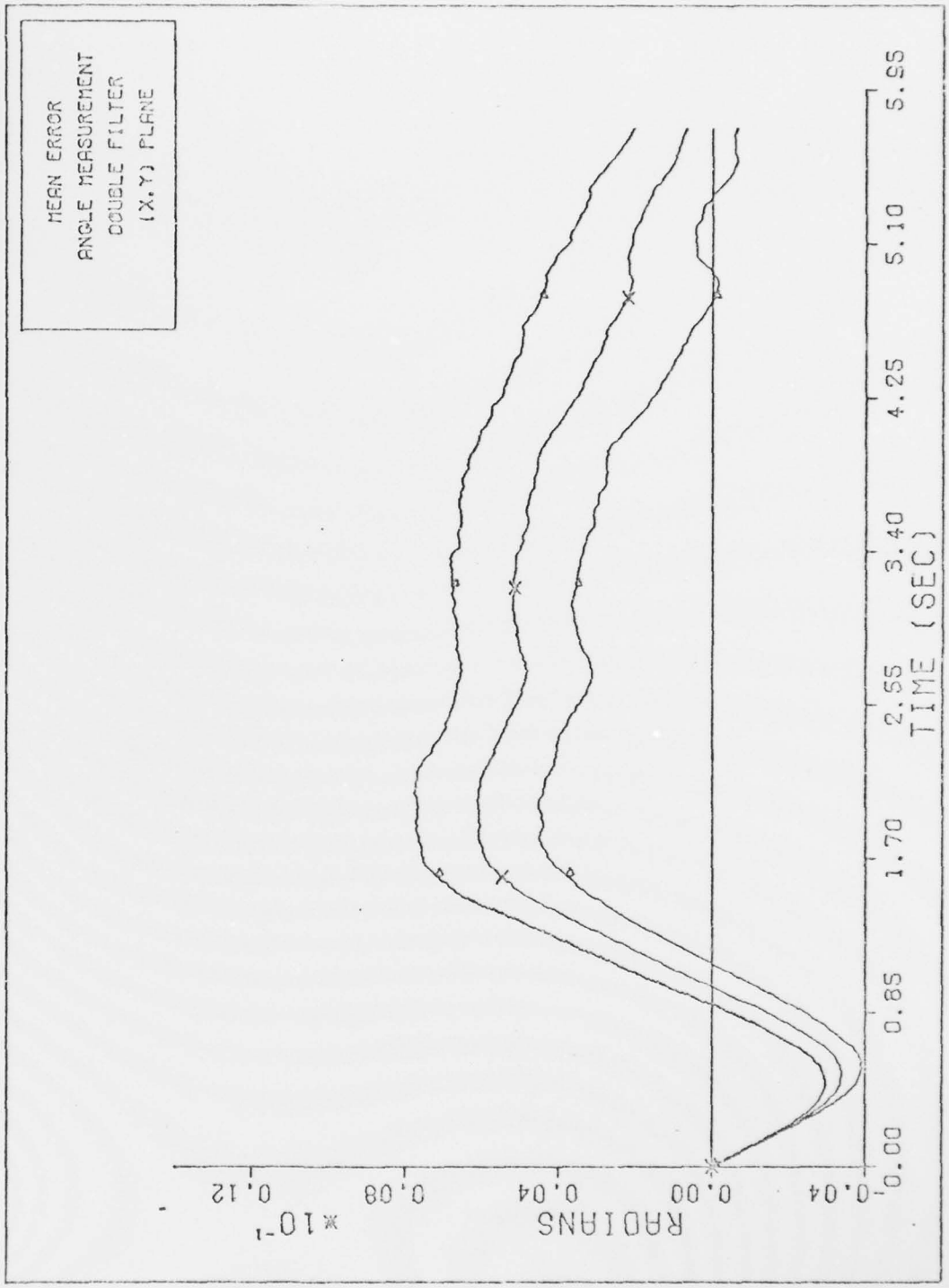


Fig. 29. ANGLE MEASUREMENT DOUBLE FILTER

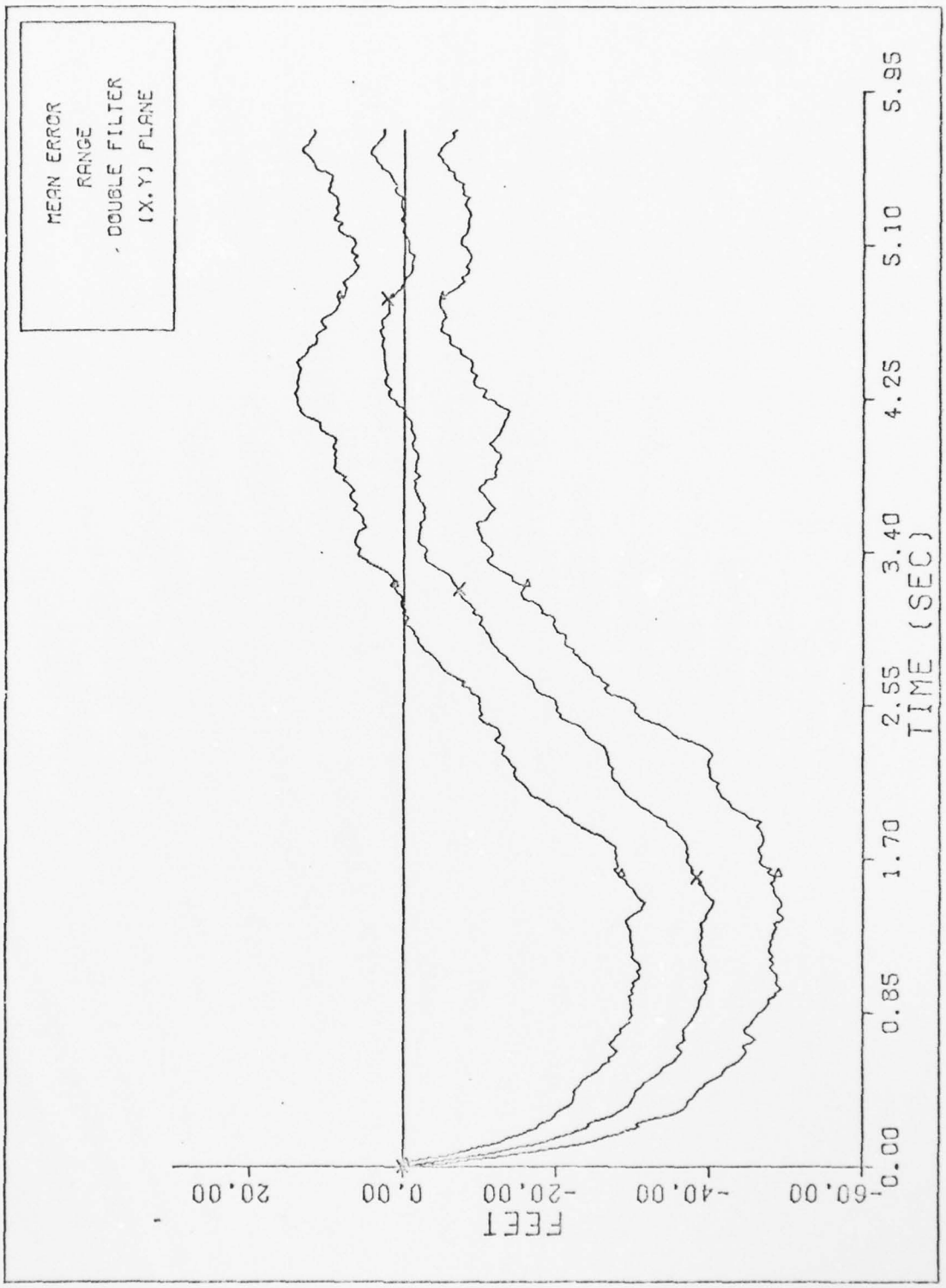


Fig. 30. RANGE DOUBLE FILTER

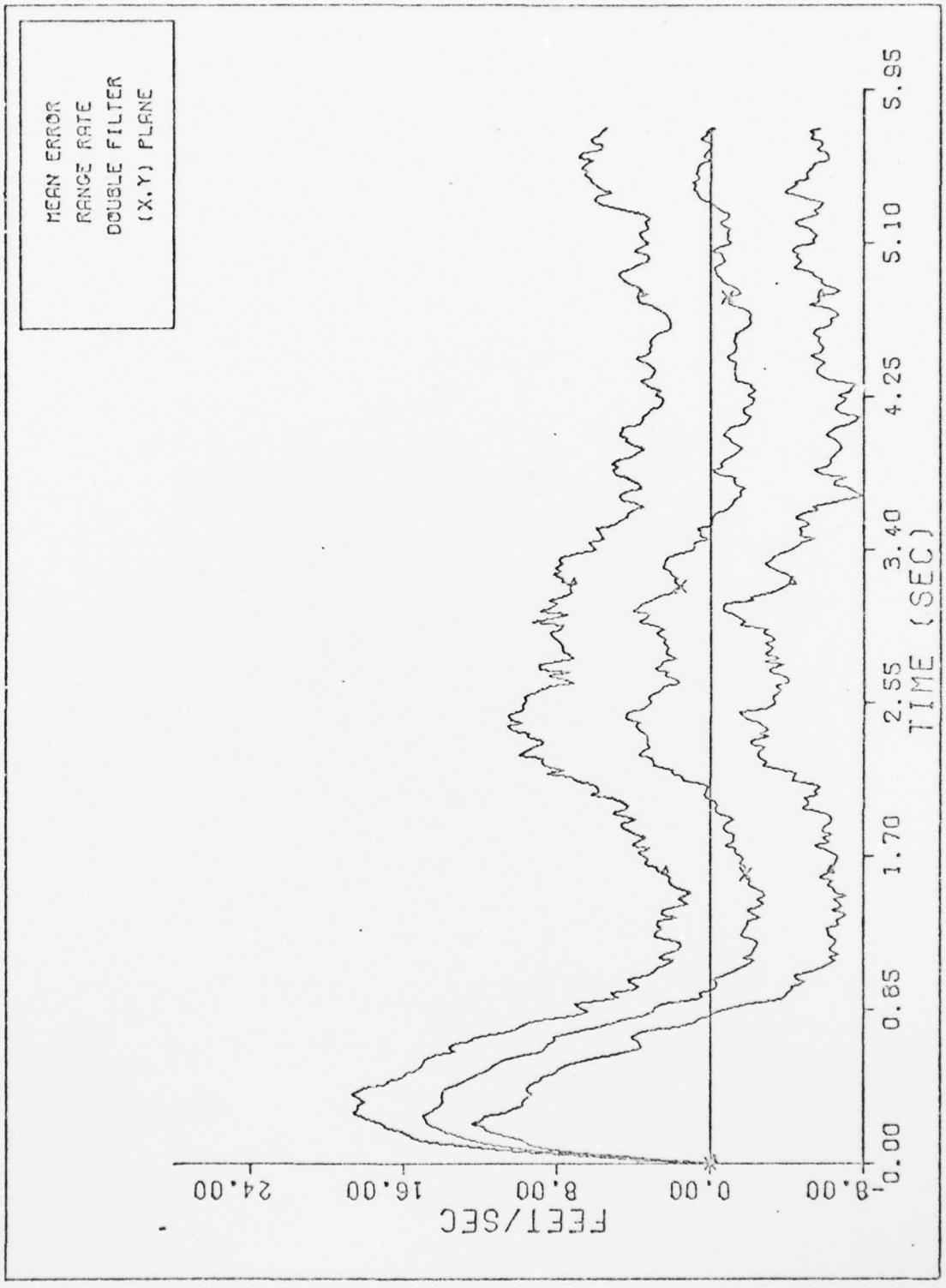


Fig. 31. RANGE RATE DOUBLE FILTER

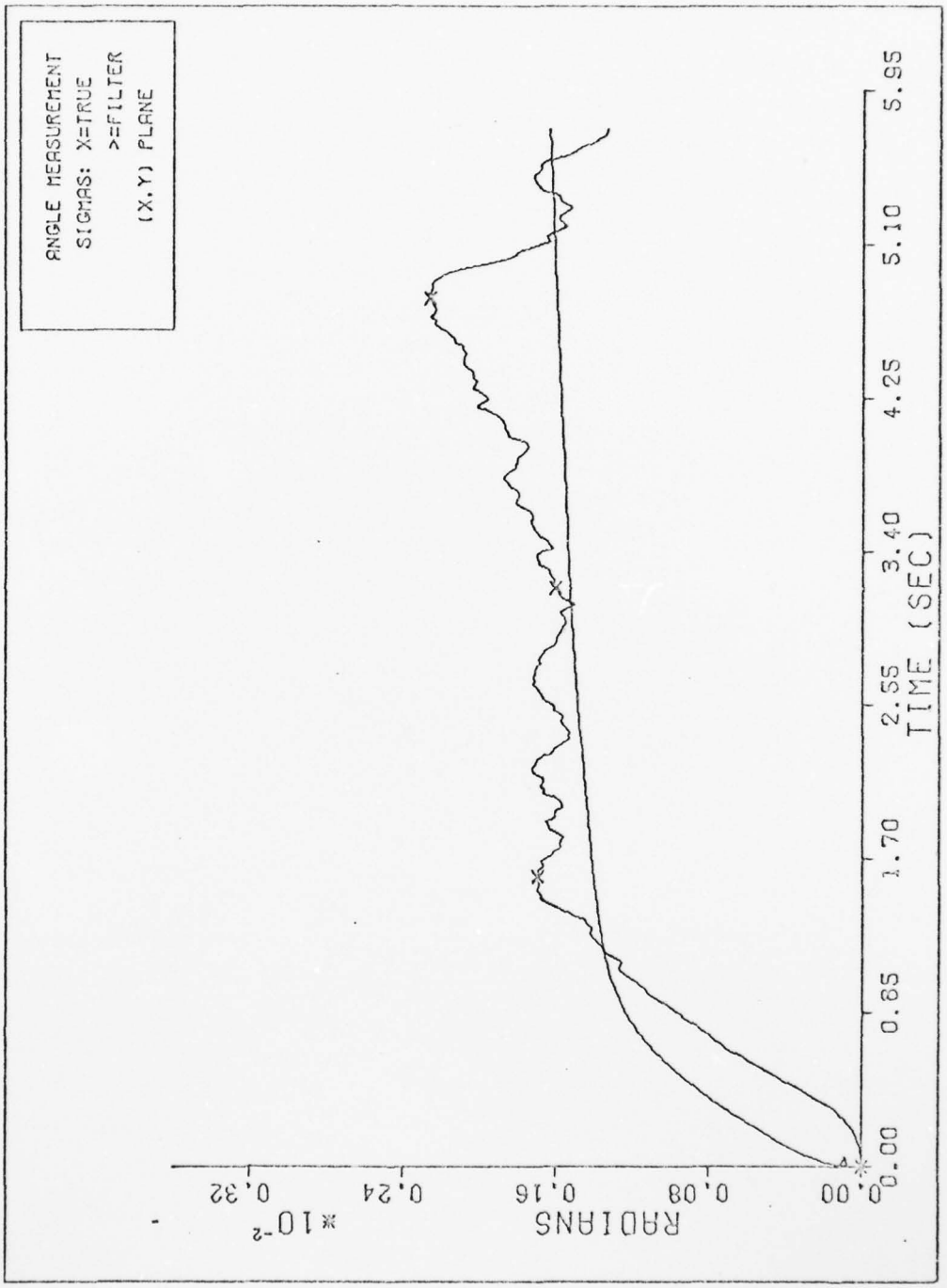


Fig. 32. ANGLE MEASUREMENT SIGMAS DOUBLE FILTER

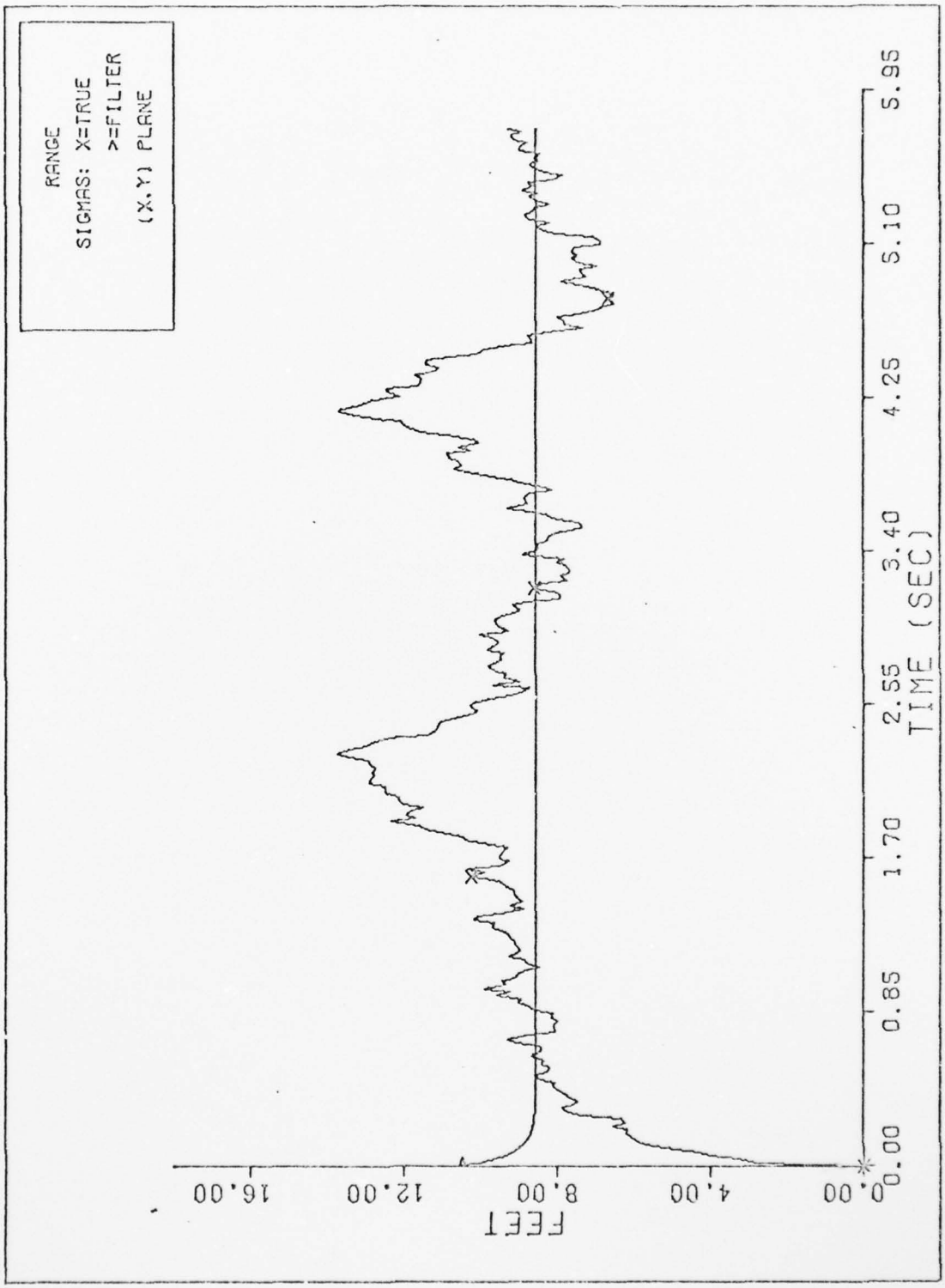


Fig. 33. RANGE SIGMAS DOUBLE FILTER

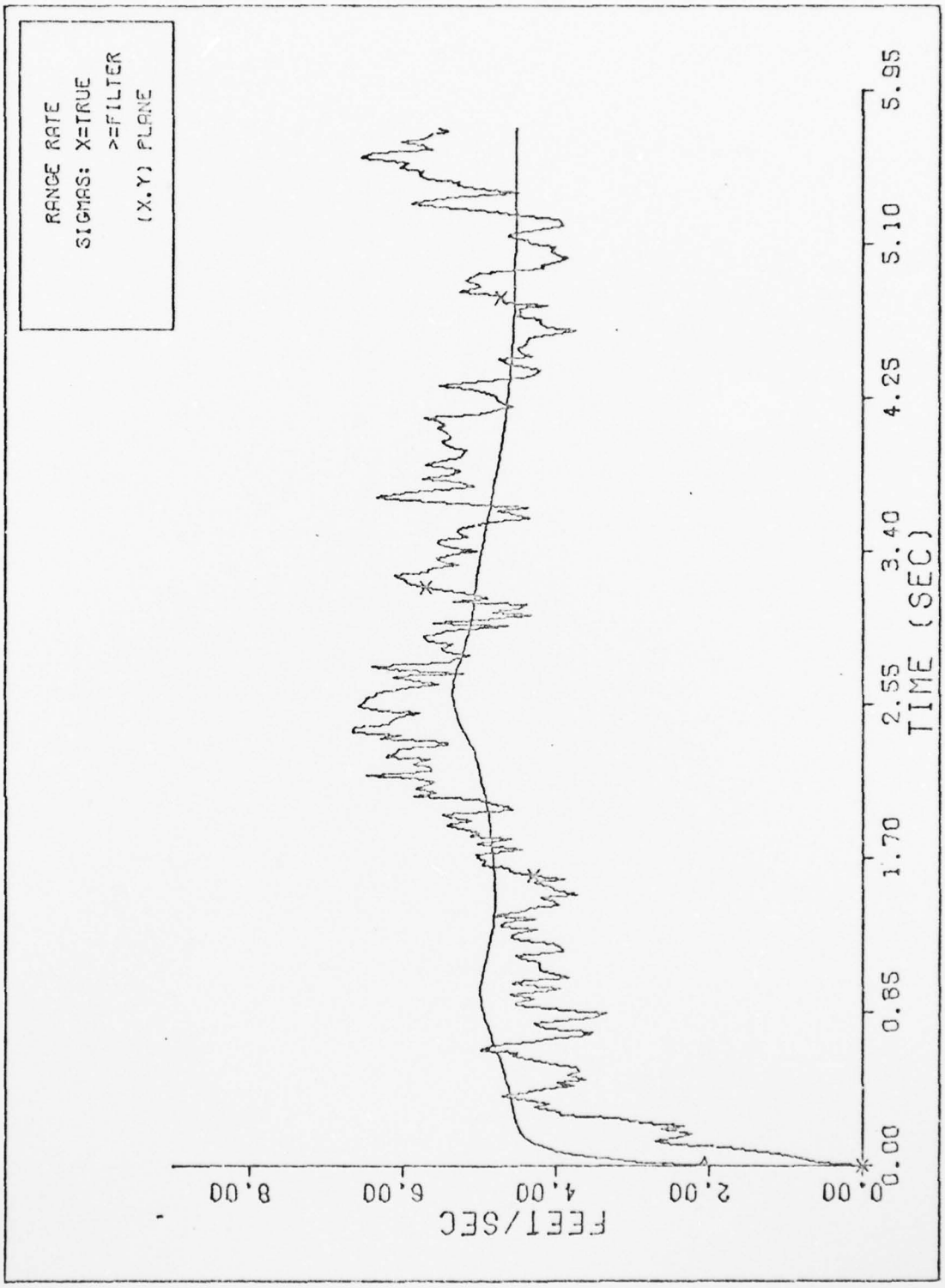
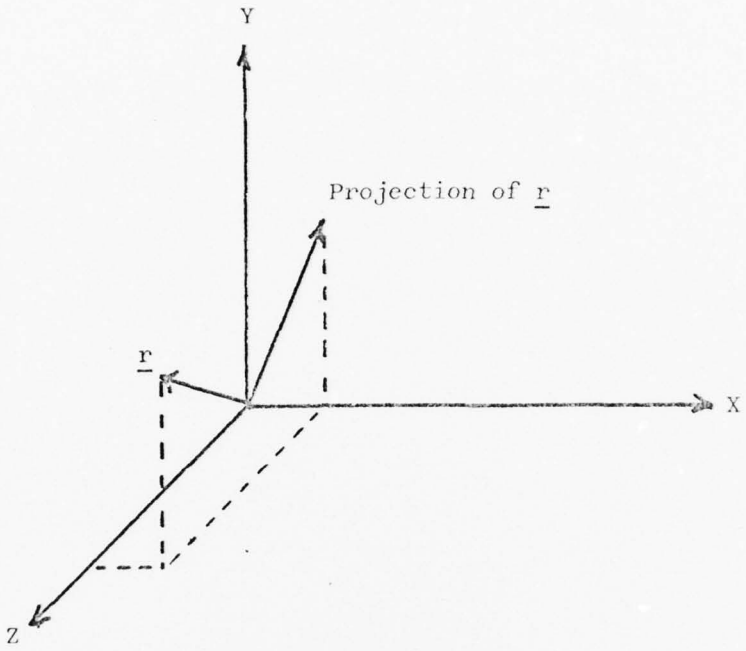
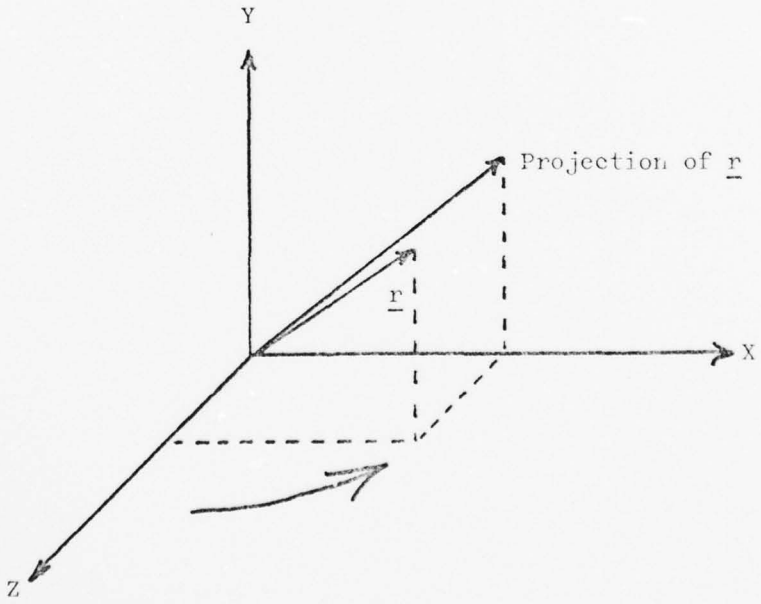


Fig. 34. RANGE RATE SIGMAS DOUBLE FILTER

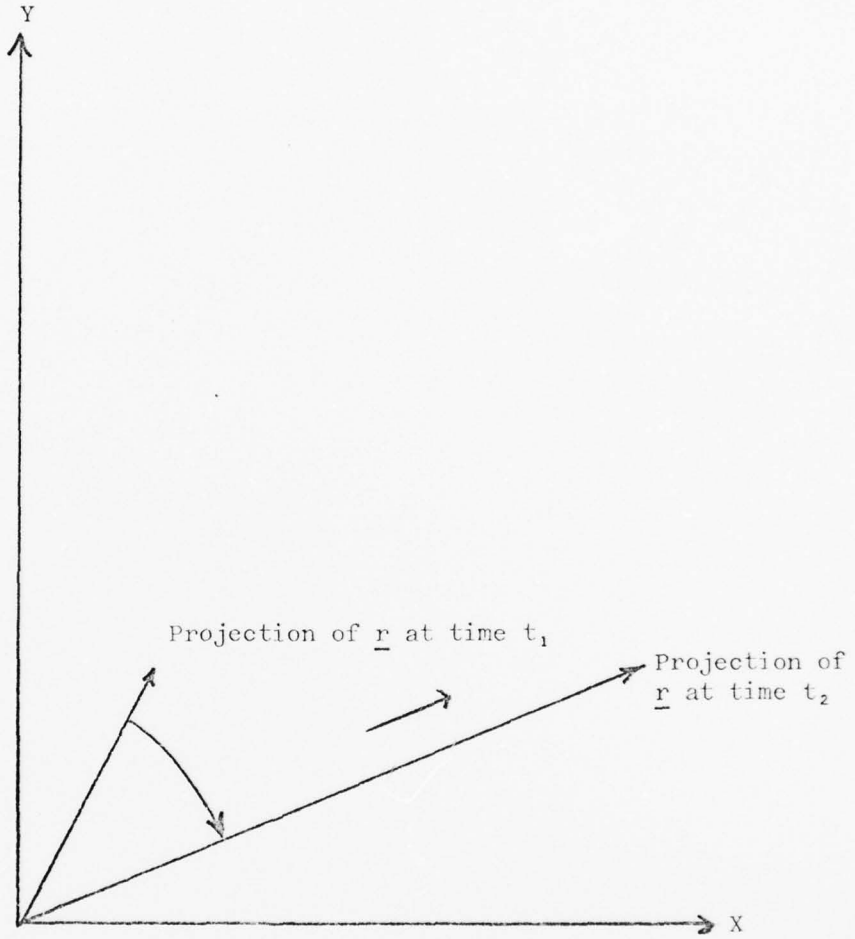


Projection of Unit Vector $\underline{r}$ at Time t_1



Projection of Unit Vector $\underline{r}$ at Time t_2

Fig. 35. Vector Rotation Effects on Its Planar Projection



Unit vector rotation causes a growth in projected $\underline{r}$ and a change in orientation.

Fig. 36. Summarized Filter Plane Results of Figure 35

of sight accelerations. In this case, transverse line of sight motion induces the most error on the line of sight's linear acceleration (as computed by the filter). To see the effect of this induced error on the 2D filter, a free body diagram of the missile is constructed. It reveals that the filter's estimate of missile drag and lateral accelerations must directly account for any errors in the line of sight acclerations as computed from the measurements (see Figure 37). Filter tuning, as well as acceleration vector orientations, determine state sensitivities to errors in the calculated line of sight accelerations. In this case (m/s) is most sensitive to induced line of sight linear acceleration errors since (m/s) is used to compute drag. Therefore, the filter's (m/s) variance encounters numerical difficulties when the (m/s) state must change considerably to balance the filter's acceleration model. When a similar test is run with the filter's (m/s) state constrained to its true value, the A_L variance encounters numerical difficulties, confirming this analysis. Therefore, a constant transformation constant is not feasible. Three dimensional evasion maneuvers by the target result in induced acceleration effects, which are unmodeled by the filter and are significant. No testing of periodically updated transformation constants is performed.

Third Proposal

The final three dimensional proposal - the double filter which processes angle measurements only - is tested against K set four. This trajectory is again chosen to avoid possible trajectory-caused tuning problems. In this test, the errors in the R and $\dot{R}$ state estimates exceed 100 ft and 100 ft/sec - an unacceptable level of error

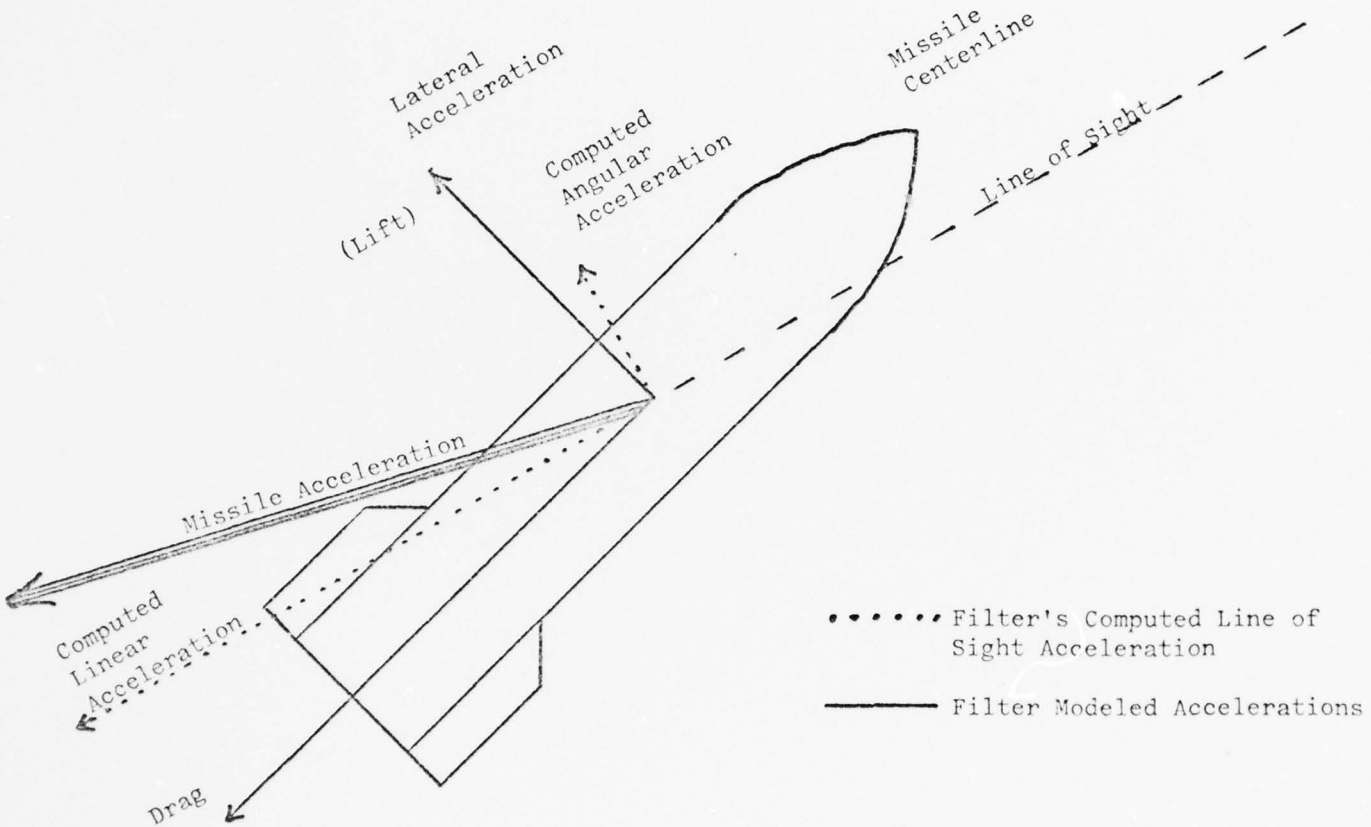


Fig. 37. Relationship Between Computed Line of Sight Accelerations and Filter Modeled Accelerations

(see Figures 38, 39, and 40). The standard deviations of the state estimates are generally more than the filter's estimates of the standard deviations, indicating a tuning problem (see Figures 41, 42, and 43). Yet, because this filter ignores available information, retuning is not accomplished, allowing more time to be devoted to the development of the 11 state filter. It is felt that even with retuning, error levels for the pointing-tracking states in this filter would be too high.

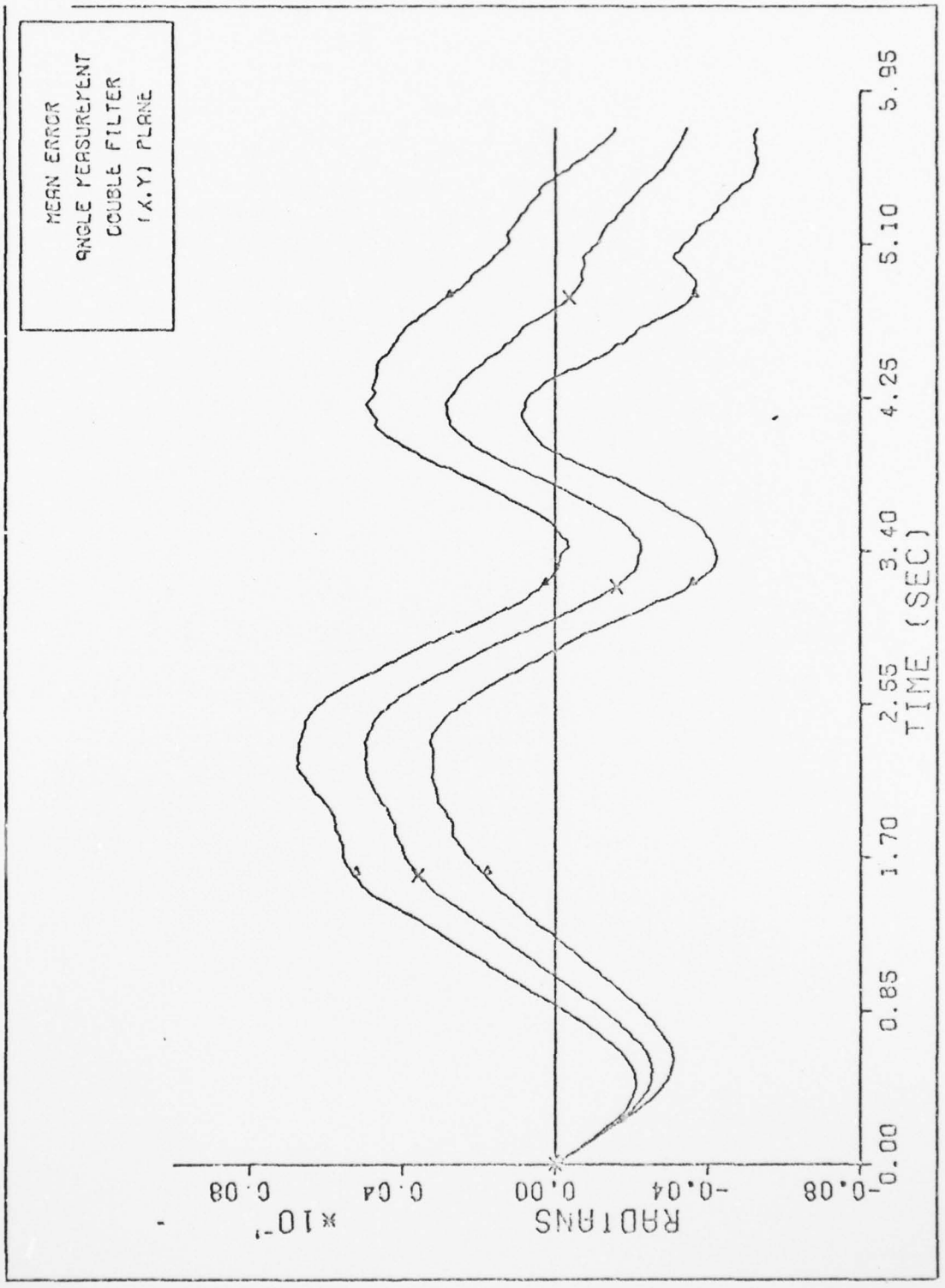


Fig. 38. ANGLE MEASUREMENT DOUBLE FILTER

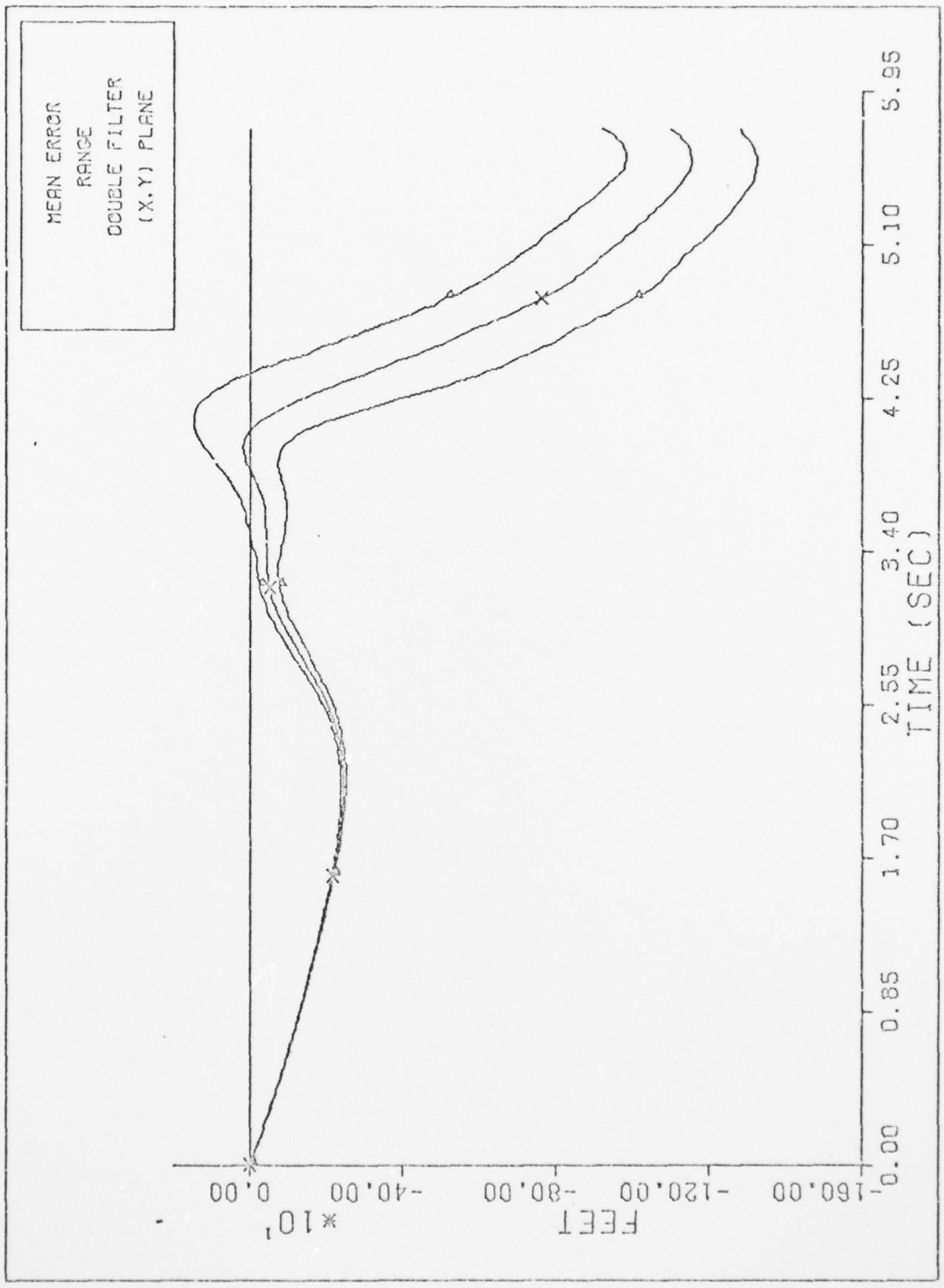


Fig. 39. RANGE DOUBLE FILTER

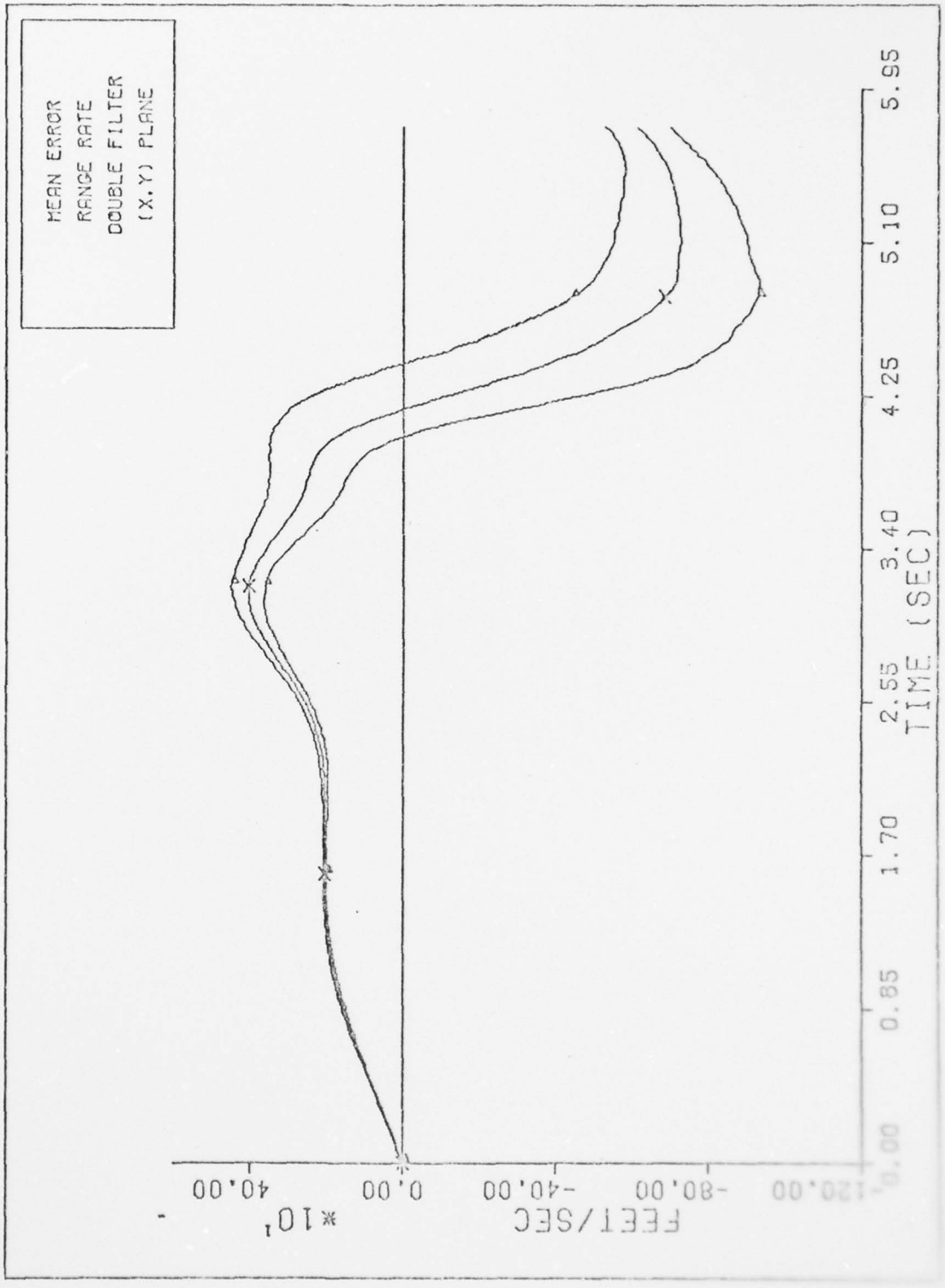


Fig. 40. RANGE RATE DOUBLE FILTER

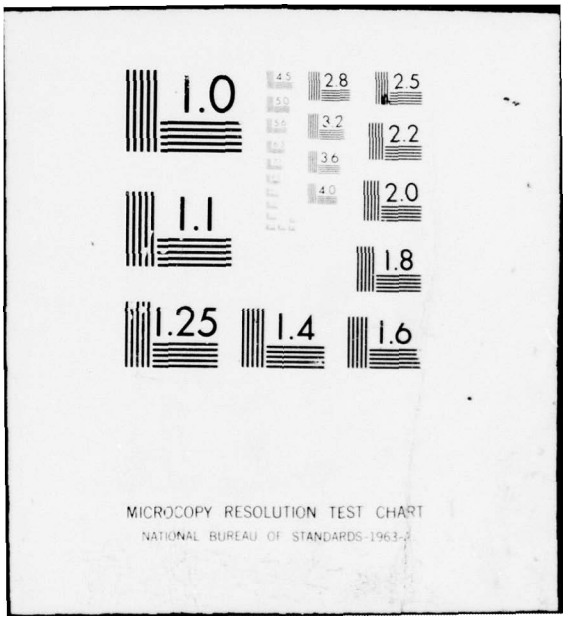
AD-A064 759 AIR FORCE INST OF TECH WRIGHT-PATTERSON AFB OHIO SCH--ETC F/G 15/3.1
A PRACTICAL THREE DIMENSIONAL , 11 STATE EXTENDED KALMAN FILTER--ETC(U)
DEC 78 C W HLAVATY

UNCLASSIFIED AFIT/GGC/EE/78-7-VOL-1 NL

2 OF 2
AD
AD 64759



END
DATE
FILMED
4 -79
DDC


1.0
1.1
1.25
1.4
1.6
1.8
2.0
2.2
2.5
2.8
3.2
3.6
4.0
4.5
5.0
5.6
6.3
MICROCOPY RESOLUTION TEST CHART
NATIONAL BUREAU OF STANDARDS-1963-A

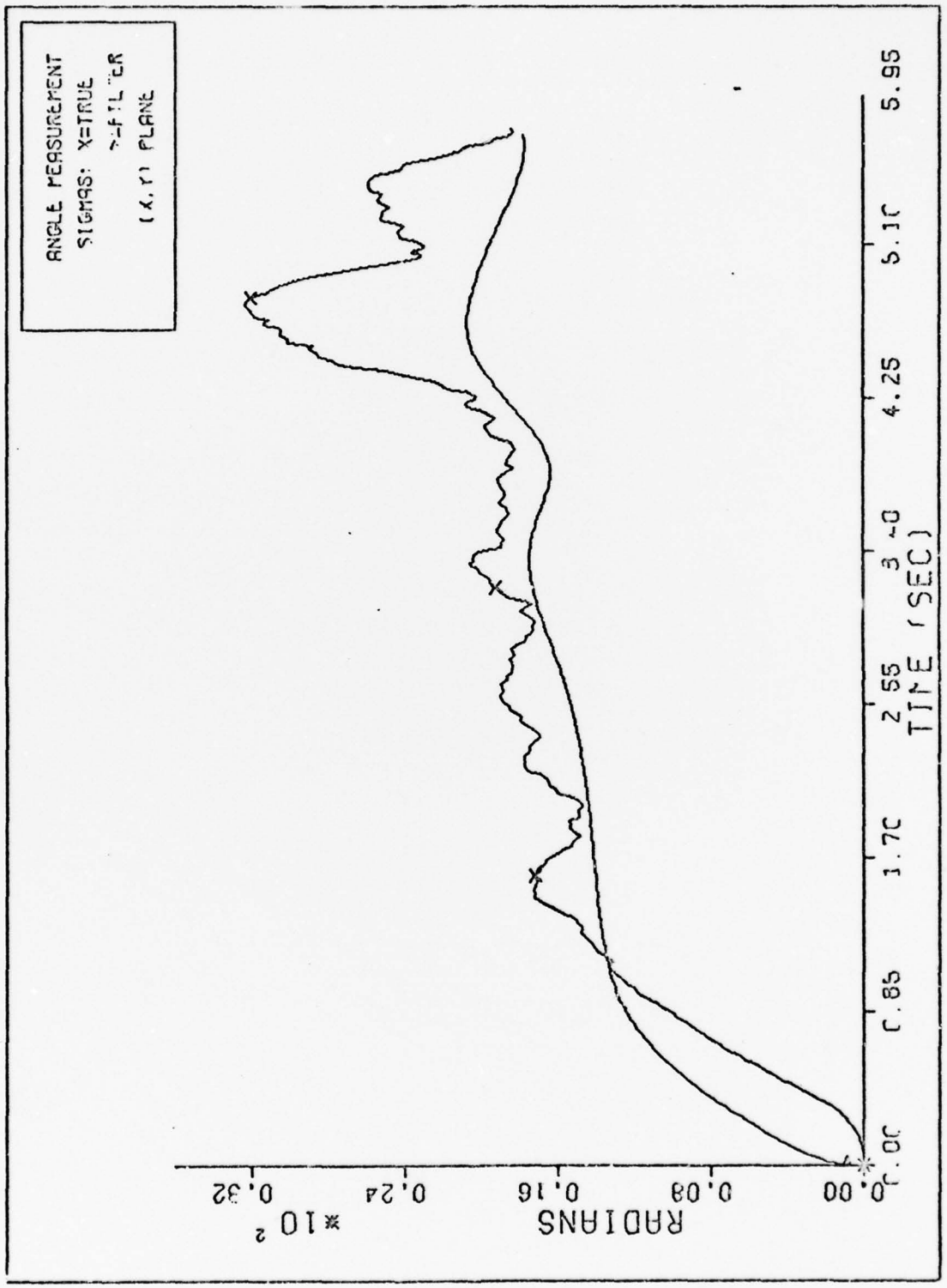


Fig. 41. ANGLE MEASUREMENT SIGMAS DOUBLE FILTER

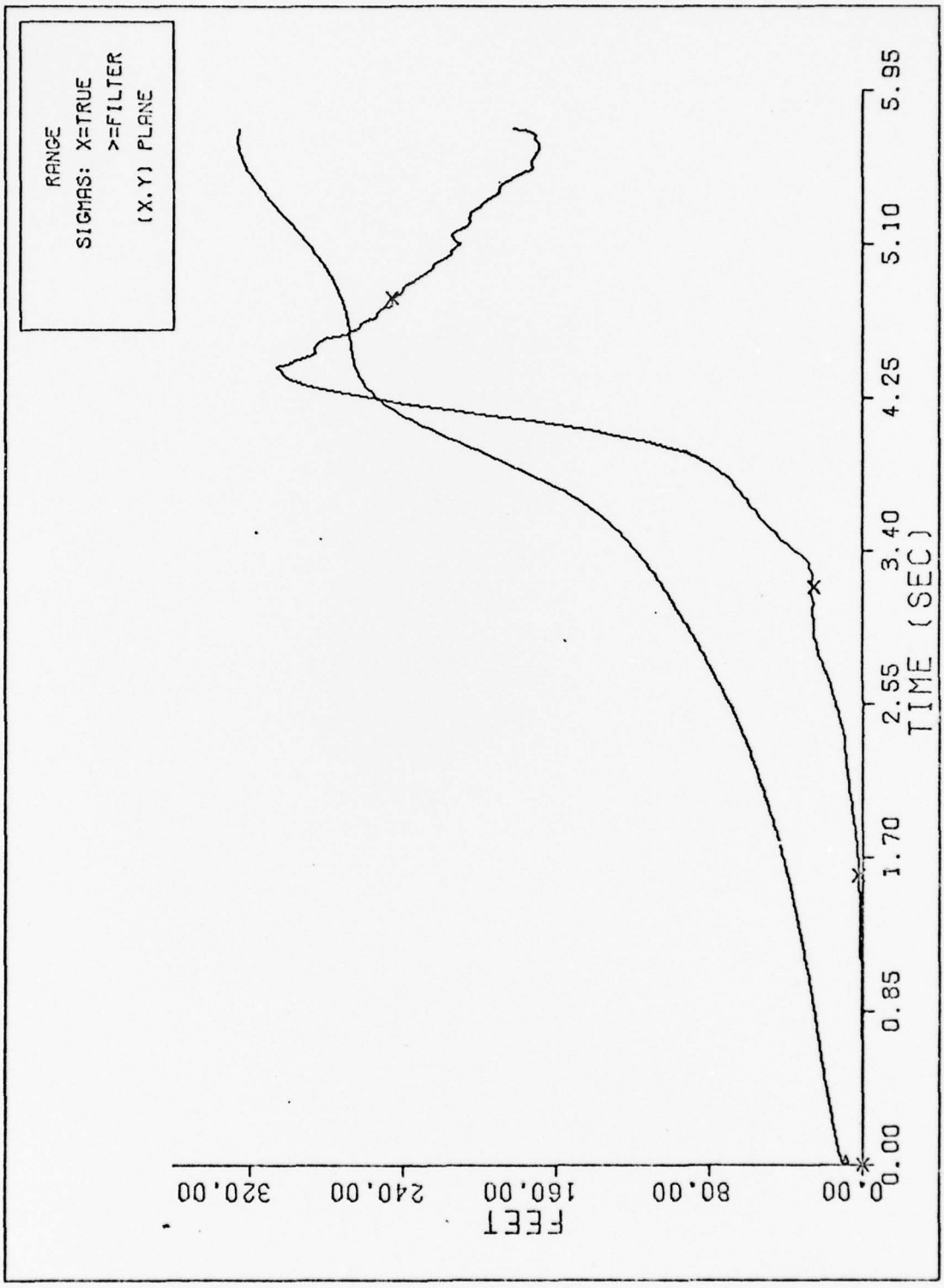


Fig. 42. RANGE SIGMAS DOUBLE FILTER

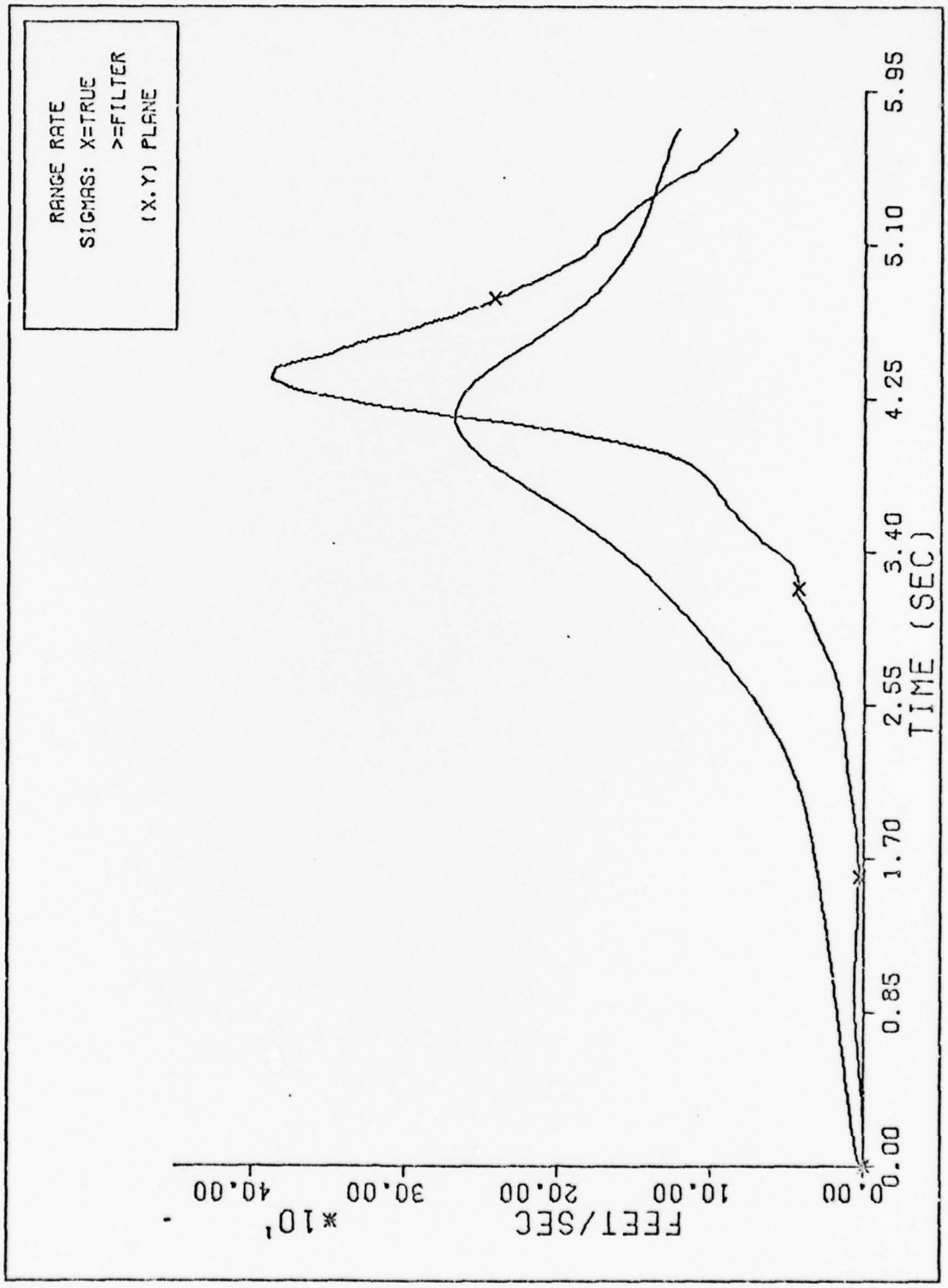


Fig. 43. RANGE RATE SIGMAS DOUBLE FILTER

IV. Three Dimensional Filter and Model

Introduction

The hardest and most important task in designing a model is choosing a state space. A good choice of states can produce an excellent filter; a bad choice can cause problems or even fail completely. Generally, the problems that need to be avoided are redundant states and a wide eigenvalue range on the state transition matrix (Ref 7,8). Previous pointing and tracking research has found favorable results with a polar coordinate frame state space (Ref 4,9).

Many pointing-tracking systems measure more than line of sight orientation, range, and range rate. Line of sight inertial angular velocities can also be measured if the system is dedicated to one missile. Cusumano and DePonte, as well as Lutter, assume that one pointing-tracking system will both scan for oncoming missiles (scanner) and provide position-velocity information to a fire control system (Ref 1:1,5:1-2,27). Therefore, their filters only process range, range rate, and line of sight orientation information, with no angular velocity measurements.

If, however, a remote scanner is used for threat evaluation, each weapon system can have a colocated pointing-tracking system dedicated to tracking one missile. This avoids transfer alignment errors and provides more measurements to the extended Kalman filter, which increases pointing-tracking accuracies. Therefore, the designed model should be capable of processing range, range rate, and line of sight

orientation, to take advantage of any and all available information.

Filter State Space

Based upon the previous ideas, the filter state space is chosen in polar coordinates. Eleven states completely describe the system. These states are:

θ_1 - first Euler rotation from inertial frame to line of sight frame (rad)

θ_2 - second Euler rotation from inertial frame to line of sight frame (rad)

ω_1 - inertial angular velocity of line of sight frame, along first line of sight frame axis (rad/sec)

ω_2 - inertial angular velocity of line of sight frame, along second line of sight frame axis (rad/sec)

R_{tm} - missile position relative to target position in line of sight frame (kiloft = 10^3 ft)

$\dot{R}_{tm}$ - rate of change of R_{tm} as observed in the line of sight frame (kiloft/sec)

A_{L1} - lateral acceleration of missile along first missile velocity frame axis (kiloft/sec^2)

A_{L2} - lateral acceleration of missile along second missile velocity frame axis (kiloft/sec^2)

n_f - proportional navigation constant, as estimated by the filter

τ_f - first order lag time constant for filter model of missile response (sec)

$(m/s)_f$ - mass to effective surface ratio of missile, as modeled by the filter (slug/kiloft^2)

The units of length are chosen to avoid computer numerics problems in computing the Kalman filter gains. The three coordinate frames inherent with this state space are: inertial (i), true line of sight (1), and missile velocity (v). These frames and the states associated with them, are depicted in Figure 44. Euler rotations relate one frame to the other. These relationships are depicted in Figures 45 and 46. A complete derivation of state equations, as well as the derivation of α_1 and α_2 (the Euler rotations from the v frame to the 1 frame), is contained in Appendix B.

In the derivation, the state space equations for ω_1, ω_2, and $\dot{R}_{tm}$ are developed from the theorem of Coriolis. Missile velocity, as measured by the target's pointing-tracking system, is related to the missile velocity as expressed in the v frame, to obtain expressions for the Euler rotation angles α_1 and α_2. The missile's drag and lateral accelerations, which are modeled in the v frame, are transformed to the 1 frame via α_1 and α_2. Missile acceleration due to gravity is transformed from the i frame to the 1 frame via θ_1 and θ_2 - two of the eleven filter states. Gravity, drag, and lateral accelerations are combined in the 1 frame to produce state equations for ω_1, ω_2, and $\dot{R}_{tm}$ through the theorem of Coriolis. The state equations for θ_1, θ_2, and R_{tm} are developed directly from state definitions. A first order lag, proportional navigation missile model is used for the A_{L1} and A_{L2} state equations. Finally, white Gaussian noise of appropriate strength is employed to model the parameters n_f, τ_f, and $(m/s)_f$.

This three dimensional filter model contains four assumptions:

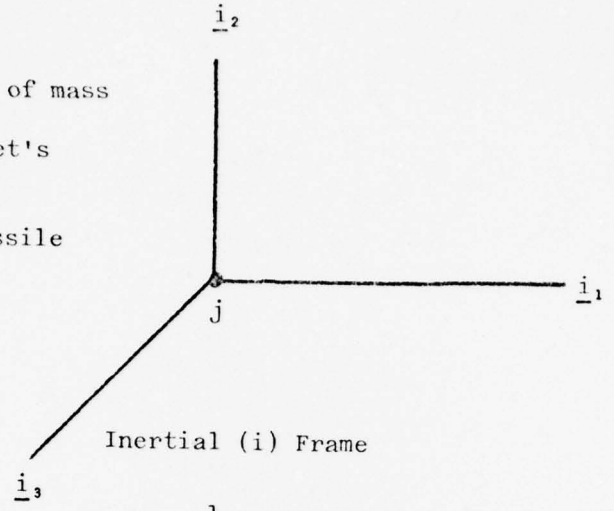
1. The actual missile's guidance scheme approximates proportional navigation.

Note:

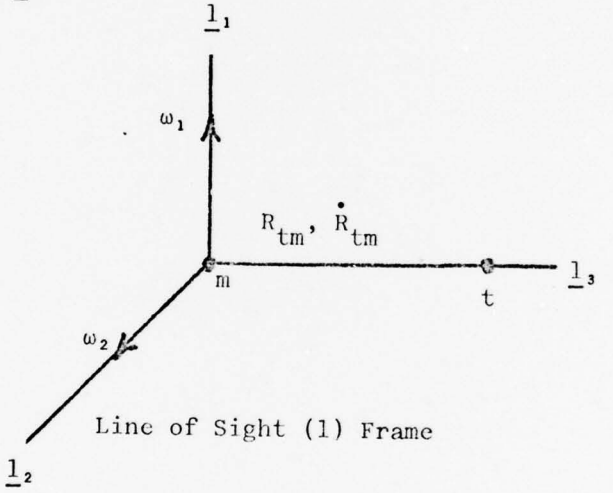
m = missile center of mass

t = center of target's tracking radar

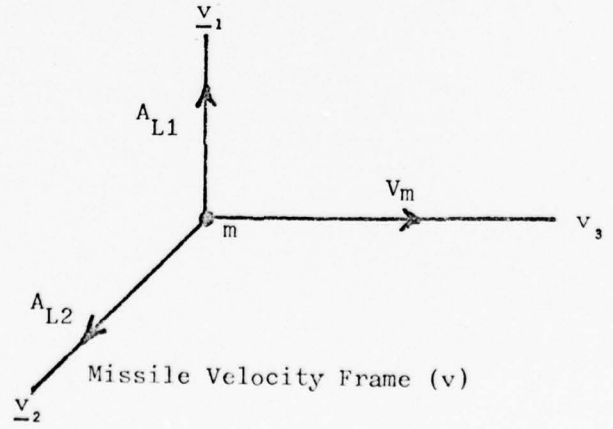
V_m = velocity of missile



Inertial (i) Frame



Line of Sight (l) Frame



Missile Velocity Frame (v)

Fig. 44. The Three Filter Frames

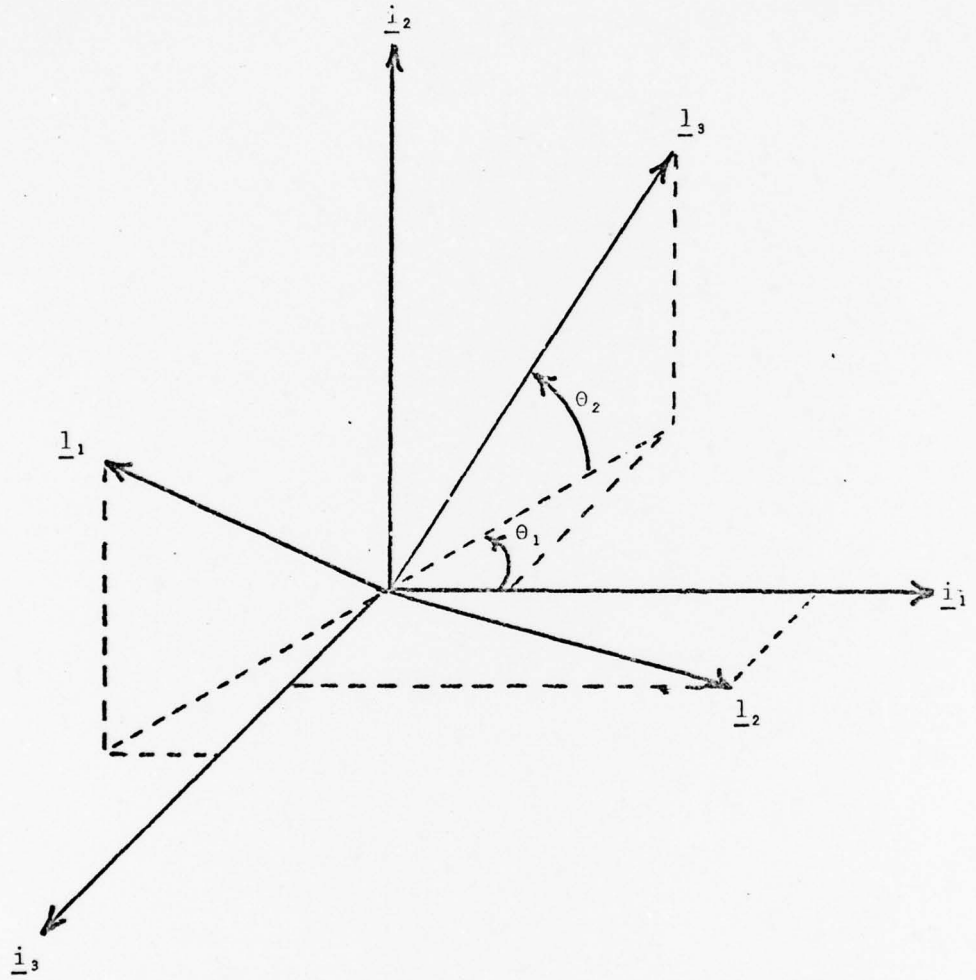


Fig. 45. Angular Orientation Between i and l Frames

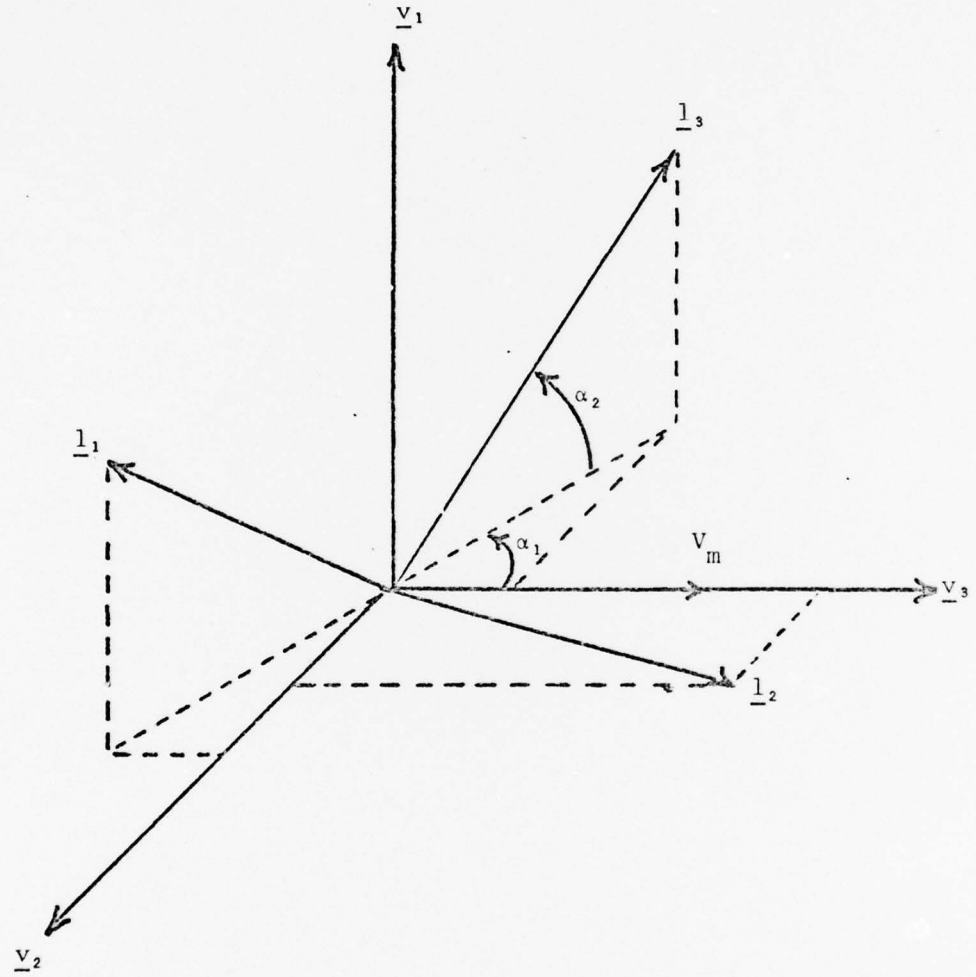


Fig. 46. Angular Orientation Between v and l Frames

2. The actual missile is non-thrusting.

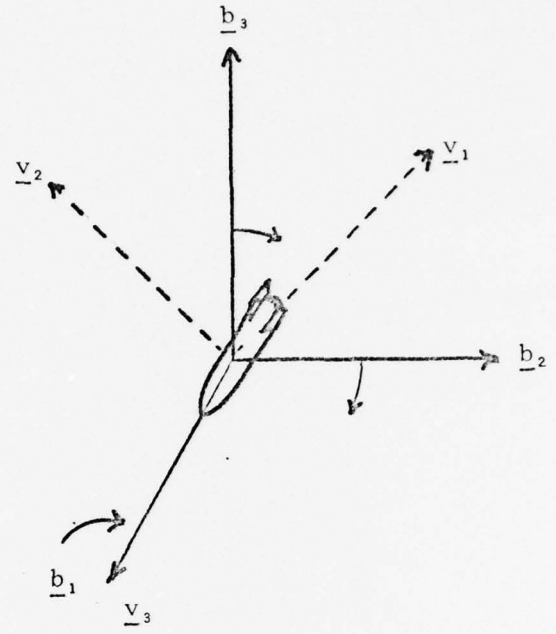
3. Actual pitch and yaw missile responses are adequately modeled by two independent, symmetrical (identical), first order lag networks.

4. The actual missile's pitch axis is constrained to the ($\underline{l}_1$, $\underline{l}_3$) plane; while simultaneously, the $\underline{l}_2$ axis is constrained to the ($\underline{i}_1$, $\underline{i}_3$) plane.

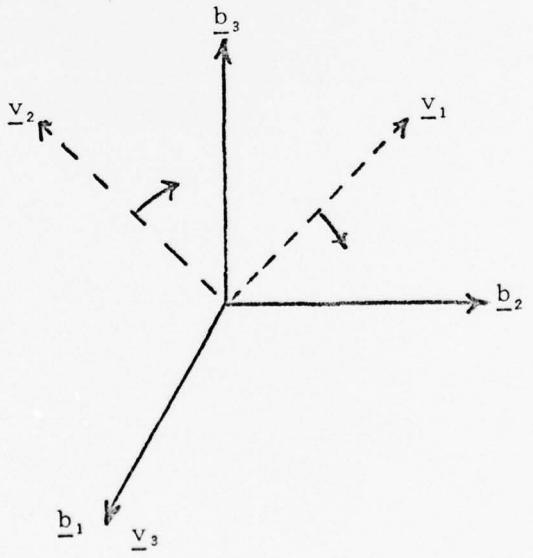
The first two assumptions limit the scope of the problem. The third assumption is shown to be adequate in the literature (Ref 1). The fourth assumption must still be demonstrated.

In reality, the fourth assumption is an approximation that is made to reduce the complexity of the filter equations. Analysis shows that if the actual missile's response is symmetrical (assumption 3), then the angle between the actual missile's response planes and the corresponding response planes in the filter's model does not introduce error to the model provided roll axes of 2 missile models remain colinear. This is not true for asymmetrical missiles, nor is it true if the angle is not constant. Under the assumptions of this thesis, there are two ways the angle can change - through inertial missile roll and/or through inertial model roll (see Figure 47).

Inertial missile roll is a physical phenomena associated with missiles and is composed of two quantities - roll stablization and induced missile roll. Roll stabilization is a constant, or near constant, inertial angular velocity along the missile's roll axis that is present when the missile is flying a straight line. It is assumed to be zero for the purposes of this thesis. Induced missile roll, which is also an inertial quantity, is zero except when the missile performs a



Inertial Missile Roll (Model Inertially Non-rolling)



Inertial Model Roll (Missile Inertially Non-rolling)

Fig. 47. Missile-Model Roll

turn (see Chapter II, Target Model). The effects of induced missile roll are assumed to be negligible to reduce the complexity of the filter equations. The truth model, however, models induced missile roll to insure that this assumption is valid.

Inertial model roll is a modeling error induced when the angle between the missile centerline and the line of sight changes. It is caused by the constraint on the missile's pitch axis, i.e. assumption 4 of the filter model. It can be eliminated if α_1 and α_2 are defined to be Euler rotation angles from the v frame to the i frame, rather than from the v to 1 frames. However, the mathematical relationships for the state model become much more complex under this new definition. In addition, preliminary analysis indicates minimal adverse effects from model roll (see Appendix B). Therefore α_1 and α_2 are defined to be Euler rotation angles from the v to 1 frame to simplify the filter equations.

Filter Tests

The three dimensional filter is tested against each K set trajectory. The complete computer program (except a matrix inversion routine called MINV) that is used for the tests is contained in Appendix D. A complete set of statistical plots, as well as tuning specifications, is contained in Appendix E.

For each test, the filter states are initialized to the true values. The initial true values for θ_1, θ_2, ω_1, ω_2, R_{tm}, and $\dot{R}_{tm}$ are calculated from the missile's and target's initial position and velocity. Missile lateral accelerations are set equal to zero. The parameters n_f and $(m/s)_f$ are set to the values used by the truth model.

τ_f, however, is set to the value that hopefully best approximates the missile's response characteristics. In this thesis, the true value is set at 0.7 seconds, causing initial transients in the filter's estimate of τ_f. These transients are characteristic of an initial state error. In Cusumano and DePonte's thesis, the true value is estimated at 0.85 seconds (Ref 1:85). Since the missile truth model that is used in this thesis is an extension of Cusumano and DePonte's missile truth model, the true value of τ_f should be 0.85 seconds. Time constraints on this thesis prevent correction of this error.

The tuning parameters for all tests are identical and are obtained by tuning the 11-state filter for the K set one trajectory. Due to time limitations, the filter is not fine tuned for maximum performance on K set one (but reasonably good tuning is achieved), nor is any tuning attempted with the other trajectories. Therefore, the filter is not fully designed for use in a three dimensional environment. It is felt that these tests will provide insights and indications of potential filter accuracies and problem areas, as well as insights for final tuning.

The tuning philosophy used to tune the 11-state filter is identical to the philosophy used by Cusumano and DePonte (Ref 1:74-76). Basically, the values chosen for the filter's measurement noise model are derived from the tracker radar's performance specifications. The pseudo-noise strength, Q_f, and the initial filter covariance P_0, are varied until the variance of the filter's state estimate is less than the filter's estimate of the variance for that state. This insures that the filter's confidence in its state estimates reflect the estimate's true statistical nature. After this variance matching is accomplished,

noise strengths are further increased to remove any residual biases in the state estimates.

V. Results and Recommendations

Results

The 11-state filter provides good state estimation for the three dimensional K set one trajectory. Its results are compared to the corresponding results obtained by Cusumano and DePonte for a two dimensional system (Ref 2). Better accuracies in the pointing-tracking states (θ_1, θ_2, ω_1, ω_2, R_{tm}, and $\dot{R}_{tm}$) are achieved probably due to the additional angular velocity measurements. Accuracies similar to Cusumano and DePonte's are achieved for the lateral acceleration and parameter states. It is at this level of performance that filter tuning is stopped, since time limitations prevented further investigation. Therefore, this performance is not necessarily the best that the filter can do, although enough tuning was accomplished to show that it is close.

To test the robustness of the K set one filter tuning, the K set one tuned filter is tested against the K sets two, three, and four trajectories. In each of these tests, the filter's estimation of the pointing-tracking states is degraded, yet still within the accuracies demonstrated by Cusumano and DePonte (Ref 2), making these states usable in an aided pointing-tracking system. The estimates of the lateral acceleration states and their corresponding parameters (n_f and τ_f) are more seriously degraded making them unusable for threat evaluation or threat avoidance in some trajectories. Close inspection of the results reveals that the n_f and τ_f parameters are allowed to

vary too much too quickly due to a rather large value for the corresponding pseudonoise strength. Thus, the filter has less confidence in its estimate of these parameters than the statistics show is warranted, i.e. the filter is too conservative (see Appendix E). For K set one (and Cusumano and DePonte's filter versus their trajectory), this large pseudonoise strength is appropriate since good estimation is achieved. But for other trajectories, this conservative tuning degrades the filter's performanace.

The parameters n_f and τ_f are both used to compute the lateral accelerations of the missile. If an error is present in one of the parameter estimates (such as τ_f), the other is affected. Since each trajectory affects the lateral accelerations of the missile differently, the parameter interaction is different for each trajectory. For K set two, for instance, the effects of the n_f and τ_f parameter errors on the lateral acceleration estimates tend to add, causing a serious degradation in the filter's estimate of lateral accelerations. At the end of the trajectory, this degradation becomes important enough to "pull" some of the pointing-tracking states away from their true value. For K set three, the effects of these parameter errors tend to cancel. Thus, lateral acceleration estimates are better than in K set two. Different tuning specifications are necessary to stablize the performance of the n_f and τ_f filter states. Unfortunately, time limitations prevent the accomplishment of any additional tuning tests.

These tests demonstrate the filter's robustness for the pointing-tracking states. Pointing and tracking accuracies equal to or better than those achieved by Cusumano and DePonte are demonstrated over four trajectories. The performance of the parameter states indicate that

different parameter pseudonoise values are required to increase the accuracies of the n_f, τ_f, A_{L1}, and A_{L2} state estimates against K sets two, three, and four trajectories. Further tuning and testing of this filter is required to determine if one appropriate set of tuning specifications will provide adequate performance of these states for all trajectories.

Recommendations

The following recommendations are made to guide future research:

1. Optimal tuning should be accomplished for each remaining trajectory. The robustness of each set of tuning specifications should be investigated to find which set, or if a compromise set, of tuning specifications can provide adequate performance over all trajectories.
2. The performance of an adaptive gain version of this filter should be investigated to see if the additional performance achieved is worth the additional filter complexity.
3. First order Markov models for missile lateral acceleration should be investigated. This model should provide better performance against those missiles whose guidance does not approximate the proportional navigation rule. In addition, it should decrease the filter complexity. However, this model will not be as accurate as the 11-state filter if it engages a proportional navigation missile.
4. The 11-state filter should be tested with the gravity vector defined along the $-\underline{i}_2$ axis. If feasible, this step will simplify the filter equations.

5. A missile acceleration model based upon a polar coordinate system should be investigated. It might be possible to model both the missile's acceleration magnitude and the acceleration vector's position angle as the outputs of first order lags. Missile roll can be modeled easily this way as the derivative of the position angle. In addition, time lags that cause a spiraling missile trajectory, such as in the sidewinder missile, would be easily handled by this system. However, asymmetrical missiles may cause problems.
6. The time between measurement updates should be lengthened to discover its effects on filter performance.
7. A thrusting missile should be modeled to increase the effective use of this filter. An adaptive filter could change the $(m/s)_f$ state to an acceleration due to thrust state, thus modeling thrust as a random walk without an increase in states. This may be possible if missile thrusts are generally much greater than drag, making the drag induced by the missile's lateral acceleration negligible. Otherwise, drag may require modeling as well as thrust.

Bibliography

1. Cusumano, S. J. and M. DePonte. An Extended Kalman Filter Fire Control System Against Air to Air Missiles (Vol. I). Unpublished thesis. Wright-Patterson Air Force Base, Ohio: Air Force Institute of Technology, December 1977.

2. Cusumano, S. J. and M. DePonte. An Extended Kalman Filter Fire Control System Against Air to Air Missiles (Vol. II). Unpublished thesis. Wright-Patterson Air Force Base, Ohio: Air Force Institute of Technology, December 1977.

3. D'Azzo, J. J. and C. H. Houpis. Linear Control System Analysis and Design. New York: McGraw-Hill Book Company, 1975.

4. Fitts, J. M. "Aided Tracking as Applied to High Accuracy Point Systems." IEEE TRANSACTIONS on Aerospace and Electronic Systems, AES-9: 350-368, May 1973.

5. Lutter, R. N. Application of an Extended Kalman Filter to an Advanced Fire Control System. Unpublished thesis. Wright-Patterson Air Force Base, Ohio: Air Force Institute of Technology, December 1976.

6. Kjesbo, L. A. Terminal Miss Sensitivity of a Radar Guided Air-to-Air Missile System. Unpublished thesis. Wright-Patterson Air Force Base, Ohio: Air Force Institute of Technology, June 1974.

7. Maybeck, P. S. Stochastic Estimation and Control Systems (Part I). Unpublished manuscript. Wright-Patterson Air Force Base, Ohio: Air Force Institute of Technology, February 1975.

8. Maybeck, P. S. Stochastic Estimation and Control Systems (Part II). Unpublished manuscript. Wright-Patterson Air Force Base, Ohio: Air Force Institute of Technology, February 1975.

9. Pearson, J. B. III. and E. B. Stear. "Kalman Filter Applications in Airborne Radar Tracking". IEEE TRANSACTIONS on Aerospace and Electronic Systems, AES-10: 319-329, May 1974.

10. Price, C. F. and W. D. Koeningsburg. Adaptive Control and Guidance for Tactical Missiles. TASC TR-170-1. Reading, Massachusetts: The Analytic Sciences Corporation, June 1970.

11. Stallard, D. V. Classical and Modern Guidance of Homing Interceptor Missiles. Technical report. Presented to Seminar of Department of Aeronautics and Astronautics, Cambridge, Massachusetts: Massachusetts Institute of Technology, April 1968.

12. Stockum, L. A. A Study of Guidance Controllers for Homing Missiles. Unpublished Dissertation. Columbus, Ohio: Ohio State University, 1974.

13. Taylor, J. D. "An Introduction to Air-to-Air Missile (AAM) Trajectories with Proportional Navigation or The Vulture Missile System", working paper written for 6586th Test Group, Holloman Air Force Base, New Mexico, May 1975.

14. Thomson, W. T. Introduction to Space Dynamics. New York: John Wiley & Sons, Inc., 1961.

15. Van Cott, H. P. and R. G. Kinkade. Human Engineering Guide to Equipment Design (Second Edition). Washington, D. C: U. S. Government Printing Office, 1972.

16. Wrigley, W. and W. M. Hollister and W. G. Denhard. Gyroscopic Theory, Design, and Instrumentation. Cambridge, Massachusetts: The Massachusetts Institute of Technology Press, 1969.

Appendix A

Rotation of a Vector

Throughout the missile model, numerous rotations of a unit vector must be accomplished, such as in the application of noise to the line of sight. This appendix describes the method used in this thesis to determine the resulting direction of a unit vector after one planar rotation.

Three conditions are required by this method:

1) Two unit vectors, $\underline{a}$ and $\underline{b}$, must define the plane of rotation: ρ is the angle of rotation, θ is the angle between $\underline{a}$ and $\underline{b}$.
2) Unit vector $\underline{b}$ is the vector to be rotated, resulting in unit vector $\underline{c}$.
3) Positive θ is from $\underline{a}$ to $\underline{b}$; positive ρ is from $\underline{b}$ to $\underline{c}$.

These three conditions are depicted in Figure A-1. The angle θ can be found through the dot product formula to be:

$$\theta = \cos^{-1}(\underline{a} \cdot \underline{b}) \tag{49}$$

With the given conditions and the defined angle θ, three equations can be generated to describe vector $\underline{c}$:

$$(\underline{a} \times \underline{b}) \cdot \underline{c} = 0 \tag{50}$$

$$\underline{a} \cdot \underline{c} = \cos(\theta + \rho) \tag{51}$$

$$\underline{b} \cdot \underline{c} = \cos(\rho) \tag{52}$$

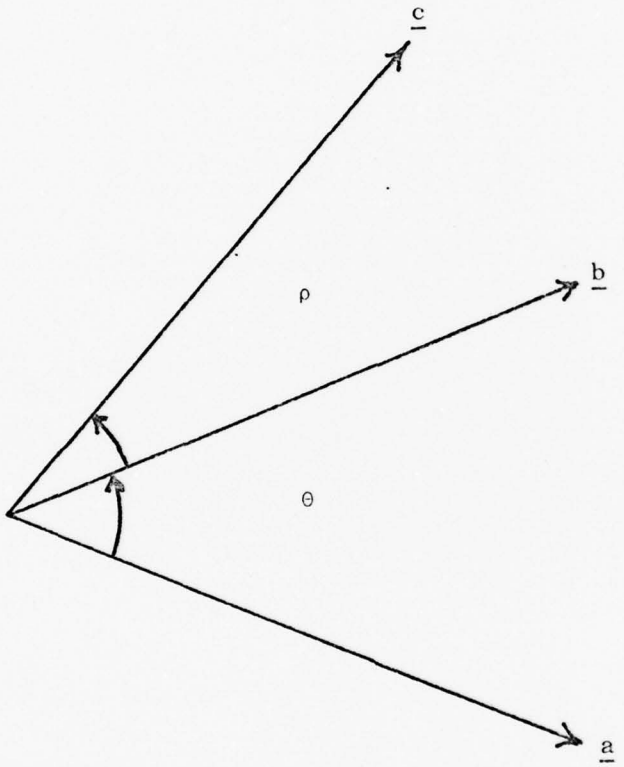


Fig. A-1. Rotation of a Unit Vector (All vectors are in the plane of this paper.)

Let $\underline{a} = \begin{bmatrix} a_1 \\ a_2 \\ a_3 \end{bmatrix}$ $\underline{b} = \begin{bmatrix} b_1 \\ b_2 \\ b_3 \end{bmatrix}$ $\underline{c} = \begin{bmatrix} c_1 \\ c_2 \\ c_3 \end{bmatrix}$

When equations (50), (51), and (52) are put in the matrix form $T\underline{C} = \underline{D}$,

$$\begin{bmatrix} a_2b_3 - a_3b_2 & a_3b_1 - a_1b_3 & a_1b_2 - a_2b_1 \\ a_1 & a_2 & a_3 \\ b_1 & b_2 & b_3 \end{bmatrix} \begin{bmatrix} c_1 \\ c_2 \\ c_3 \end{bmatrix} \quad \begin{bmatrix} 0 \\ \cos(\theta+\rho) \\ \cos(\rho) \end{bmatrix} \tag{53}$$

Premultiplying by T^{-1} yields $\underline{c} = T^{-1}\underline{D}$. T^{-1} is

$$\left(\frac{1}{X_1^2 + X_2^2 + X_3^2} \right) \begin{bmatrix} X_1 & b_2X_3 - b_3X_2 & X_2a_3 - X_3a_2 \\ X_2 & b_3X_1 - b_1X_3 & X_3a_1 - X_1a_3 \\ X_3 & b_1X_2 - b_2X_1 & X_1a_2 - X_2a_1 \end{bmatrix} \tag{54}$$

where $X_1 = a_2b_3 - a_3b_2$

$X_2 = a_3b_1 - a_1b_3$

$X_3 = a_1b_2 - a_2b_1$

Solving for the components of $\underline{C}$ yield:

$$c_1 = \frac{(b_2X_3 - b_3X_2)\cos(\theta+\rho) + (X_2a_3 - X_3a_2)\cos(\rho)}{X_1^2 + X_2^2 + X_3^2}$$

$$c_2 = \frac{(b_3X_1 - b_1X_3)\cos(\theta+\rho) + (X_3a_1 - X_1a_3)\cos(\rho)}{X_1^2 + X_2^2 + X_3^2}$$

$$c_3 = \frac{(b_1X_2 - b_2X_1)\cos(\theta+\rho) + (X_1a_2 - X_2a_1)\cos(\rho)}{X_1^2 + X_2^2 + X_3^2}$$

The computer program that employs this technique is subroutine TIN in Appendix D.

Appendix B

Appendix B contains the mathematical derivation of the filter state equations. The eleven states used in the filter are:

θ_1 - first Euler rotation from inertial frame to line of sight frame (rad)

θ_2 - second Euler rotation from inertial frame to line of sight frame (rad)

ω_1 - inertial angular velocity of line of sight frame along first line of sight frame axis (rad/sec)

ω_2 - inertial angular velocity of line of sight frame along second line of sight frame axis (rad/sec)

R_{tm} - missile position relative to tracker position in line of sight frame (kiloft = 10^3 ft)

$\dot{R}_{tm}$ - rate of change of R_{tm} along the line of sight (kiloft/sec)

A_{L1} - lateral acceleration of missile along first missile velocity frame axis (kiloft/sec^2)

A_{L2} - lateral acceleration of missile along second missile velocity frame axis (kiloft/sec^2)

n_f - proportional navigation constant

τ_f - first order lag time constant for filter model of missile (sec)

$(m/s)_f$ - mass to effective surface ratio of missile (slug/kiloft^2)

The state units are so chosen to insure that each element of the Kalman filter gain matrix is of the same order of magnitude, thus avoiding computer numerical difficulties.

Three reference frames are required for the derivation: the missile velocity frame, v; the line of sight frame, 1; and the inertial frame, i. The relationship between each frame is part of the derivation and will be described at the appropriate time. The first part of the derivation develops the relationship between the missile velocity frame, v, and the line of sight frame, 1, in terms of the states.

Let j be the origin of the inertial frame; m be the origin of the line of sight frame, and t be the center of the target aircraft's radar. The missile is assumed to be a point mass located at m. The target, t, is located on the $\underline{1}_3$ (line of sight frame third component) axis a distance R_{mt} from the missile (see Figure B-1). The vector relationship between the points j, m, and t is:

$$\underline{R}_{jm} = \underline{R}_{jt} - \underline{R}_{mt} \tag{55}$$

Taking the first derivative of equation (55) to determine missile velocity,

$$p_i \, \underline{R}_{jm} = p_i \, \underline{R}_{jt} - p_i \, \underline{R}_{mt} \tag{56}$$

where p_i = rate of change as seen from the i frame

The theorem of Coriolis is

$$p_i \, \underline{R} = p1 \, \underline{R} + \underline{\Omega}_{i1} \times \underline{R} \tag{57}$$

where $\underline{R}$ = any vector

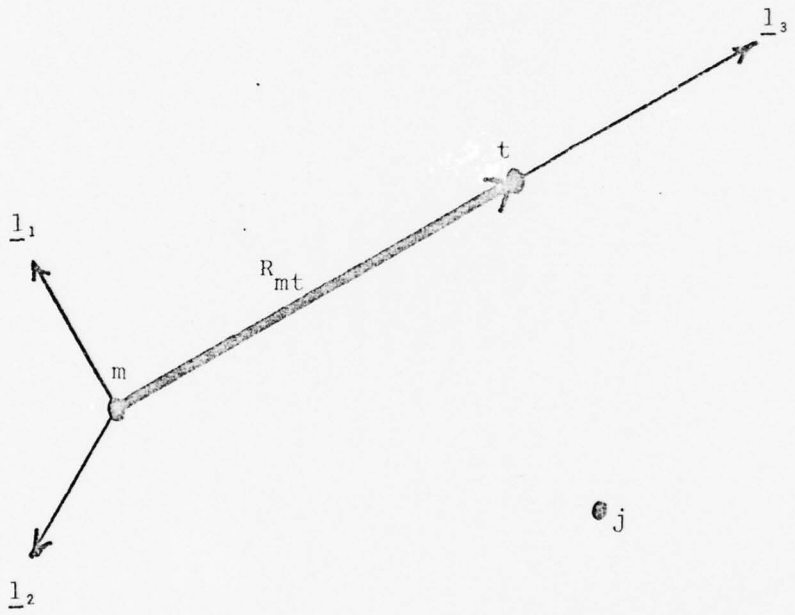


Fig. B-1. Points m, t, and j in the Line of Sight Frame

$\underline{\Omega}_{il}$ = angular velocity of 1 frame with respect to i frame

p_1 = rate of change as seen from the 1 frame

Substituting (57) into (56) yields

$$p_i \underline{R}_{jm} = p_i \underline{R}_{jt} - p_1 \underline{R}_{mt} - \underline{\Omega}_{il} \times \underline{R}_{mt} \tag{58}$$

Equation (58) can be coordinatized in the 1 frame and expressed in vector form as:

$$(p_i \underline{R}_{jm})^1 = (p_i \underline{R}_{jt})^1 - (p_1 \underline{R}_{mt})^1 - (\underline{\Omega}_{il} \times \underline{R}_{mt})^1 \tag{59}$$

or

$$\begin{bmatrix} V_{m_1} \\ V_{m_2} \\ V_{m_3} \end{bmatrix} = \begin{bmatrix} V_{t_1} \\ V_{t_2} \\ V_{t_3} \end{bmatrix} - \begin{bmatrix} 0 \\ 0 \\ \dot{R}_{mt} \end{bmatrix} - \begin{bmatrix} \omega_1 \\ \omega_2 \\ \omega_3 \end{bmatrix} \times \begin{bmatrix} 0 \\ 0 \\ R_{mt} \end{bmatrix} \tag{60}$$

Performing the operation on equation (60) yields the following three scalar equations for inertial missile velocity coordinatized in the line of sight frame:

$$V_{m1} = V_{t_1} - \omega_2 R_{mt} \tag{61}$$

$$V_{m2} = V_{t_2} + \omega_1 R_{mt} \tag{62}$$

$$V_{m3} = V_{t_3} - \dot{R}_{mt} \tag{63}$$

V_{t_1}, V_{t_2}, and V_{t_3} are the inertial velocities of the target, which are obtained from the target's navigation system. These values are considered deterministic since the measurement precision of the target

velocity is much greater than the measurement precision of the states.

The $\underline{v}_3$ axis of the right hand orthogonal missile velocity frame, v, is defined to be along the missile velocity vector. Two Euler angles, α_1 and α_2, are defined in Figure B-2 to describe the rotations from the v frame to the 1 frame. The transformation matrix from the v to 1 frame is:

$$C_v^1 = \begin{bmatrix} \cos\alpha_2 & \sin\alpha_1 \sin\alpha_2 & -\cos\alpha_1 \sin\alpha_2 \\ 0 & \cos\alpha_1 & \sin\alpha_1 \\ \sin\alpha_2 & -\sin\alpha_1 \cos\alpha_2 & \cos\alpha_1 \cos\alpha_2 \end{bmatrix} \tag{64}$$

The relationship between the missile velocity in the v and 1 frames is:

$$\begin{bmatrix} 0 \\ 0 \\ V_m \end{bmatrix}^v = \begin{bmatrix} \cos\alpha_2 & 0 & \sin\alpha_2 \\ \sin\alpha_1 \sin\alpha_2 & \cos\alpha_1 & -\sin\alpha_1 \cos\alpha_2 \\ -\cos\alpha_1 \sin\alpha_2 & \sin\alpha_1 & \cos\alpha_1 \cos\alpha_2 \end{bmatrix} \begin{bmatrix} V_{m_1} \\ V_{m_2} \\ V_{m_3} \end{bmatrix}^1 \tag{65}$$

Solving equation (65) for the first component of the missile velocity in the v frame, and substituting in equations (62) and (63) yields:

$$\alpha_2 = \tan^{-1}\left(\frac{-V_{t_1} + \omega_2 R_{mt}}{V_{t_3} - \dot{R}_{mt}}\right) \tag{66}$$

Solving equation (65) for the second component and using equations (61), (62), and (63) yields:

$$\alpha_1 = \tan^{-1}\left(\frac{V_{t_2} + \omega_1 R_{mt}}{(V_{t_3} - \dot{R}_{mt})\cos\alpha_2 - (V_{t_1} - \omega_2 R_{mt})\sin\alpha_2}\right) \tag{67}$$

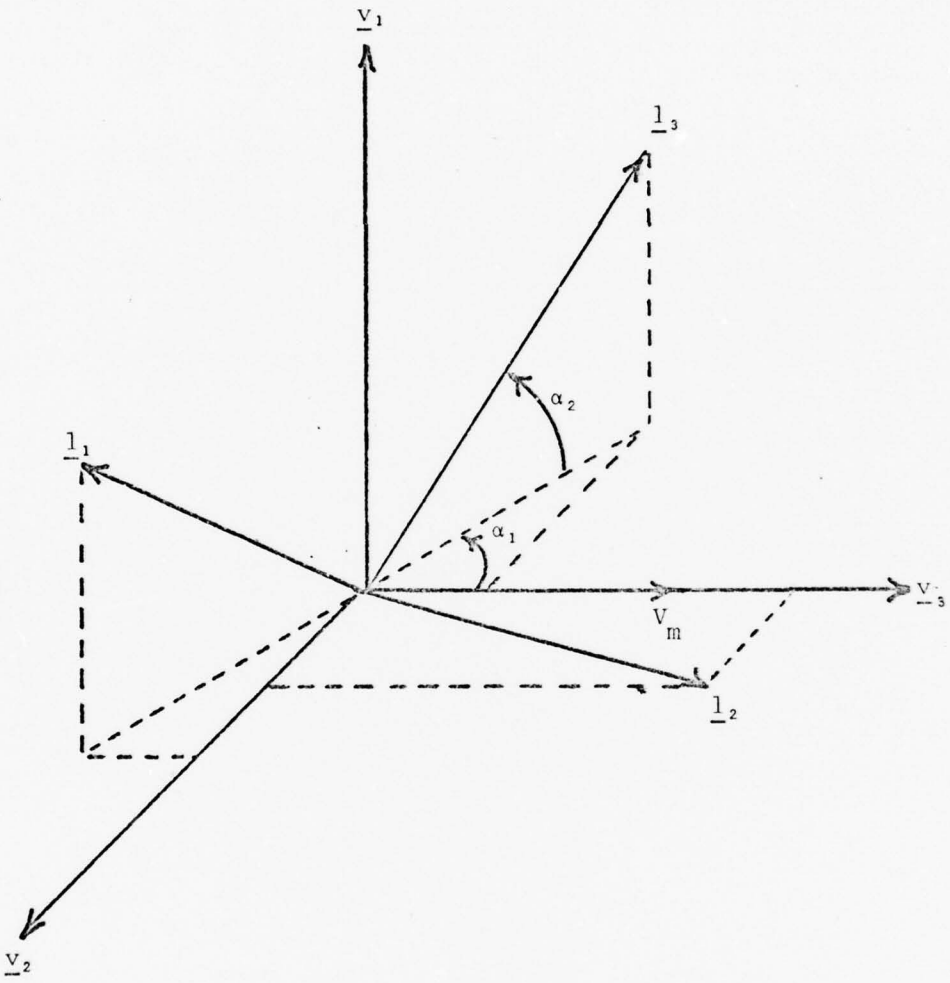


Fig. B-2. Angular Orientation Between v and l Frames

If equation (66) is solved for $-(V_{t_1} - \omega_2 R_{mt})$ and substituted into equation (67), equation (67) reduces to:

$$\alpha_1 = \tan^{-1}\left(\frac{(V_{t_2} + \omega_1 R_{mt})\cos\alpha_2}{V_{t_3} - \dot{R}_{mt}}\right) \tag{68}$$

Since $R_{mt} = -R_{tm}$ and $\dot{R}_{mt} = -\dot{R}_{tm}$,

$$\alpha_2 = \tan^{-1}\left[\frac{-V_{t_1} - \omega_2 R_{tm}}{V_{t_3} + \dot{R}_{tm}}\right] \tag{69}$$

$$\alpha_1 = \tan^{-1}\left[\frac{(V_{t_2} - \omega_1 R_{tm})\cos\alpha_2}{V_{t_3} + \dot{R}_{tm}}\right] \tag{70}$$

Thus, the relationship between the v and 1 frames is established in terms of the states. Note: α_1 and α_2 are the Euler angles from the missile velocity to the line of sight. If the two limits, $-\pi/2 \leq \alpha_1 \leq \pi/2$, $-\pi/2 \leq \alpha_2 \leq \pi/2$ are exceeded, it can be assumed that the missile is in an invalid regime for intercept.

The proportional navigation law is used to develop state equations for A_{L1} and A_{L2}. This law in equation form is (Ref 11:13)

$$\underline{A}_p = n(\underline{\Omega}_{i1} \times \dot{R}_{tm}) \tag{71}$$

where $\underline{A}_p$ = acceleration required perpendicular to the line of sight and $\underline{\Omega}_{i1}$

$\underline{\Omega}_{i1}$ = line of sight inertial angular velocity

n = proportionality constant

However, missiles produce accelerations perpendicular to the missile

velocity, not the line of sight (see Chapter II, Guidance Block, for more detail). The proportional navigation equations most missiles implement are:

$$A_{c_1} = n\ \omega_2\ \dot{R}_{tm} \tag{72}$$

$$A_{c_2} = -n\ \omega_1\ \dot{R}_{tm} \tag{73}$$

where A_{c_1} and A_{c_2} are commanded accelerations perpendicular to the missile velocity.

To obtain A_{L1} and A_{L2}, the produced accelerations, the time response of the missile must be taken into account. Cusumano and DePonte found that the time response of a missile can be adequately modeled by a first order lag, since the bandwidth effects of the guidance prefilter are dominant (Ref 1:117). Using this model, equations (72) and (73) become

$$A_{L1} = \frac{n_f\ \omega_2\ \dot{R}_{tm}}{\mathcal{s}\tau_f + 1} \tag{74}$$

$$A_{L2} = \frac{-n_f\ \omega_1\ \dot{R}_{tm}}{\mathcal{s}\tau_f + 1} \tag{75}$$

where $\mathcal{s}$ = Laplace transform "s"

Manipulation of equations (74) and (75) yields

$$\dot{A}_{L1} = \frac{n_f\ \omega_2\ \dot{R}_{tm} - A_{L1}}{\tau_f} \tag{76}$$

$$\dot{A}_{L2} = \frac{-n_f\ \omega_1\ \dot{R}_{tm} - A_{L2}}{\tau_f} \tag{77}$$

which are the state equations of A_{L1} and A_{L2} in terms of the other

states. To allow possible asymmetrical missile response, the n_f and/or τ_f could be different between equations (76) and (77), adding one or two additional filter states. This concept is not investigated.

To develop state equations for states ω_1, ω_2, and R_{tm}, the acceleration of the missile in the line of sight frame is derived. The second derivative of equation (55) is:

$$p_i^2 \underline{R}_{jm} = p_i^2 \underline{R}_{jt} - p_i^2 \underline{R}_{mt} \tag{78}$$

or

$$p_i^2 \underline{R}_{jm} = p_i^2 \underline{R}_{jt} + p_i^2 \underline{R}_{tm} \tag{79}$$

Applying the theorem of Coriolis (equation (57)) twice to equation (79) yields:

$$p_i^2 \underline{R}_{jm} = p_i^2 \underline{R}_{jt} + p_1^2 \underline{R}_{tm} + 2\underline{\Omega}_{i1} \times p_1 \underline{R}_{tm} + p_1 \underline{\Omega}_{i1} \times \underline{R}_{tm} + \underline{\Omega}_{i1} \times (\underline{\Omega}_{i1} \times \underline{R}_{tm}) \tag{80}$$

Coordinatizing equation (80) into the 1 frame,

$$\begin{bmatrix} A_{m_1} \\ A_{m_2} \\ A_{m_3} \end{bmatrix} = \begin{bmatrix} A_{t_1} \\ A_{t_2} \\ A_{t_3} \end{bmatrix} + \begin{bmatrix} 0 \\ 0 \\ \dot{R}_{tm} \end{bmatrix} + \begin{bmatrix} 2\omega_1 \\ 2\omega_2 \\ 2\omega_3 \end{bmatrix} \times \begin{bmatrix} 0 \\ 0 \\ \dot{R}_{tm} \end{bmatrix} + \begin{bmatrix} \dot{\omega}_1 \\ \dot{\omega}_2 \\ \dot{\omega}_3 \end{bmatrix} \times \begin{bmatrix} 0 \\ 0 \\ R_{tm} \end{bmatrix} + \begin{bmatrix} \omega_1 \\ \omega_2 \\ \omega_3 \end{bmatrix} \times \begin{bmatrix} \omega_1 \\ \omega_2 \\ \omega_3 \end{bmatrix} \times \begin{bmatrix} 0 \\ 0 \\ R_{tm} \end{bmatrix} \tag{81}$$

where A_{m_1}, A_{m_2}, A_{m_3} = inertial acceleration of missile along $\underline{1}_1$, $\underline{1}_2$, $\underline{1}_3$ axes, respectively

A_{t_1}, A_{t_2}, A_{t_3} = inertial acceleration of tracker along $\underline{1}_1$, $\underline{1}_2$, $\underline{1}_3$ axes, respectively

The acceleration of the target is assumed to be deterministic and known to the estimation algorithm residing in the target. The inertial acceleration of the missile, $p_i{}^2\underline{R}_{jm}$, is composed of gravity, induced accelerations (A_{L1} and A_{L2}), and drag (A_D). Note that the missile is modeled as non-thrusting. In addition, the lateral accelerations, A_{L1} and A_{L2}, are assumed to be along the $\underline{v}_1$ and $\underline{v}_2$ axes, respectively; this assumption requires the missile angle of attack to be small, which is quite appropriate. Moreover, the missile must not roll with respect to the v frame. The zero roll assumption is not appropriate when missiles are roll stablized, nor may it be appropriate when the line of sight frame rotates with respect to the inertial frame. Two effects degrade the validity of the zero roll assumption when the line of sight rotates - model induced roll and induced missile roll. Model induced roll is present when the angle between the line of sight vector and the missile velocity vector changes. It is caused by the definition of α_1 and α_2 in the model, i.e. constraining the v frame to the rotating l frame rather than to the non-rotating inertial frame. Induced missile roll is a physical phenomena caused by the missile's inertial turn (see Chapter II, Target Model).

Model induced roll is demonstrated by analyzing the three coordinate frames (i, v, and 1) and their relationship to each other. The $\underline{v}_2$ axis is constrained to the ($\underline{1}_2$, $\underline{1}_3$) plane, and the $\underline{1}_2$ axis is constrained to the ($\underline{i}_1$, $\underline{i}_3$) plane by the model's definitions. In Figure B-3, the $\underline{v}_2$ axis is in the ($\underline{i}_1$,$\underline{i}_3$) plane. But in this same

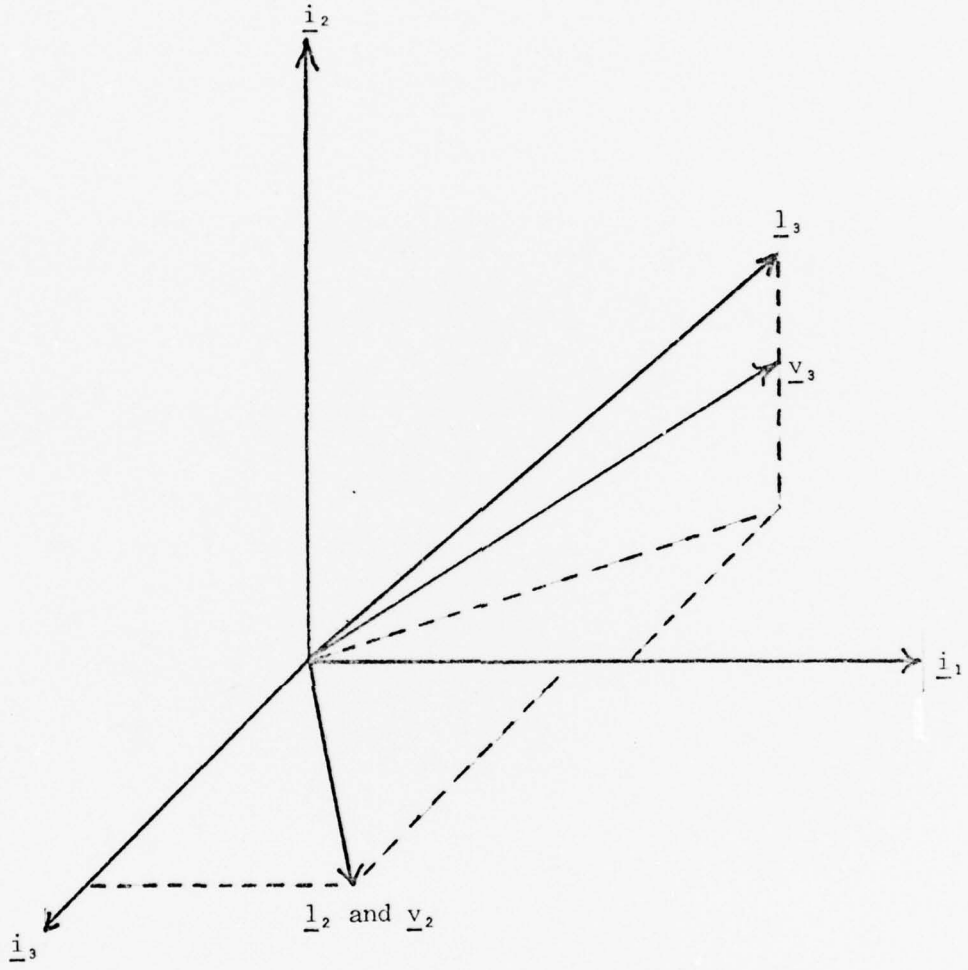


Fig. B-3. 11 State Filter Model's $\underline{v}_2$ Relationship for Time t_1

scenario at a later time instant as depicted in Figure B-4, the line of sight vector has moved. Although the missile does not physically roll, the $\underline{v}_2$ axis must be in a different plane to remain in the $(\underline{1}_2, \underline{1}_3)$ plane. To achieve this effect, there must be an inertial angular velocity along the $\underline{v}_3$ axis, i.e. the model must roll. The amount of roll induced by the model is trajectory dependent.

The model induced roll can be eliminated if α_1 and α_2 are defined as Euler rotation angles from the v to i frame rather than from the v to 1 frame. But the mathematics become more complex. In many encounters, the missile velocity is much greater than the aircraft velocity. This results in a small missile lead angle. Model induced roll effects become less significant as the lead angle becomes small, and vanish completely for zero lead angle. Therefore, an assumption is made that the model induced roll effects will be insignificant. This assumption must be verified by the Monte Carlo analyses.

The induced missile roll, however, is a physical phenomena associated with the actual missile. As a missile performs a turn, a roll is induced upon it. A full explanation of this effect is presented in Chapter II, Target Model. Two methods can be used to account for this roll - direct modeling and indirect modeling. In the direct method, the three dimensional missile model is rotated the appropriate amount as calculated by an accurate model of induced missile roll. In the indirect method, the three dimensional missile model is developed for a missile that rolls. The missile roll is modeled as a constant parameter plus a white Gaussian noise of appropriate strength. However, these techniques are not employed since it is assumed that induced missile roll effects, present only when the line of sight rotates, are negligible.

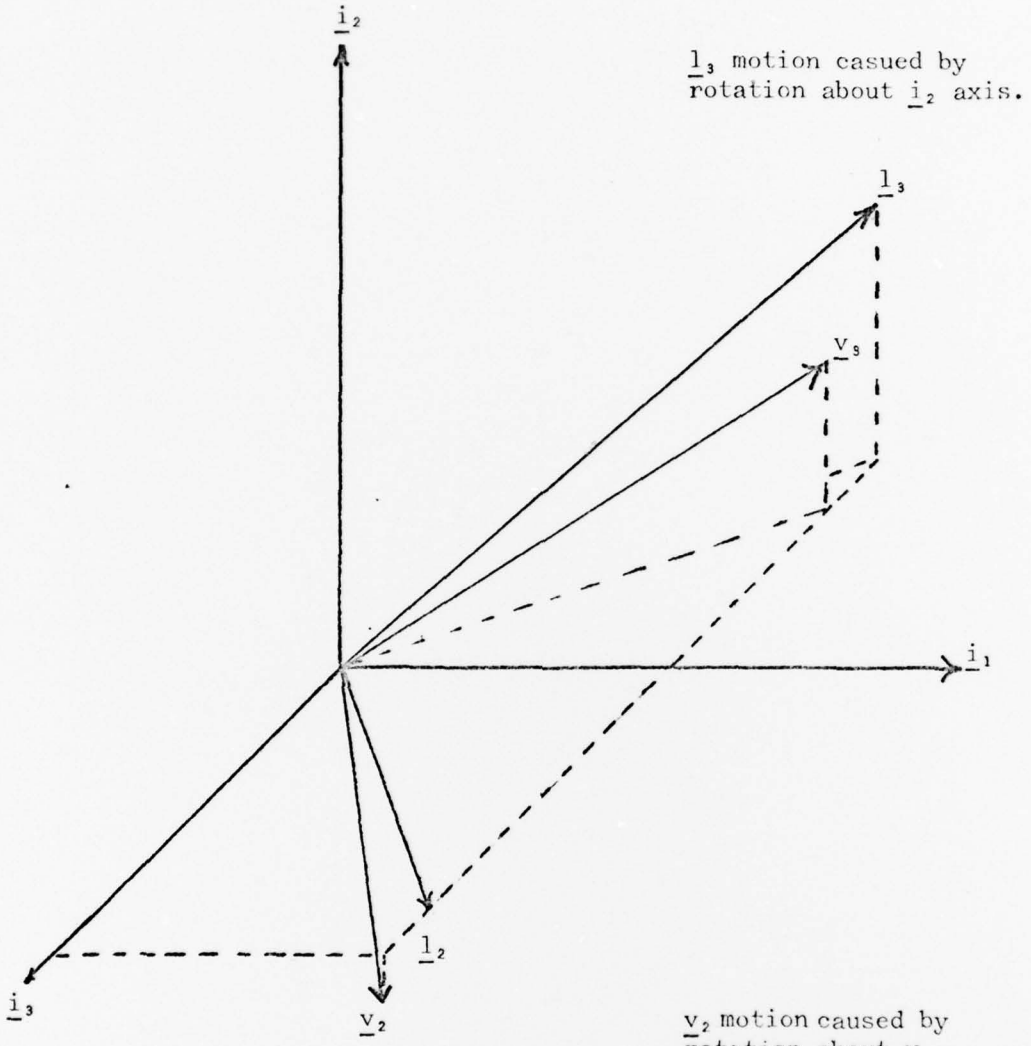


Fig. B-4. 11 State Filter Model's $\underline{v}_2$ Relationship for Time t_2

With these assumptions, then, the inertial acceleration of the missile, in the v frame, is:

$$(p_i{}^2\underline{R}_{jm})^v = \begin{bmatrix} A_{L1} \\ A_{L2} \\ -A_D \end{bmatrix} + C_i^v \, \underline{G}^i \tag{82}$$

where C_i^v = the transformation from the i frame to the v frame

$\underline{G}^i$ = gravity vector in the i frame

Multiplying each term of equation (82) by C_v^l from equation (64) transforms the missile acceleration to the 1 frame:

$$(p_i{}^2\underline{R}_{jm})^l = \begin{bmatrix} A_{L1}\cos\alpha_2 + \sin\alpha_2(A_{L2}\sin\alpha_1 + A_D\cos\alpha_1) \\ A_{L2}\cos\alpha_1 - A_D\sin\alpha_1 \\ A_{L1}\sin\alpha_2 - \cos\alpha_2(A_{L2}\sin\alpha_1 + A_D\cos\alpha_1) \end{bmatrix} + C_i^l \, \underline{G}^i \tag{83}$$

To define gravity in the 1 frame, the transformation from the inertial frame to the 1 frame, C_i^l, must be specified. With θ_1, θ_2, and the coordinate frame relationships as depicted in Figure B-5, the transformation from the i to 1 frame is:

$$C_i^l = \begin{bmatrix} -\cos\theta_1\sin\theta_2 & \cos\theta_2 & \sin\theta_1\sin\theta_2 \\ \sin\theta_1 & 0 & \cos\theta_1 \\ \cos\theta_1\cos\theta_2 & \sin\theta_2 & -\sin\theta_1\cos\theta_2 \end{bmatrix} \tag{84}$$

At this point, an interesting dilemma develops. If gravity is defined to be in the $-\underline{i}_2$ direction, $C_i^l \, \underline{G}^i$ has no component that is dependent upon θ_1. Therefore, none of the states are a function of θ_1. It is felt that this weak coupling of θ_1 might have an adverse effect upon filter performance. This hypothesis is not tested due to time

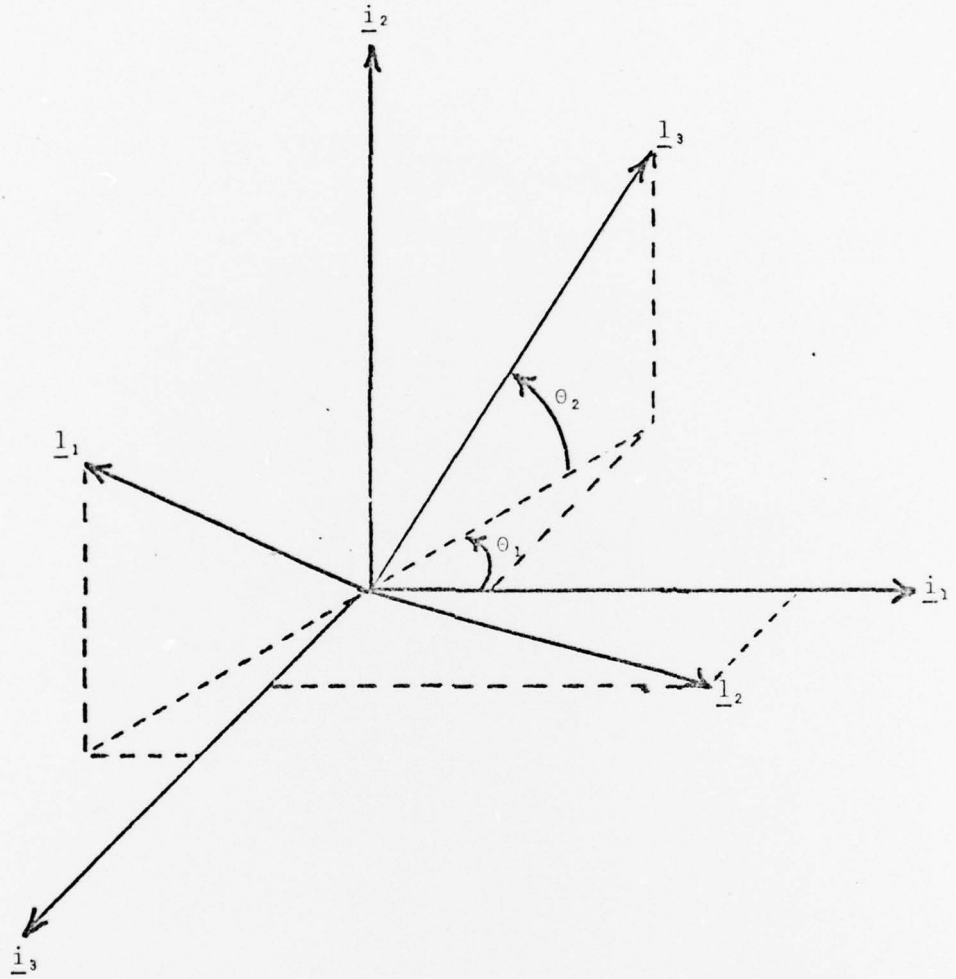


Fig. B-5. Angular Orientation Between i and l frames

limitations. To test it, the truth model gravity vector must be defined in the $-\underline{i}_2$ direction and all terms involving θ_1 must be eliminated in the filter equations (see Appendix B). Therefore, the filter's inertial coordinate frame is physically rotated 45° about the $\underline{i}_1$ axis, such that:

$$\underline{G}^i = \begin{bmatrix} 0 \\ -g/\sqrt{2} \\ -g/\sqrt{2} \end{bmatrix} \tag{85}$$

where g = acceleration due to gravity (kiloft/sec^2)

This definition of the inertial frame couples both θ_1 and θ_2 into the filter equations, avoiding a weakly coupled state. In the computer simulation, the missile truth model is also physically rotated 45° about the $\underline{i}_1$ axis of the truth model's inertial frame. Thus, the filter's i frame and the truth model's i frame have identical orientation. This allows the truth model states to be directly utilized, after unit conversion, for filter measurements and analysis. Putting equation (84) and (85) into (83), and the resulting equation into (81) yields the three scalar equations for missile acceleration:

$$A_{L1} \cos\alpha_2 + \sin\alpha_2(A_{L2} \sin\alpha_1 + A_D \cos\alpha_1) - \frac{g(\cos\theta_2 + \sin\theta_1 \sin\theta_2)}{\sqrt{2}} =$$

$$A_{t_1} + 2\omega_2 \dot{R}_{tm} + \dot{\omega}_2 R_{tm} + \omega_1 \omega_3 R_{tm} \tag{86}$$

$$A_{L2} \cos\alpha_1 - A_D \sin\alpha_1 - \frac{g \cos\theta_1}{\sqrt{2}} = A_{t_2} - 2 \omega_1 \dot{R}_{tm} - \dot{\omega}_1 R_{tm} +$$

$$\omega_2 \omega_3 R_{tm} \tag{87}$$

$$A_{L1} \sin\alpha_2 - \cos\alpha_2 (A_{L2} \sin\alpha_1 + A_D \cos\alpha_1) - \frac{g}{\sqrt{2}} (\sin\theta_2 - \sin\theta_1 \cos\theta_2) =$$

$$A_{t_3} + \ddot{R}_{tm} - (\omega_1^2 + \omega_2^2) R_{tm} \tag{88}$$

Now an expression for ω_3 must be generated. From equation (84) and Figure 53, the state equations for θ_1 and θ_2 are developed as

$$\dot{\theta}_1 = \omega_{i_2} \tag{89}$$

$$\dot{\theta}_2 = \omega_2 \tag{90}$$

where ω_{i_2} = the inertial angular rate of the line of sight frame along the $\underline{i}_2$ axis

Notice that equation (84) requires the line of sight frame inertial angular rate to be a vector in the $(\underline{i}_2, \underline{1}_2)$ plane. This can only happen if the vector sum of the line of sight angular velocities which lie along the $\underline{1}_1$ and $\underline{1}_2$ axes points in the $\underline{i}_2$ direction, i.e.

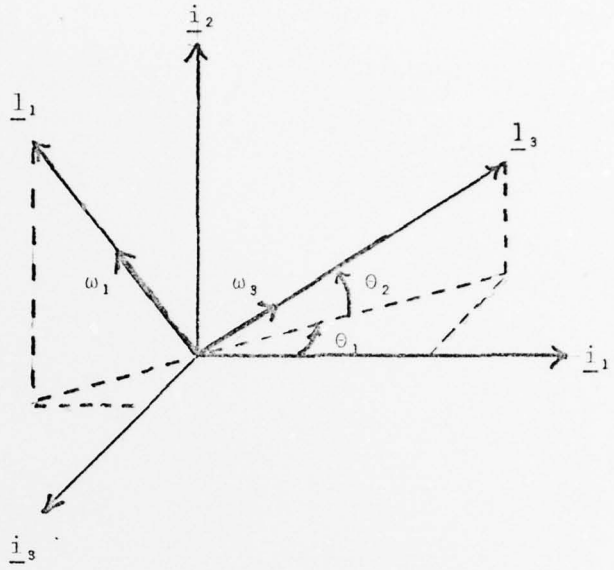
$$\omega_1 \underline{1}_1 + \omega_3 \underline{1}_3 = \omega_{i_2} \underline{i}_2 \tag{91}$$

which is depicted in Figure B-6. Taking the dot product of each term of equation (91) with $\underline{i}_2$ yields

$$\omega_1 \cos\theta_2 + \omega_3 \sin\theta_2 = \omega_{i_2} \tag{92}$$

From the Pythagorean theorem,

$$\omega_3 = \omega_1 \tan\theta_2 \tag{93}$$



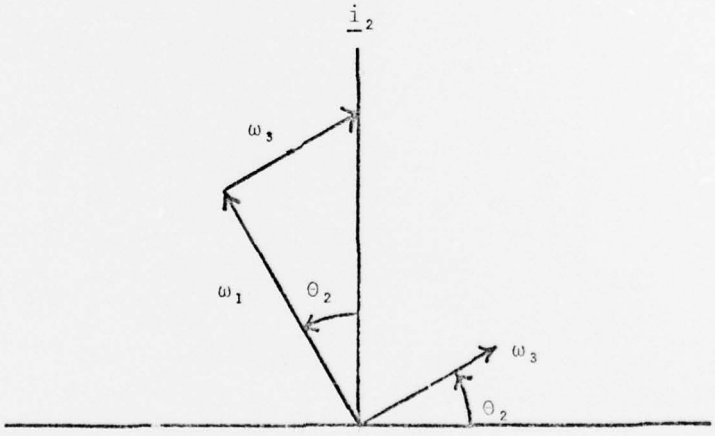


Fig. B-6. Mathematical Constraint on ω_3

Substituting equation (93) into (92) and the result into (89) yields

$$\dot{\theta}_1 = \omega_1 \sec\theta_2 \tag{94}$$

Substituting equation (93) into (87), (86), and (88); and then solving for $\dot{\omega}_1$, $\dot{\omega}_2$, and $\ddot{R}_{tm}$ yields the state equations for ω_1, ω_2, and $\dot{R}_{tm}$:

$$\dot{\omega}_1 = \frac{1}{R_{tm}}\left[A_D \sin\alpha_1 - A_{L2}\cos\alpha_1 + \frac{g\cos\theta_1}{\sqrt{2}} + A_{t_2} - 2\omega_1 \dot{R}_{tm} + \omega_1 \omega_2 R_{tm}\tan\theta_2\right] \tag{95}$$

$$\dot{\omega}_2 = \frac{1}{R_{tm}}\left[A_{L1}\cos\alpha_2 + \sin\alpha_2(A_{L2}\sin\alpha_1 + A_D\cos\alpha_1) - \frac{g}{\sqrt{2}} \cdot (\cos\theta_2 + \sin\theta_1\sin\theta_2) - A_{t_1} - 2\omega_2 \dot{R}_{tm} - \omega_1^2 R_{tm}\tan\theta_2\right] \tag{96}$$

$$\ddot{R}_{tm} = A_{L1}\sin\alpha_2 - (A_{L2}\sin\alpha_1 + A_D\cos\alpha_1)\cos\alpha_2 - \frac{g}{\sqrt{2}} \cdot (\sin\theta_2 - \sin\theta_1\cos\theta_2) - A_{t_3} + (\omega_1^2 + \omega_2^2)R_{tm} \tag{97}$$

where g = the acceleration of gravity (kiloft/sec^2)

A_D = acceleration due to drag (kiloft/sec^2)

The acceleration of drag can be approximated as (Ref 1:58)

$$A_D = \frac{\rho\sqrt{a\,V_m^3}}{(m/s)_f} + \frac{2(m/s)_f\,(A_{L1}^2 + A_{L2}^2)}{\rho\,a\,V_m\,(57.3)} \tag{98}$$

where ρ = air density (slugs/kiloft^3)

a = speed of sound (kiloft/sec)

V_m = velocity magnitude of the missile (kiloft/sec)

57.3 = radian to degree conversion

Note that neither Lutter, who developed this approximation, nor Cusumano and DePonte, include the conversion factor in the text of their theses. However, both use it in the computer program (Ref 5:209). Therefore it is included here to provide appropriate scaling. This approximation is within 3% of the truth model value for drag.

The missile velocity can be found in terms of the states from equations (61) through (63):

$$V_m = \sqrt{V_{m1}^2 + V_{m2}^2 + V_{m3}^2} \tag{99}$$

Thus, the state equations for the first eight states have been completely specified.

The final states, n_f, τ_f, and $(m/s)_f$ are constant parameters. Since the missile model used by the filter is not exact, it is possible for the filter to acquire an incorrect initial parameter estimate. If the parameters are modelled as a random bias, the gain in the extended Kalman filter approaches zero, inhibiting corrective changes. Thus, this filter model is inappropriate. To prevent this phenomena, pseudonoise can be added to each parameter model (Ref 7:204), changing the model from a form such as $\dot{b} = 0$ to $\dot{b} = W$. Through appropriate choice of the pseudonoise variance, the filter gain will be large enough to compensate for errors, yet small enough to maintain the essentially constant nature of the parameters. This technique proved successful in the two dimensional case (Ref 1:118). The state equations for the parameters are, therefore:

$$\dot{n}_f = W_1(t) \tag{100}$$

$$\dot{\tau} = W_2(t) \tag{101}$$

$$(m/s)_f = W_3(t) \tag{102}$$

where $W_1(t)$, $W_2(t)$, and $W_3(t)$ are independent white Gaussian noises with mean of zero and variance kernels $Q_1\delta(t)$, $Q_2\delta(t)$, and $Q_3\delta(t)$ respectively.

The final state equations, as used by the filter, are: NOTE: IF gravity is defined in the $-\underline{i}_2$ direction, ALL terms with θ_1 in the following equations are zero.

$$\dot{\theta}_1 = \omega_1 \sec\theta_2 \tag{94}$$

$$\dot{\theta}_2 = \omega_2 \tag{90}$$

$$\dot{\omega}_1 = \frac{1}{R_{tm}}\left[A_D \sin\alpha_1 - A_{L2}\cos\alpha_1 + \frac{g}{\sqrt{2}}\cos\theta_1 + A_{t2} - 2\omega_1 \dot{R}_{tm} + \omega_1\,\omega_2\,R_{tm}\tan\theta_2\right] \tag{95}$$

$$\dot{\omega}_2 = \frac{1}{R_{tm}}\left[A_{L1}\cos\alpha_2 + \sin\alpha_2(A_{L2}\sin\alpha_1 + A_D\cos\alpha_1) - \frac{g}{\sqrt{2}}\cdot(\cos\theta_2 + \sin\theta_1\sin\theta_2) - A_{t1} - 2\omega_2\dot{R}_{tm} - \omega_1{}^2 R_{tm}\tan\theta_2\right] \tag{96}$$

$$(\dot{R}_{tm}) = \dot{R}_{tm} \tag{103}$$

$$\ddot{R}_{tm} = A_{L1} \sin\alpha_2 - (A_{L2} \sin\alpha_1 + A_D \cos\alpha_1)\cos\alpha_2 - \frac{g}{\sqrt{2}} (\sin\theta_2 -$$

$$\sin\theta_1 \cos\theta_2) - A_{t_3} + (\omega_1^2 + \omega_2^2)R_{tm} \tag{97}$$

$$\dot{A}_{L1} = \frac{n_f \omega_2 \dot{R}_{tm} - A_{L1}}{\tau_f} \tag{76}$$

$$\dot{A}_{L2} = \frac{-n_f \omega_2 \dot{R}_{tm} - A_{L2}}{\tau_f} \tag{77}$$

$$\dot{n}_f = W_1(t) \tag{100}$$

$$\dot{\tau}_f = W_2(t) \tag{101}$$

$$(\dot{m/s})_f = W_3(t) \tag{102}$$

where

$$A_D = \frac{\rho\sqrt{a\ V_m^3}}{(m/s)_f} + \frac{2(m/s)_f\ (A_{L1}^2 + A_{L2}^2)}{\rho\ a\ V_m\ (57.3)} \tag{98}$$

$$\alpha_2 = \tan^{-1}\left[\frac{-V_{t_1} + \omega_2 R_{mt}}{V_{t_3} - \dot{R}_{mt}}\right] \tag{66}$$

$$\alpha_1 = \tan^{-1}\left[\frac{(V_{t_2} + \omega_1 R_{mt})\cos\alpha_2}{V_{t_3} - \dot{R}_{mt}}\right] \tag{68}$$

$$V_m = \sqrt{V_{m_1}^2 + V_{m_2}^2 + V_{m_3}^2} \tag{99}$$

$$V_{m_1} = V_{t_1} - \omega_2 R_{mt} \tag{61}$$

$$V_{m_2} = V_{t_2} - \omega_1 R_{mt} \tag{62}$$

$$V_{m_3} = V_{t_3} - \dot{R}_{mt} \tag{63}$$

The partial derivatives of these state equations, which are required by an extended Kalman filter, are contained in Appendix D, Subroutine FMAT.

Vita

Charles W. Hlavaty was born 6 October, 1949 in Davenport, Iowa. He graduated from Bettendorf High School in 1967 and entered the electrical engineering curriculum at Iowa State University in Ames, Iowa. After receiving his Bachelor of Science degree in Electrical Engineering in 1971, he entered the Air Force to become a navigator. He flew C-141's from Travis AFB, California and HC-130's from Kadena AB, Okinawa. While at Kadena, he obtained a Master of Science degree in Systems Management from the University of Southern California. After completion of his overseas tour of duty in 1977, he entered the School of Engineering at the Air Force Institute of Technology to pursue a Masters degree in Electrical Engineering.

UNCLASSIFIED

SECURITY CLASSIFICATION OF THIS PAGE (When Data Entered)

REPORT DOCUMENTATION PAGE		READ INSTRUCTIONS BEFORE COMPLETING FORM
1. REPORT NUMBER AFIT/GGC/EE/78-7	2. GOVT ACCESSION NO.	3. RECIPIENT'S CATALOG NUMBER
4. TITLE (and Subtitle) A PRACTICAL THREE DIMENSIONAL, 11 STATE EXTENDED KALMAN FILTER FOR USE IN A FIRE CONTROL SYSTEM AGAINST NON-THRUSTING MISSILES		5. TYPE OF REPORT & PERIOD COVERED MS Thesis 6. PERFORMING ORG. REPORT NUMBER
7. AUTHOR(s) Charles W. Hlavaty, Captain, USAF		8. CONTRACT OR GRANT NUMBER(s)
9. PERFORMING ORGANIZATION NAME AND ADDRESS Air Force Institute of Technology/AFIT/EN Wright-Patterson AFB OH 45433		10. PROGRAM ELEMENT, PROJECT, TASK AREA & WORK UNIT NUMBERS
11. CONTROLLING OFFICE NAME AND ADDRESS Air Force Avionics Laboratory/RWA Wright-Patterson AFB OH 45433		12. REPORT DATE December 1978 13. NUMBER OF PAGES (Vol I) 131 (Vol II) 210
14. MONITORING AGENCY NAME & ADDRESS(if different from Controlling Office)		15. SECURITY CLASS. (of this report) UNCLASSIFIED 15a. DECLASSIFICATION/DOWNGRADING SCHEDULE

16. DISTRIBUTION STATEMENT (of this Report)

Approved for public release; distribition unlimited

17. DISTRIBUTION STATEMENT (of the abstract entered in Block 20, if different from Report)

18. SUPPLEMENTARY NOTES

Approved for public release; IAW AFR 190-17

JOSEPH P. HIPPS, Major, USAF
Director of Information 1-23-79

19. KEY WORDS (Continue on reverse side if necessary and identify by block number)

Kalman Filter
Aided Tracking
Fire Control
Missile Model

20. ABSTRACT (Continue on reverse side if necessary and identify by block number)

A previously designed extended Kalman filter, based upon the proportional guidance law, aerodynamic drag equation, and a first order lag model of the missile time response; is modified for three dimensional use. Its purpose is to estimate various states of an offensive missile by processing the line of sight measurements made by the target aircraft. A six-degree-of-freedom, stochastic missile model is developed and presented in Fortran code. Monte Carlo analyses

DD FORM 1 JAN 73 1473 EDITION OF 1 NOV 65 IS OBSOLETE UNCLASSIFIED

SECURITY CLASSIFICATION OF THIS PAGE (When Data Entered)

of the filter's performance are generated for four different trajectories. These trajectories test for different orientations of the line of sight, different accelleration profiles of the missile, and different amount of roll induced upon the missile by a three dimensional, conic turn.

The extended Kalman filter is designed in the line of sight frame and is composed of eleven states. They are: two line of sight orientation angles, two inertial angular velocities of the line of sight, range, closing velocity, two lateral accelerations of the missile, and three constant parameters. The constant parameters are the proportional navigation constant (which exploits an assumed missile guidance scheme), a time constant (for the first order lag model of missile time response), and the missile's mass over surface ratio (for computing aerodynamic drag of the missile). The filter assumes that the missile is non-rolling with respect to the line of sight frame, and that the line of sight frame is non-rolling with respect to the inertial frame. It also assumes that the missile is non-thrusting.

Preliminary results are promising. The filter is only tuned for one trajectory due to time limitations, yet its estimation of the pointing-tracking states provide good aiding for all trajectories. Parameter estimates and missile accleration estimates for the other trajectories are degraded due to improper tuning of two parameters. However, it is felt that additional tuning of those parameters will increase the filter's accuracy for the other trajectories. Plots of the Monte Carlo results are provided, as well as the Fortran computer program used in the simulation.